Schweizerische Eidgenossenschaft
Confédération suisse
Confederazione Svizzera
Confederaziun svizra

Swiss Confederation

Federal Department of Home Affairs FDHA
Federal Office of Meteorology and Climatology MeteoSwiss

Scientific Report MeteoSwiss No. 90

A study of Convective Events in Switzerland with Radar and a High-Resolution NWP Model

Mario Betschart

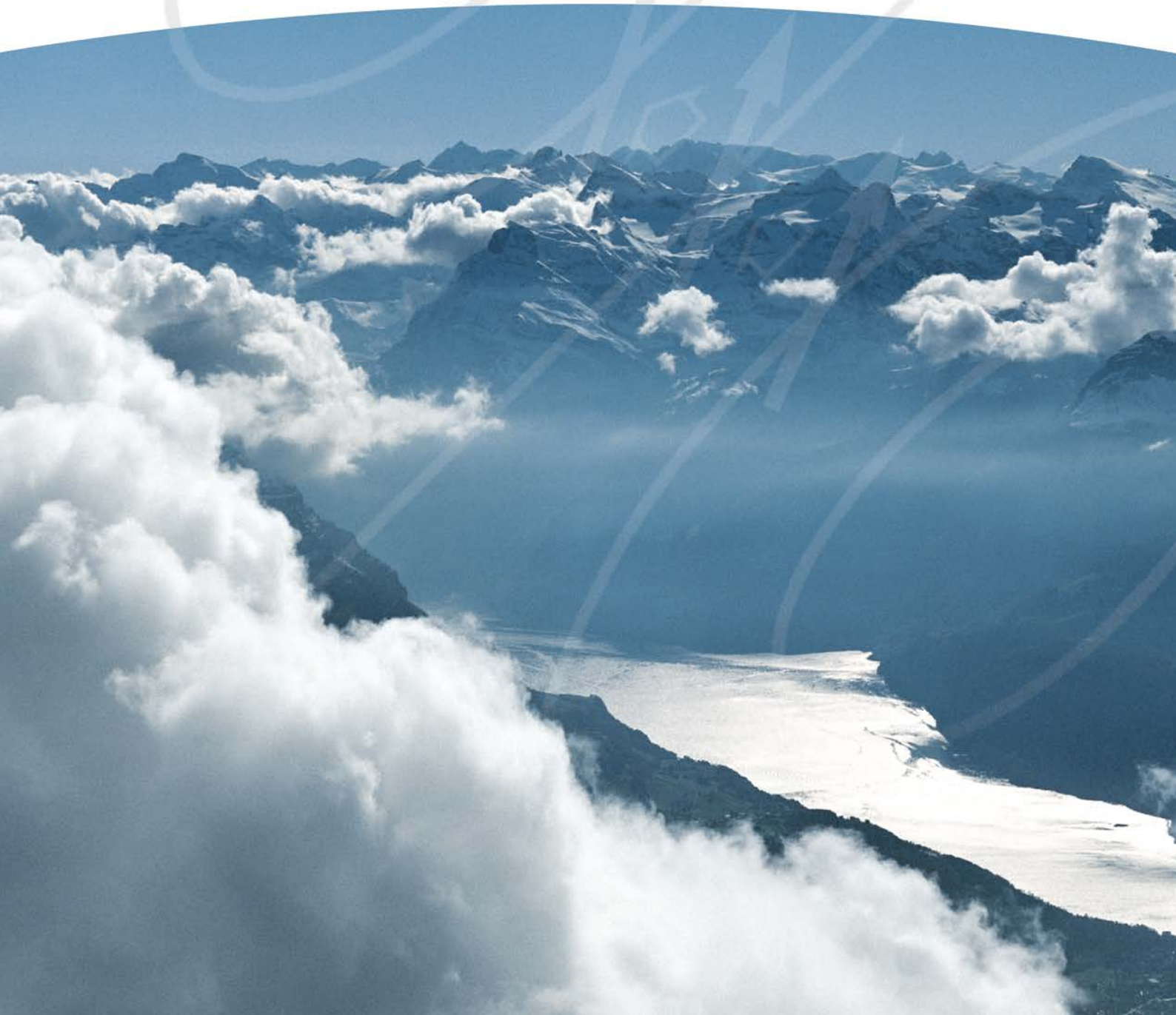

ISSN: 1422-1381

Scientific Report MeteoSwiss No. 90

A study of Convective Events in Switzerland with Radar and a High-Resolution NWP Model

Mario Betschart

Master Thesis
Supervisor: Prof. Dr. Olivia Romppainen-Martius, Institute of Geography and Oeschger Centre for Climate Change Research, Berne
Co-supervisor: Dr. Marco Arpagaus and Dr. Alessandro Hering, MeteoSwiss

Recommended citation:
Betschart, M: 2012, A Study of Convective Events in Switzerland with Radar and a High-Resolution NWP Model, *Scientific Report MeteoSwiss,* **90,** 119 pp.

Editor:
Federal Office of Meteorology and Climatology, MeteoSwiss, © 2012

MeteoSwiss
Krähbühlstrasse 58
CH-8044 Zürich
T +41 44 256 91 11
www.meteoschweiz.ch

Acknowledgement

I would like to thank my girlfriend and my family who supported me throughout all the long years and encouraged me in difficult times of the education from the beginning till the end which comes true with this Master Thesis. Thanks to all people who supported me and contributed to the realization of this study. In particular I would like to express my gratitude to Prof. Dr. Olivia Romppainen-Martius, the supervisor and head of the Climate Impact Group at the Geographical Institute of the University of Bern, for the possibility to do research on an applied topic at the frontline of research and the helpful advices. Special thanks go to Dr. Marco Arpagaus who supported me at MeteoSwiss. He guided me through the problems, and challenges. He had always time to answer my questions and reviewed many hours. Thank you Marco, for your help and patience! In addition, I would like to thank Dr. Daniel Leuenberger and Dr. Alessandro Hering from MeteoSwiss, who supported and introduced me to the field of NCL and IDL programming with a lot of patience. Both were never too busy to answer all my questions and however find time to review my work. Thanks are also owing to Dr. Ulrich Blahak from the DWD who gave helpful advices and interpretation inputs in a difficult topic. Very special thanks go to the rest of APN and APS at MeteoSwiss who helped me and made this time not only interesting but also amusing. The time at MeteoSwiss was just great, I will never forget it.

Abstract

Three hailstorms which caused significant damage in Switzerland were simulated with the COSMO (Consortium for Small-scale Modeling) one-moment microphysical scheme as well as with the new COSMO two-moment microphysical scheme and qualitatively verified with real radar measurements of the operational Swiss radar network in order to investigate the model capability to realistically simulate convective storms. To this end, a new COSMO radar forward operator was implemented and applied within this study to compute synthetic radar volume data which are then directly compared with the radar derived reflectivities. This is the first time the COSMO two-moment scheme as well as the COSMO radar forward operator is used for COSMO-2 simulations over Switzerland. Using the COSMO two-moment microphysical scheme in forecast mode, resulted in the almost complete absence of convective cells in the simulations. Using the same model in analysis mode and investigating the synthetic radar reflectivities, realistic structures were observed. The reasons why the COSMO two-moment scheme does not simulate any convection for all three cases are not understood. Investigations of the vertical structure showed the capability of the COSMO two-moment scheme to simulate hail in the strong updraft areas. High reflectivity cores ($\geq$ 55 dBZ) are simulated similar to the radar data. The COSMO one-moment microphysical scheme shows the capability to predict the three hailstorms with small deviations in terms of the location and time, but with too low intensity, lifetime and geographical extension. Applied radar-based hail detection algorithms highlight the capability of the COSMO one-moment scheme to forecast whether and where hail can occur within the next hours. The analyses of the COSMO one-moment scheme showed better results than the forecasts but not as good as the case of the COSMO two-moment scheme analysis. The study also found that probably a wrong mass-size parameterization of the COSMO one-moment scheme results in an underestimation of the convective vertical extent in terms of synthetic reflectivity. In both schemes too high synthetic reflectivities were simulated close to the ground mostly due to high hydrometeor densities of rain.

Table of Contents

1. Introduction and Motivation

Thunderstorms and especially hailstorms have been one of the main natural hazards since many centuries to crops, infrastructures, and buildings. For Switzerland, the total insurance costs of the year 2009 due to hail were three times higher than all other elemental damages together (storms, floods, landslides, rock falls, snow pressure, and avalanches) and exceeded the old record hail losses of 2005 by a factor of two (Schweizer Hagel, 2009). A study by Kunz et al. (2009) found an almost constant annual number of thunderstorm days in the mean, but a significant increase of hail damages and hail days in the last three decades for southwestern Germany. In Switzerland, Schiesser (2003) reports evidence of more extreme hail events within the last 10 years. Therefore, similar trends in terms of losses can be expected for Switzerland.

Numerical weather prediction (NWP) is the use of computer power and mathematical models of the atmosphere, oceans, and land surface to predict the weather based on current weather conditions. In Switzerland, the main precipitation types in summer are convective precipitation and stratiform precipitation with embedded convective cells. NWP models are used to simulate and forecast (large-scale) stratiform precipitation as well as (small-scale) convective phenomena which are associated with the warm season and for which operational models tend to perform poorly (Droegmeier et al., 2000; Ebert et al., 2003).

National weather services have developed and deploy a new generation of mesoscale models operating at a horizontal resolution of only a few kilometers with the aim of explicitly resolving convection (Pfeifer et al., 2008). Quantitative precipitation forecasts show better or equal results for high-resolution convection-permitting models than for lower-resolution models which employ a convection parameterization scheme (Weusthoff et al., 2010). The numerical simulation of convective phenomena, with its various highly non-linear cloud microphysical processes, is still a challenge for state-of-the-art atmospheric models (Seifert and Beheng, 2006b). One-moment schemes , which simulate the evolution of one moment (typically the mass density or mass fraction) of the particle size distribution of all hydrometeors are commonly used in operational forecast models and have proven to

be successful to describe large scale precipitation systems, but high-resolution mesoscale NWP demand for a more accurate approach (Seifert and Beheng, 2006a).

In recent years, different two-moment-microphysical schemes have been developed (e.g., Ferrier, 1994; Meyers, 1997; Reisner et al., 1998; Seifert and Beheng, 2006a), which consider both the number and the mass densities for all hydrometeors. Seifert and Beheng (2006a) developed a two-moment bulk microphysical scheme, which comprises the 5 hydrometeor categories cloud water, rain water, cloud ice, snow, and graupel. Noppel et al. (2006) suggested to use two graupel categories and to distinguish clearly between graupel created by rimed ice particles (RIME-graupel) and graupel created by freezing raindrops (FRI-graupel). Based on Noppel's work the two-moment bulk scheme was extended with an additional hail class by Blahak (2008b), who made several modifications and extensions to the two-moment scheme. The outcome of freezing rain into ice was split to lower- and to higher density graupel, according the raindrop size. Finally, the relation between mass- and number density and the size range (diameter) was used to apply two size thresholds. The category below the first threshold size was defined as cloud ice particles, the second category between those threshold sizes was defined as graupel (formerly RIME graupel) and the last category as hail (formerly FRI-graupel). Blahak (2008b) then implemented the new two-moment microphysical scheme into the Consortium for Small Scale Modeling (COSMO) NWP model. We will henceforth refer to this two-moment microphysical scheme as the COSMO two-moment scheme.

Keil et al. (2003) showed the potential of radar observations for the evaluation of high-resolution model forecasts as radar systems provide multidimensional information at a high temporal and spatial resolution. The retrieval of the microphysical model variables of a two-moment scheme, i.e., the various hydrometeor mass and number densities, from radar measurements is however quite cumbersome if not impossible (Seifert and Beheng, 2006b). Two paradigms coexist in literature for model evaluations using observations that are not directly linked to the model parameters. Either the observations are converted into model variables (observation-to-model approach; e.g., Illingworth et al. (2007)) or synthetic observables are simulated from model output by applying a so-called forward operator and performing comparisons in terms of observables (model-to-observation-approach; Chevallier and Bauer (2003)).

Therefore, a new radar forward operator for simulating terrestrial weather radar measurements from NWP model output was developed by Blahak (2007). This radar forward operator calculates radar reflectivity and radial wind (synthetic radar volume data) and was implemented as a module in the COSMO-model. According to Blahak (2007), radar forward operators are suitable for a broad range of applications, e.g., radar data assimilation in the framework of Ensemble Kalman Filter Systems, or verification of cloud microphysical parameterizations.

Case studies with different two-moment schemes have shown improved simulations and higher forecasts skills compared with one-moment schemes (e.g., Tao et al., 2003). Baldauf et al. (2011) conclude that the two-moment scheme by Seifert and Beheng (2006a) shows only minor differences in most cases with the exception of strong squall-line situations. Comparisons of model simulations (one-moment scheme 3D cloud resolving model) with radar measurements of an isolated thunderstorm have already been done by Bertram et al. (2004). A study by Pfeifer et al. (2008) with synthetic quantities of a polarimetric radar forward operator has shown consistence of simulated model (one-moment scheme) data and observations. The sensitivity study of the COSMO two-moment scheme to the assumed cloud condensation nuclei density for the simulation of a severe hailstorm over southwestern Germany was tested by Noppel et al. (2010) and did not produce conclusive results.

The purpose of this study is the qualitative comparison of COSMO-2 model simulations with radar measurements of recently observed hailstorms in Switzerland in order to investigate the model capability to realistically simulate convective storms. Based on a previous study (Betschart and Hering, 2012) three different hailstorms are investigated. Model results employing both the one- and two-moment microphysical schemes are compared to classical observations. In addition, the COSMO radar forward operator was used to generate synthetic radar volume data which we then directly compared with the radar derived reflectivities. This is the first time the COSMO two-moment scheme as well as the COSMO radar forward operator was used for COSMO-2 simulations over Switzerland.

To summarize, this study aims at answering the following question:

How realistic can COSMO-2 simulate hail events over Switzerland, and what are the main differences between the one-moment and two-moment microphysical schemes in modeling the convective storms?

To address different facets of the principle question, we formulate a number of sub questions as follows:

- What are the differences of the two microphysical schemes in simulating surface precipitation?
- How well does the model generated synthetic radar data, such as maximum reflectivity and vertically integrated quantities, compare with the radar data, and what are the differences for the two microphysical schemes?
- How realistic are the vertical structures of the hydrometeor fields and how well do the radar forward operator generated three-dimensional reflectivity fields compare with the radar derived reflectivities?
- How do radar-based hail detection algorithm outputs look like for the simulations in comparison with the radar derived data and what are the differences between the simulations with the one-moment and two-moment scheme?

The data and method which are used in this study as well as theory about the COSMO model, the COSMO two-moment microphysical scheme, and the COSMO radar forward operator and theory about convection and hail are introduced in chapter 2. Model results and their corresponding discussions are presented in chapter 3. Summary, conclusions and an outlook are presented in chapter 4.

2. Data and Method

In this study the capability of the COSMO model to simulate convection and especially hailstorms is investigated in a qualitative way. First, the qualitative investigations of the COSMO one-moment and two-moment microphysical schemes should give a prime insight into how well the model simulates deep convection. Such a method is already applied in other studies (e.g., Noppel et al. 2010). Due to the limitation to three hail events, no statistical analysis is applied. Therefore, a number of visual products and outputs from the COSMO model and the COSMO radar forward operator are generated in order to analyze them in comparison with radar measurements.

2.1. Radar Observations

2.1.1. Radar Equations

The weather radar (radio detecting and ranging) is an active remote sensing instrument, which sends out electromagnetic pulses, detects the returning echo, and computes its reflectivity Z as well as other moments. The electromagnetic pulse is scattered by the hydrometeors. The scattering depends on the properties of the different hydrometeors such as diameter or the dielectricity constant, as well as the number density of hydrometeors in the pulse volume. Weather radars operate in different frequency bands (typically in the range of GHz) and wavelengths (typically in the range of cm). MeteoSwiss operates a C-Band Doppler radar with a frequency of 5.4 GHz

Weather radar equation for multiple scatterers

The back scattered signal for a multiple scatterer such as rain, hail or snow is considered per pulse volume V (Figure 2.1.1).

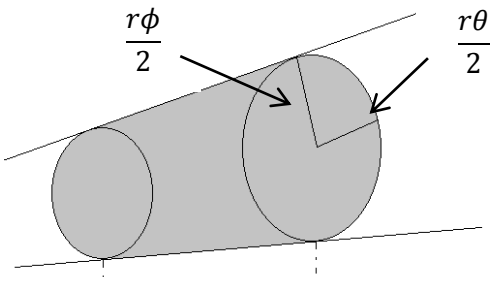

Figure 2.1.1: Schematic presentation of a single pulse volume (grey area) of a multiple scatterer after Wüest (2011). See text below for explanations.

The pulse Volume V is defined as:

$$V = \frac{c\tau}{2}\frac{r\phi}{2}\frac{r\theta}{2}\pi \quad (1)$$

where c is the speed of light, r is the distance from the radar site, ϕ and θ are the angles in elevation and azimuth, respectively, and τ is the pulse duration.

According to Uijlenhoet (2001), the radar equation describes the relationship between the received power, the properties of the radar, the properties of the targets and the distance between the radar and the targets. The radar itself measures the received power (P_r) which is given at non-attenuated wavelengths as:

$$P_r = C\frac{|K|^2}{r^2}Z \quad (2)$$

where P_r [W] is the mean power received from hydrometeors at range r [km], C is the so-called radar constant, $|K|^2$ is a coefficient related to the dielectric constant of water (~0.93) and Z [mm^6m^{-3}] is the radar reflectivity factor or simple radar reflectivity. All radar properties are contained in C, and all raindrop properties in $|K|^2$ and Z (Uijlenhoet, 2001).

The reflectivity factor Z is defined as (Wüest, 2011):

$$Z = \frac{1}{V}\sum D^6 = \int_0^\infty N(D)D^6 dD \quad (3)$$

where D is the spherical particle diameter [mm] and $N(D)dD$ represents the mean number of raindrops with equivalent spherical diameters between D and $D+dD$ (mm) per unit volume of air. Therefore the reflectivity factor is dependent of the diameter to the power of six.

The standard units of Z are mm^6/m^3. Because of the huge spread of typical radar measured Z values, usually logarithmic units are used. The transformation is computed as follows:

$$dBZ = Z[dB] = 10log\frac{Z}{1mm^6m^{-3}} \quad (4)$$

Further information about radar basics and equations can be found in e.g. Rinehart (2010).

The transformation between measured reflectivity (dBZ) values and the more common mm/h unit for precipitation measurements can be done in general assuming the Marshall-Palmer (Marshall and Palmer, 1948) distribution for correlations between radar reflectivity and the rain rate on the ground. MeteoSwiss uses the empirical relationship (Joss et al., 1997).

$$Z = 316\,R^{1.5} \quad (5)$$

where R is given in mm/h and Z in mm^6/m^3. Table 2.1 gives information of the different levels of precipitation intensity used by MeteoSwiss.

Table 2.1: Levels of intensity for reflectivity [dBZ] and rain rate [mm/h] used by MeteoSwiss (Joss et al., 1997).

Class	Reflectivity [dBz]	Rain rate [mm/h]
00	<13	< 0.16
01	13 - 16	0.16 - 0.25
02	16 - 19	0.25 - 0.40
03	19 - 22	0.40 - 0.63
04	22 - 25	0.63 - 1.00
05	25 - 28	1.00 - 1.60
06	28 - 31	1.60 - 2.50
07	31 - 34	2.50 - 4.00
08	34 - 37	4.00 - 6.30
09	37 - 40	6.30 - 10.0
10	40 - 43	10.0 - 16.0
11	43 - 46	16.0 - 25.0
12	46 - 49	25.0 - 40.0
13	49 - 52	40.0 - 63.0
14	52 - 55	63.0 - 100.
15	> 55	> 100.

Putting a weather radar in a mountainous region, is challenging. The orography interferes both with what a radar should observe and the way how a radar can observe it (Germann and Joss, 2004; Germann et al., 2006). According to these authors, several geometrical and physical problems play a role when detecting precipitation in an orographic environment such as the Alps. The orography complicates precipitation measurements by radar because of beam shielding (orographic shadow), partial shielding, overshooting, and severe ground clutter (echos due to terrestrial objectives), as well as difficult operating conditions on mountain sites. The influence of an orographic barrier, on the other hand, on the distribution of precipitation is glaring when looking at climatological maps (Frei and Schär, 1998). Germann (1999) mentioned also beam-broadening, partial beam filling, variations in the relation between radar reflectivity and rainfall rate (Z-R relation), hardware faults, as well as attenuation in heavy rain, in the melting layer, and in the water cover on the radome as dominant sources of errors involved in quantitative precipitation measurements by radars. It is therefore possible that a severe thunderstorm cell shields another cell from the radar which is directly behind the first cell. Therefore, composites of all three Swiss radar stations are used in order to see more. The shielding effect might have an influence on the radar measurement when considering extreme events. In this study, no shielding effects were observed.

In order to see and to understand the most challenging problems such as shielding, partial shielding and ground echos, which often inhibit a direct view on precipitation close to the ground, the radar visibility map can be obtain (Figure 2.1.2). To fill the

holes in badly visible regions, measurements from several km above the ground or from neighboring regions must be extrapolated in order to estimate the precipitation on the ground (Germann and Joss, 2004). In the Swiss radar network, the clutter removal is done using a sophisticated clutter elimination algorithm. Further information about the clutter elimination and additional technics to improve the radar scan quality can be found in e.g. Germann and Joss (2004) and Germann (1999).

2.1.2. Swiss radar network

MeteoSwiss operates a network of three C-band (3.75-7.5 cm wavelength) Doppler radar stations with the radar sites Albis, La Dôle, and Monte Lema. Figure 2.1.2 shows the locations of the three radar stations and the composite visibility map, showing the height above sea level of the lowest radar beam which is unshielded by topography. High (low) values denote regions with bad (good) visibility. The network is renewed since 2011 towards double polarized radars (4th generation), two additional radars will be added in Grisons and Valais. For this study only single-polarized radar data are used. Further information about the Swiss radar network can be found in the literature (e.g., Joss et al., 1997; Hering et al., 2004; Germann et al., 2006).

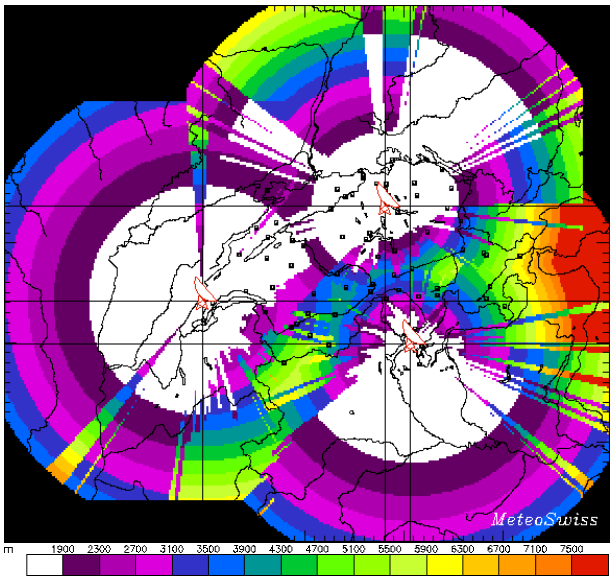

Figure 2.1.2: Radar sites and their visibilities in the Swiss radar composite. Low (high) values denote good (bad) visibility. The Albis radar is located in the north of Switzerland near Zurich, the La Dôle radar is located in the western part of Switzerland near Geneva and the Monte Lema radar is placed in the south of Switzerland near Lugano.

2.1.3. Radar Products

In the following, some specific radar products, which were used within this study, are introduced, with the aim of a better understanding of the products and their properties. Short product names (except for the products POH, MESHS and VIL, see below) contain three letters (e.g. OMC). The last one describes the radar (A, D or L) or stands for the entire composite (C).

MAX-ECHO

The MAX-ECHO (or maximum reflectivity) product gives information about the maximum occurred reflectivity in a vertical column for a certain time step as radar composite of all three radar stations. The product short form is called OMC for the 3th generation and CZC for the new 4th generation. Within this study OMC is used for radar data and CZC for synthetic radar volume data. Maximum reflectivity products do not give accurate information about the precipitation at the ground, but they can give an overview of the locations where high reflectivities occur.

PKC

The PKC (1x1 km) product displays the best estimate of the precipitation at ground level using the experience accumulated in the past. The PKC product is especially (low rest-clutter, consider the past) made for the use of assimilation in the COSMO model in order to force the model towards more or less surface precipitation.

Vertical Integrated Liquid (VIL)

The VIL product shows the vertically integrated liquid water content derived by the radar reflectivities of a 2x2 km column for the 3th generation (DLC) and a 1x1 km column for the 4th generation (LZC) which are transformed (equation 5) in kg/m^2 water equivalent. The liquid water content of a cloud can be used to determine the amount of condensation and dynamic development that has taken place. Changes in the liquid water content are also associated with thermodynamic energy changes (Greene and Clark, 1972). Johnson et al. (1998) developed an enhanced cell identification and tracking algorithm based on VIL values. A similar cell tracking algorithm is implemented as Thunderstorm Radar Tracking (TRT; e.g., Hering et al. 2004; Hering 2010) system at MeteoSwiss. Reflectivity based VIL products can be used as an estimate for the potential for severe thunderstorms in each radar grid

box. To compute VIL at MeteoSwiss, reflectivity values are limited to 57 dBZ. Values above 57 dBZ are set to 57 dBZ in order to reduce the effect of high reflectivity values e.g. due to wet hail. Then the values are integrated over the entire vertical column.

Vertical cross sections (OYC)

The product OYC contains full volume information of the reflectivity [dBZ], updated every 5 minutes. This product is useful, for example, to obtain vertical sections in any desired azimuthal direction, for a 3-dimensional impression. The spatial resolution is 2x2 km (Joss et al., 1997).

Vertical cross sections of reflectivity can be generated for each single radar site (only) and give the view of a single radar station on the corresponding plane, where the cross section is made. They were used in this study to investigate the vertical structure of convective cells. According to the location of a convective cell, the radar station which is closest to the cell is chosen for the vertical cross section in order to have the best possible resolution. Due to the radar scan strategy, radar pixels do not cover the entire cross section and single scans are clearly visible as small scan bands. Spatial displacements of the cells between radar data and model simulations make it necessary to choose the location and the length of each vertical cross section individually. Therefore, vertical cross sections of the same cell must not be exactly at the same location or of the same length within this study. The cuts were chosen to produce similar plots about similar situations between different time steps and the two different parameterization schemes.

Vertical contour plots of hydrometeor densities were plotted in order to learn more about the behavior of the vertical reflectivities. Vertical winds were only plotted within the hydrometeor plots where interesting structures such as rain in high altitudes or hail cores (two-moment scheme) were co-located with strong up- or downdrafts.

Probability of Hail (POH)

The POH product shows the grid-based probability of hail for each pixel (2x2 km for the 3th generation products and 1x1 for the 4th generation). The algorithm estimates the probability of hail of any size on the ground (Hering, 2010). The basic criterion of the POH algorithm was introduced by Waldvogel et al. (1979) and is the distance between the 45 dBZ contour height (H_{45}) and the melting level (H_{T0}). Witt et al. (1998) then found a probability of hail as a function of $H_{45} - H_{T0}$. The probability of hail increases with the height difference. Differences greater than 6 km have 100% probability and less than 1.6 km give 0% probability of hail. For the MeteoSwiss POH product, the zero degree height is extracted from the latest available COSMO-2 model runs. Missing H_{T0} values due to the height of the Alps are horizontally interpolated for this approach (from Betschart and Hering, 2012).

Maximum Expected Severe Hail Size (MESHS)

The Maximum Expected Severe Hail Size (MESHS) is an estimation of the maximum expected hail diameter for each pixel within the radar composite. Treloar (1998) developed a heuristic method in order to detect different severe (> 2 cm) hail size diameters, using the difference between the maximum height of the 50 dBZ altitude and the height of the freezing level. For the MeteoSwiss MESHS algorithm, the 51 dBZ height is used instead due to the specifications of the Swiss radar network. The maximum hail size is categorized in 0.5 cm classes. Hail sizes of less than 2 cm are not computed. The zero degree height is extracted from the latest available COSMO-2 model run. The missing H_{T0} values due to the higher elevation of the Alps are horizontally interpolated (from Betschart and Hering, 2012).

Radar-based hail detection algorithms

The radar-based hail detection algorithms POH and MESHS were used to produce synthetic hail products directly from the model. Therefore, clear statements can be made whether the COSMO model is able to simulate equal or similar hail products as they are derived by the radar. Despite the fact that the COSMO one-moment scheme does not simulate hail as a separate category, the applied radar-based hail algorithms POH and MESHS provide explicit information about hail. From a forecasting perspective, it is interesting to see whether these synthetic POH and MESHS products can be used for a hail forecast or to be more specific about the

location where hail can be expected or whether hail is predicted or not. The main advantage of these products is the direct comparability with radar derived POH and MESHS product in terms of hail. Due to the straight forward computation process and its relation the height of high reflectivity values (45 dBZ, 51 dBZ), these two products are immediately influenced by the vertical extent of high reflectivity values.

The synthetic POH products will be verified with the corresponding SHVDB[1] as far as possible. Therefore, the quality of the synthetic POH product are verified with the same method and the same data as was done for the corresponding radar derived POH products (Betschart and Hering, 2012). This approach quantitative conclusions for the cases for which it makes sense to apply this method.

2.2. COSMO NWP Model

The COSMO model (Doms et al., 2011a; Schättler et al., 2011) is a non-hydrostatic limited-area atmospheric prediction model and has been designed for operational numerical weather prediction (NWP) as well as research applications, with focus on the meso-β to meso-γ scale (grid spacings of 50 km down to 50m). The COSMO model was originally developed at the Deutscher Wetterdienst (DWD; German weather service) and is maintained and further developed in the Consortium for Small Scale Modeling (COSMO), a group of meteorological services from Germany, Greece, Italy, Poland, Romania, Russia, and Switzerland. It is in operational use in several COSMO countries, including Switzerland, since the end of 1999.

The COSMO model is based on the primitive thermo-hydrodynamical equations describing compressible flow in a moist atmosphere. Different physical processes are taken into account by parameterization schemes, such as subgrid-scale turbulence, surface layer parameterization, grid-scale clouds and precipitation, subgrid-scale clouds, shallow convection, radiation, soil processes, and terrain and surface data (Doms et al., 2011b).

MeteoSwiss operates the COSMO-7 model with 7 km grid spacing and the high resolution COSMO-2 model with 2 km grid spacing. COSMO-7 employs a convection parameterization scheme to simulate subgrid-scale deep convection, whereas COSMO-2 is expected to simulate large deep convective systems explicitly, and only

[1] Swiss Hail Verification Data Base

shallow convection is parameterized. Microphysical cloud and precipitation processes in the operational COSMO-2 are represented by a one-moment microphysical cloud scheme as described in Baldauf et al. (2011), which was extended to include riming processes for the graupel formation in order to simulate convection as well as stratiform rain. This one-moment cloud microphysical scheme predicts cloud water (cloud droplets smaller than 50 μm), rainwater (liquid-phase spherical drops with non-negligible fall velocity), cloud ice, snow (rimed ice particles and rimed aggregates), and graupel. The COSMO one-moment cloud microphysical scheme deals with mixing ratios for each hydrometeor species and does not include a separate hail class. The size distribution of graupel is described with an exponential size distribution dependent on the mass-density. For further information consider for e.g., Doms et al. (2011a; 2011b), Schättler et al. (2011), and Baldauf et al. (2011).

2.2.1. Two-moment Cloud Microphysical Scheme

For selected simulations of this study, an experimental two-moment cloud microphysical scheme after Seifert and Beheng (2006a) is used (SB-scheme). The two-moment scheme is expected to simulate microphysics in more detail by integrating rate equations in terms of number as well as mass densities, including a full treatment of cloud droplet number concentrations (Seifert and Beheng, 2006a). The diameter-mass- as well as the velocity-mass-relations of the different ice phase particles are parameterized by power laws (see Seifert and Beheng, 2006a) equations (32) and (33)). The standard SB-scheme distinguishes between five hydrometeor types, such as cloud water, rain water, cloud ice, snow, and graupel. The graupel category was separated into two classes by Noppel et al. (2006). On the one hand, graupel created by rimed ice particles (termed RIME graupel) with a lower density and on the other hand, graupel created by freezing raindrops (frozen-raindrop-induced or FRI graupel for short) with a higher density is distinguished. The most obvious effect of the new split scheme was a strong increase in the total volume of precipitation, larger rain drops, and a vertical redistribution of mass (Noppel et al., 2006). Blahak (2008b) found that especially the often observed high reflectivity values in the upper central part of active convective clouds, forming the so called reflectivity cores, could not be adequately simulated by the SB-scheme. Therefore, he changed the parameters of size-mass and velocity-mass relations of all ice categories in such a way that less RIME-graupel particles initiate by riming and then grow to a larger size by further riming because there is less competition for the available

supercooled water between the RIME-graupel particles. In addition, the initiation of high density FRI-Graupel by freezing of raindrops was changed. Before (two-moment scheme after Noppel et al., 2006), all freezing raindrops were converted to FRI-graupel. After that, only particles exceeding a certain size threshold initiate to FRI-graupel, all other convert either to cloud ice (very small raindrops) or to RIME-graupel (Blahak, 2008b). In order to define a 'hail' class, the so-called wet-growth process was added and the FRI-graupel class changed to the class 'hail'.

For this study the extended SB-scheme by Blahak (2008b) is used and further referred as COSMO two-moment scheme. For all case studies, a middle Cloud Condensation Nuclei (CCN) concentration of $\geq 500\ L^{-1}$ is used (L = liter), meaning that a minimum number of 500 CCN is available per liter air, when the model is started. This value can fluctuate due to different processes and therefore the real CCN concentration by the initiation of the cell depends on the formation processes and is different for each convective system in the model.

Further information about the microphysics of the COSMO two-moment scheme can be found in the corresponding literature (e.g., Seifert and Beheng, 2006a; Noppel et al., 2006; Blahak, 2008b).

2.2.2. Data Assimilation

The model uses initial environmental conditions in order to make a weather prediction. Atmospheric measurements such as from radiosondes, aircrafts, surface-level data, wind profilers and radar reflectivities are assimilated in the model in order to have the best estimate of the current situation. More information about the data assimilation can be found in e.g. (Schraff and Hess, 2003).

2.2.3. Latent Heat Nudging

The Latent Heat Nudging (LHN) is a relatively simple radar data assimilation method. The radar data force the model towards observed surface precipitation. The original LHN technique was proposed by Jones and Macpherson (1997). At every model grid point the model is compared to the radar measurement (PKC product). If the two are different, the vertical profile of modeled latent heat release at that grid point is scaled according to the ratio between observed and modeled precipitation rate (Stephan and Schraff, 2008). In cases where the model does not develop mesoscale disturbances that lead to the onset of convection, the radar data

assimilated with LHN can be of significant value and a positive impact can be observed during the entire lifetime of a convective storm (Leuenberger, 2005). Within this study analyses were forced to more accurate surface precipitation values using the LHN forcing.

2.2.4. Radar Forward Operator

Seifert and Beheng (2006b) suggested to develop synthetic radar reflectivities in order to allow for a more realistic comparison between measured and simulated hydrometeor distribution in space and to evaluate the development of advanced model components with measured radar data. For this study the radar forward operator by Blahak et al. (see Blahak, 2007; Blahak et al., 2011) is applied. Henceforth, the radar forward operator is referred to as the COSMO radar forward operator (RFO). The basic aim of the COSMO RFO (Blahak, 2007; Blahak et al., 2011) is the simulation of the equivalent (simulation of the real reflectivity factor Z) reflectivity factor Z_e, radial wind v_r, and polarization parameters on the native radar geometry (polar coordinates) using the model simulated meteorological fields such as wind and hydrometeor mixing ratios. For this study, only equivalent reflectivities Z_e (referred to as simulated or synthetic reflectivities) are considered. In general, the radar simulation is done in two sub-tasks. The first task is the computation of the field function Z_e (Z_e per grid box) using the model microphysical scheme (either one- or two-moment). The second task is the correction of the 3-dimensional field function by taking into account the most relevant typical radar characteristics, such as beam bending by atmospheric refraction, attenuation, beam function weighted volume averaging, and shadowing by orographic obstacles. In order to achieve these tasks, the radar quantity Z_e is computed on the COSMO model grid by using the spectral number density (number per size interval per volume) of the hydrometeors. Additional, the resulting equivalent reflectivity values Z_e are transformed and interpolated to the polar radar system because the corrected equivalent reflectivity factors in the model are still in a Cartesian system.

More detailed information about the equivalent reflectivity factor Z_e, the variables shown in the illustration above, and the concepts of the COSMO radar forward operator can be found in the corresponding literature (Blahak, 2007; Blahak, 2008a; Blahak et al., 2011).

The COSMO radar forward operator is still under development and therefore some parts of the simulation are not yet implemented, e.g., the calculation of polarization parameters and the fall velocity of hydrometeors on the model grid. Furthermore, the shading of the radar beams due to orographic obstacles such as the Alps or the Jura mountains are not considered yet. The cases, which are investigated in this study, mostly occur overt the flat Swiss Plateau and were checked that there are no adverse effects due to missing orographic obstacles in the synthetic radar data.

The application of the tools of the Swiss radar network to the synthetic reflectivity output of the COSMO model was one the main technical tasks of this study. Due to the radar renewal (4th generation), the synthetic radar volume data are computed with the 4th generation tools and have therefore in general higher spatial resolution than the corresponding original radar data, which were made with the tools of the 3th generation.

The new 4th generation radar server offers completely new computing capabilities in terms of computer power and flexibilities compared to the old system. This allows it for the first time to ingest radar data simulated by the COSMO RFO into the operational radar data chain and to compute identical formats as measured with radar. The COSMO RFO simulates 20 synthetic polar elevations as it is measured by the radar. Figure 2.2.1 shows a schematic illustration of the computation chain for synthetic radar products. In a first step, the synthetic reflectivity values (*dBZ*) are read in IDL and then transformed elevation by elevation into the Swiss radar network scan geometry. After that, synthetic PLX files (binary files) are written. These synthetic PLX files are then submitted to the new radar server (CCS4). The server is then able to compute every radar product as it is done with the real radar data. In order to produce synthetic POH and MESHS products, the COSMO H_0 files have to be transformed in the right syntax. After that these files also have to be submitted to the radar server. For daily maximum POH plot the raw data (echo tops) of the radar server have to be used together with the H_0 for a separate post-processing step.

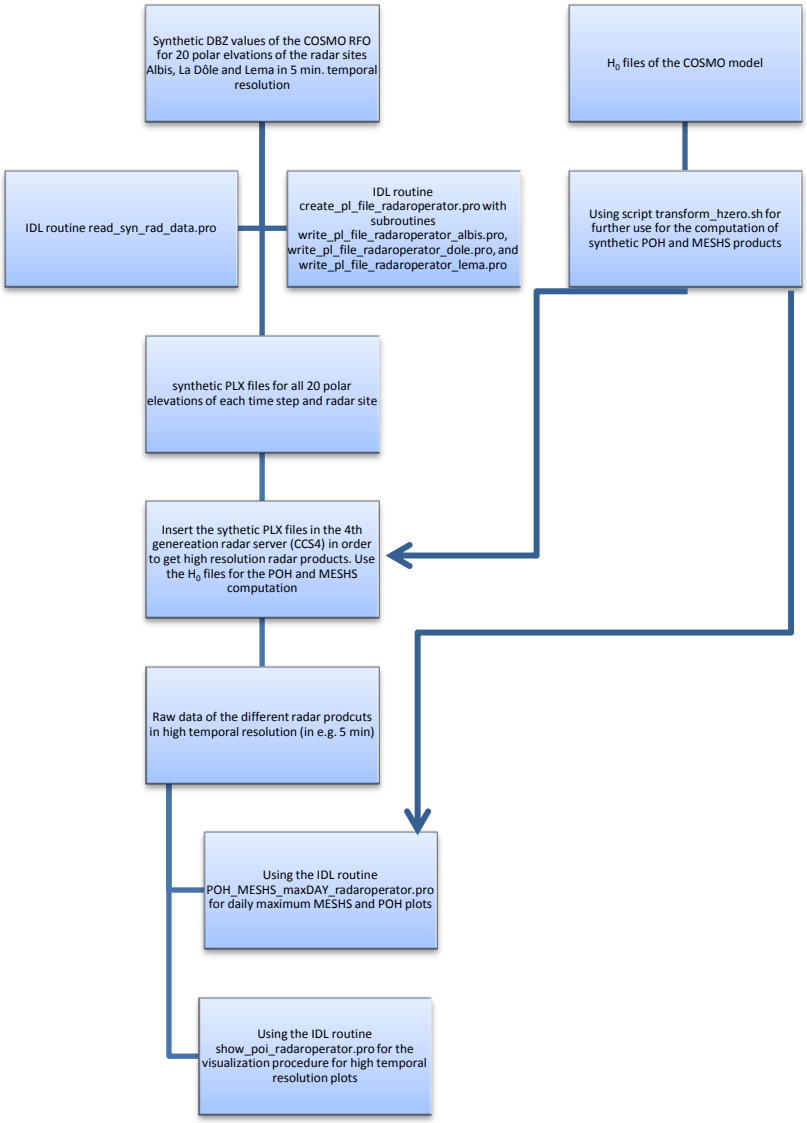

Figure 2.2.1: Schematic illustration of the computation chain for synthetic radar products. The corresponding IDL and script file routines can be found in the Appendix B.

2.3. Convection, Thunderstorms, and Hail

The formation and development of a first cumulus cloud to a mature cumulonimbus cloud as well as the development to different complex and organized convective storm systems such as single cell storms, multicell storms, supercell storms, and mesoscale convective systems (MCS) with their different distinct phenomena like gusts, bursts, splitting of the cell, squall lines and even tornados, are highly complex and the general description of these phenomena and is not part of this chapter. For further information the reader is referred to the literature. Good introductions are

given in e.g., Houze (1993), Emanuel (2005), Wallace and Hobbs (2006), and Lin (2007).

The structures of severe mesoscale precipitation systems (MPS) in Switzerland were analyzed by Schiesser et al. (1994). Organized mesoscale systems are quite common in Switzerland and are responsible for heavy rainfall and hail. Hail research has a long tradition in Switzerland. In the 1970s and 1980s, hail storm research in Switzerland was undertaken in the framework of hail suppression experiments (Federer et al., 1986). A hail climatology was done, in e.g., by Willemse (1995).

Hail

Hail is frozen hydrometeors with a diameter of more than 0.5 cm. Holleman (2001) distinguished between summer hail and winter hail. Winter hail mostly occurs when the freezing level is close to the surface and large-scale vertical motion, e.g. due to the passage of a front, forms small hail (smaller than 2 cm). Summer hail is defined as larger (greater than 2 cm) hail (terminal velocity 20-30 m/s) on a small scale, associated to summertime thunderstorms. Large summer hail with its large mass and high terminal fall velocity can cause severe damage and is potentially dangerous (Holleman, 2001).

The hail size distribution within a hail cell varies strongly. The same is true for hail stones which can be found on the ground. Severe hail is defined as hail stone sizes with 2 cm diameter or larger.

Weather radar scientists have found that a returning echo of more than 55 dBZ is usually hail. MeteoSwiss uses the 55 dBZ criterion for the HAIL product (not introduced) in order to distinguishes between hail possible (≥ 52 dBZ) and hail probable (≥ 55 dBZ). In this study, the 55 dBZ was used in order to see when, where, and whether a cell produced hail and is come along with strong convective activity. Maximum reflectivity analyses are based on the time when the most 55 dBZ values are simulated and hail is expected.

3. Case Studies; Results and Discussions

3.1. July 23, 2009

On July 23, 2009, a severe thunderstorm front with hail and strong wind gusts moved across large parts of Switzerland. Thereby, disastrous damages were caused on crops, buildings and vehicles. The sum of all loss reports for this single day reached more than 600 million Swiss Francs (Schweizer Hagel, 2009).

3.1.1. Synoptic Situation and Measurements

On July 23, 2009, a strong southwesterly flow developed due to a high-pressure system over the Mediterranean and a low-pressure system northwest of Scotland (see Figure 3.1.1). Strong foehn north of the Alps led to maximum wind speeds 10 meter above the ground up to 100 km/h. On the north side of the Alps, severe thunderstorms moved from southwest to northeast on the afternoon of July 23, 2009, embedded in an approaching cold front. The supply of warm, moist air from the Mediterranean and the particularly strong upper air flow from the southwest contributed significantly to the severity of the storms. Hailstones with diameters up to 5 cm were observed. Precipitation amounts of more than 40 mm/h were detected by the radar for the two most intense thunderstorm cells, one in the midland, moving from Geneva to the Lake of Constance (midland cell), and one in the Alps, travelling from Valais to the Bernese Oberland. The midland cell split in two cores in the area of Fribourg. Then, the south core crossed the region of Aaretal, mount Napf, and the Lake of Lucerne, whereas the northern core hit the Bernese midland, Aargau, and Zurich (Salamin et al., 2009). The cell in the Alps is not further considered in this study due to the circumstance that the midland cell was verfied by a earlier study at MeteoSwiss (Betschart and Hering, 2012) and therefore better conclusions about the cababilty of the COSMO model to simulate the midland cell can be made.

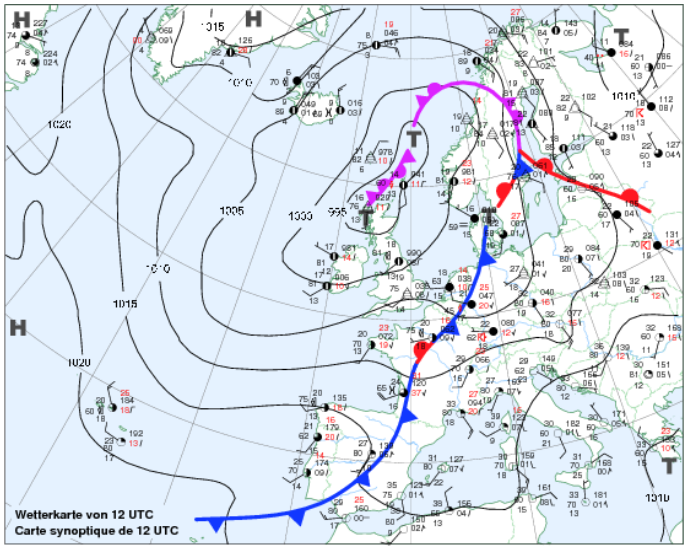

Figure 3.1.1: Synoptic weather chart of Europe on July 23, 2009. Blue signatures are surface cold fronts whereas red signatures are surface warm fronts. Purple signatures are occlusions. Black lines show the pressure [hPa] at the ground (source: MeteoSwiss).

First convective cells developed during the morning when the cold front approached Switzerland. The midland cell, which produced devastating hail later in the day, initiated in France. First weak reflectivities were detected at 11.00 UTC (not shown). The midland cell intensified over the Jura Mountains close to the La Dôle radar at 13.00 UTC (see red arrow on Figure 3.1.2, left). Later on, the main cell intensified more and more. At 14.00 UTC the main cell split in two cores in the area of Fribourg. The southern core reached the highest precipitation rates at 14.45 UTC (see red arrow on Figure 3.1.2, right). After that, the cells were getting weaker and dissipated after crossing the Lake of Constance (16.00 UTC, not shown). The cell(s) crossed entire Switzerland from Geneva to the Lake of Constance (~300 km) in about 3 hours, which results in a mean speed of around 100 km/h.

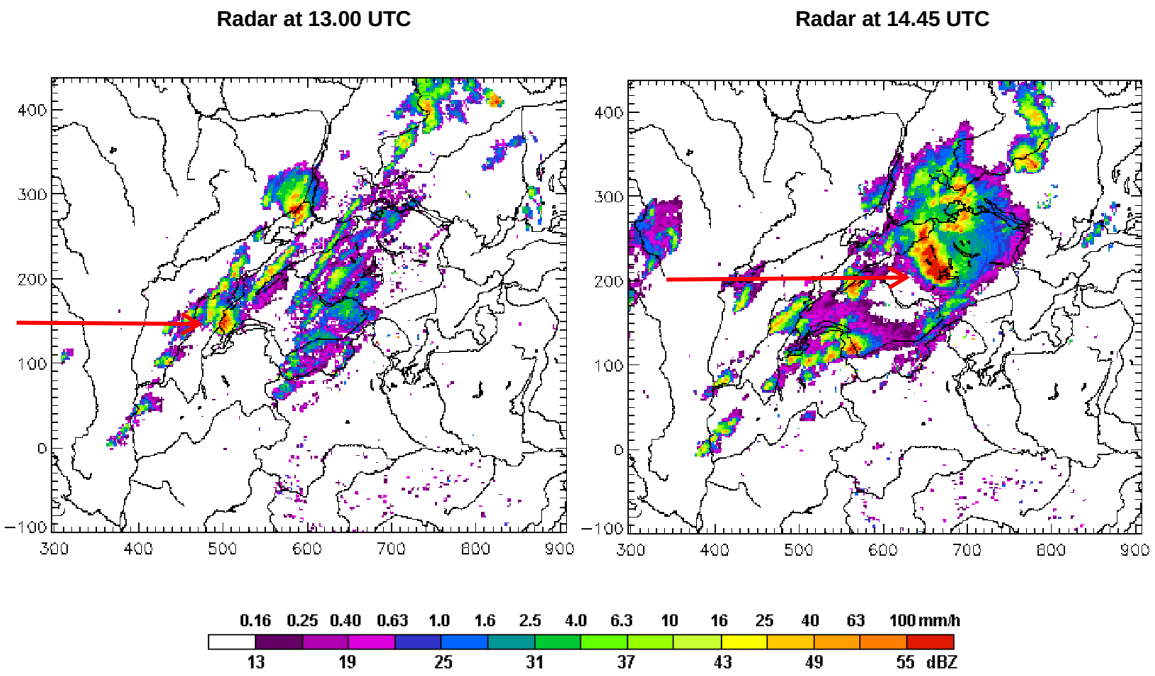

Figure 3.1.2: Precipitation [mm/h] (OMC product) at 13.00 UTC on July 23, 2009 (left), and at 14.45 UTC (right). The red arrow on the left side shows the moment of the intensification of the midland cell over the Jura Mountains close to the La Dôle radar, whereas the red arrow on the right side shows the location of the midland cell (south core) during the moment of highest intensity over the region of Lucerne.

3.1.2. 12 UTC COSMO Forecasts

We first look at the 12 UTC forecast because the first cells become visible in the radar data at 11.00 UTC and we can hence expect the model to ingest these first cells in the assimilation cycle (which is run until 12 UTC) by means of the LHN. Therefore the forecast model does not need to initiate the cells at the right place and at the right time by itself. The focus is on the intense midland cell.

3.1.2.1. Total Precipitation Sums

COSMO one-moment microphysical scheme 12 UTC forecast: data

Figure 3.1.3 shows the 24h total precipitation sum of the COSMO one-moment scheme 12 UTC forecast (left) and the corresponding radar derived measurements (right). Two swaths with values up to 100 mm/24h are simulated for the areas from the Entlebuch to the Lake of Constance as well as from Valais to the Bernese Oberland. The southern border of the simulated precipitation area corresponds well with the radar measurements.

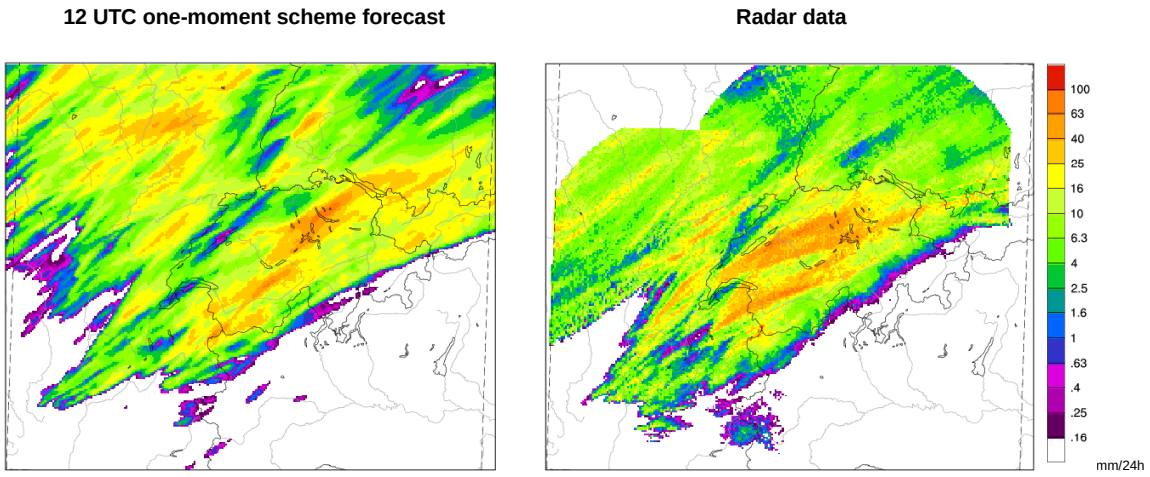

Figure 3.1.3: 24h precipitation sum (shaded) [mm/24h] of the COSMO one-moment 12 UTC forecast (left) and the radar measurements (PKC product, right) for July 23, 2009. Black solid lines are international borders and lakes, grey lines are rivers and coast lines, and the dashed lines indicate the radar domain.

COSMO two-moment microphysical scheme 12 UTC forecast: data

Figure 3.1.4 shows the 24h total precipitation sum of the COSMO two-moment scheme 12 UTC forecast (left) and the corresponding radar derived measurements (right). The simulation shows a precipitation swath from the Entlebuch to the Lake of Constance with quantities up to 63 mm/24h. The radar data shows precipitation values up to 100 mm/24h for the midland cell and the cell over the Alps. The southern border of the precipitation area can be seen in both, the simulation and the radar data.

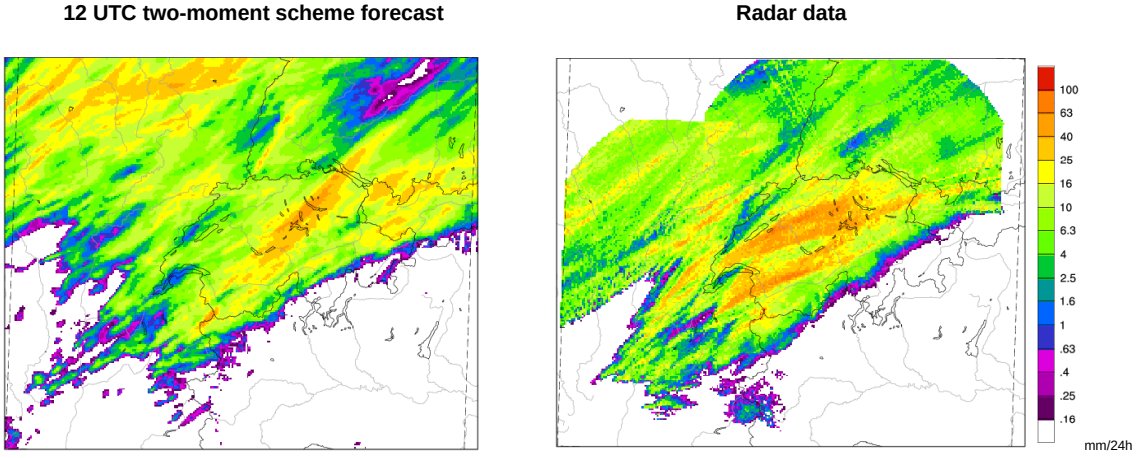

Figure 3.1.4: 24h precipitation sum (shaded) [mm/24h] of the COSMO two-moment 12 UTC forecast (left) and the radar measurements (PKC product, right) for July 23, 2009. Black solid lines are international borders and lakes, grey lines are rivers and coast lines, and the dashed lines indicate the radar domain.

12 UTC forecasts total precipitation sums: discussion

The comparison of the COSMO one-moment scheme 12 UTC forecast with the corresponding two-moment scheme 12 UTC forecast and the radar data show that both schemes simulate highest precipitation values between Entlebuch and the Lake of Constance with slightly higher 24h precipitation sum simulated in case of the one-moment 12 UTC forecast. In terms of the total precipitation, the two-moment 12 UTC forecast does not simulate the swath from Valais to the Bernese Oberland, which is not initiated due to the LHN forcing. The simulated swath from Entlebuch to the Lake of Constance looks different than seen in the radar data. Both simulations overestimate the total precipitation rates beyond the Lake of Zurich. Furthermore, the two-moment scheme simulates the midland swath a bit more in south-north direction than the one-moment scheme.

3.1.2.2. Maximum Reflectivities

COSMO one-moment microphysical scheme 12 UTC forecast: data

Figure 3.1.5 illustrates the maximum reflectivity values of the COSMO one-moment scheme 12 UTC forecast (top left panel) and the radar data (top right panel) when the simulation shows maximum intensity (14.10 UTC). The midland cell can be seen over the area of Berne. In comparison with the radar data, in general more small intense cells are visible when considering all the simulated maximum reflectivity plots of the entire day (not shown). The midland cell intensifies after crossing the Jura mountains near the La Dôle radar and looks smaller in terms of the geographical extension. In the radar measurements the maximum intensity is reached at 14.45 UTC (bottom right panel) over the area of Lucerne.

COSMO two-moment microphysical scheme 12 UTC forecast: data

Considering the maximum reflectivities of the two-moment 12 UTC forecast it can be recognized (not shown) that a midland cell intensifies after crossing the Jura mountains near the La Dôle radar. But the cell weakens when reaching Berne at 14.05 UTC and completely dissipates near Zurich until 15.00 UTC. The two-moment scheme simulates a second cell (with maximum reflectivities greater than 55 dBZ) which moves from Geneva to Lucerne and to the Lake of Constance. The cell shows its maximum intensity (when the most number of 55 dBZ pixels are seen) at Berne

at 15.15 UTC (Figure 3.1.5, bottom left panel) and therefore, the temporal displacement is about one hour, when using the second cell as the midland cell. This second cell dissipates around 17.00 UTC close to the Lake of Constance.

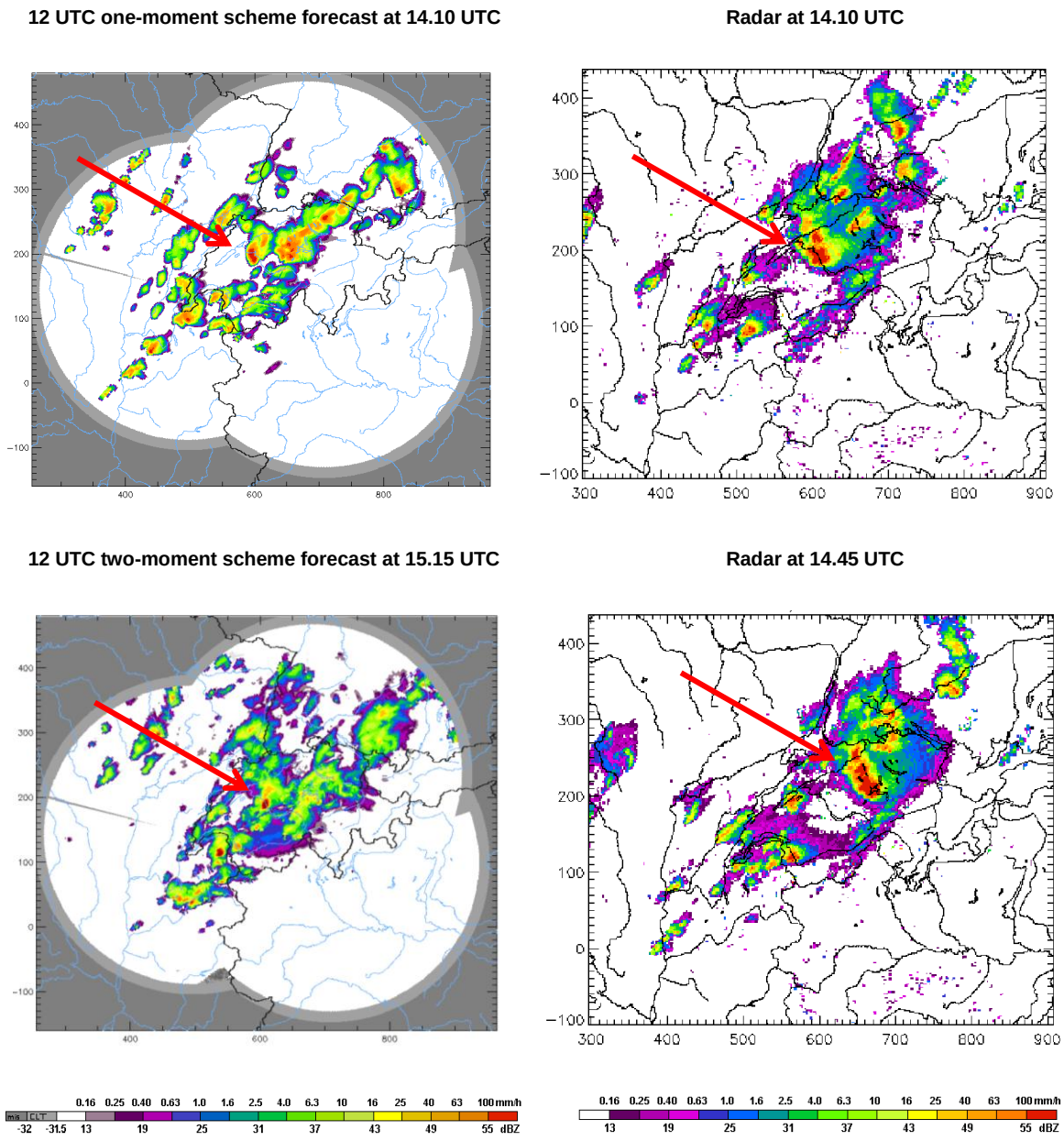

Figure 3.1.5: Maximum reflectivities (CZC product) [dBZ, mm/h] of the one-moment scheme 12 UTC forecast at 14.10 UTC (top left panel) and of the two-moment scheme 12 UTC forecast at 15.15 UTC (bottom left panel), as well as the corresponding radar derived maximum reflectivities (OMC product) at 14.10 UTC (top right panel) and at 14.45 UTC (bottom right panel). The midland cell is labeled with red arrows.

12 UTC forecasts maximum reflectivities: discussion

The investigations of the maximum reflectivities of the COSMO one- and two-moment scheme 12 UTC forecasts point out that both model forecasts simulate a midland cell with small spatial displacements. The COSMO two-moment scheme has

more problems to generate the midland cell. A second cell is simulated from Geneva to the Lake of Constance while the first dissipates. The midland (second) cell in the two-moment scheme looks smaller in terms of geographical extension than the corresponding cell in the one-moment scheme 12 UTC forecast. The temporal displacement of the cell in the COSMO one moment scheme is negligible whereas the temporal displacement is about one hour in the two-moment scheme 12 UTC forecast. Further investigations show that the cells in both schemes lose their high reflectivity values faster than it was observed with the radar measurements. The high 24h total precipitation sums between Zurich and the lake of Constance are not the result of the investigated midland cells but a result of additional cells which are simulated over this region after the investigated midland cells cross this area. This means together that the simulated midland cells are more short-lived in comparison with the measured cells by the radar. But for all that, the maximum reflectivities of the entire day are in good agreement with the corresponding total precipitation plots, not in terms of their quantities of precipitation at the ground, but in terms of the location where the reflectivities are simulated.

3.1.2.3. Vertical Structures and 3-dimensional Reflectivities

COSMO one-moment microphysical scheme 12 UTC forecast: data

Figure 3.1.6 shows different vertical cross section products of the COSMO one-moment scheme 12 UTC forecast, as well as radar data in a south-north cut around Berne at 14.10 UTC. When considering the vertical cross section of the synthetic reflectivities (bottom left panel), it can be seen that high reflectivity values above 55 dBZ are simulated up to 2 km altitude and are close to the ground. The corresponding radar data (Figure 3.1.6, bottom right panel) shows the same reflectivity values up to 11 km. Lower reflectivity values such as the 45 dBZ (yellow category) are simulated up to approximately 5 km altitude, whereas radar measurements shows these reflectivities up to 12 km or even higher (not visible). The red core in the vertical cross section of reflectivity of the COSMO one-moment scheme 12 UTC forecast has a horizontal extent of approximately 15 km, whereas the radar red core has a horizontal extent of approximately 23 km. It is clearly visible that no reflectivities are simulated above 6 km height. The vertical cross section of hydrometeor densities (top left panel) shows graupel up to 8 km height. The high reflectivity values correspond with the region of intense rainfall. The

vertical wind field of the one-moment scheme 12 UTC forecast shows correspondence between the maximum vertical extent of graupel and the updrafts (red shaded colors) as well as between the most intense rainfall and the downdrafts (blue shaded colors).

The simulated VIL at 14.10 UTC (Figure 3.1.7, left) shows maximum values up to 20 kg/m^2. The corresponding radar derived VIL (Figure 3.1.7, right) of July 23, 2009, 14.10 UTC shows maximum VIL values up to 70 kg/m^2 and a much higher geographical extension of the lowest VIL class (5-10 kg/m^2).

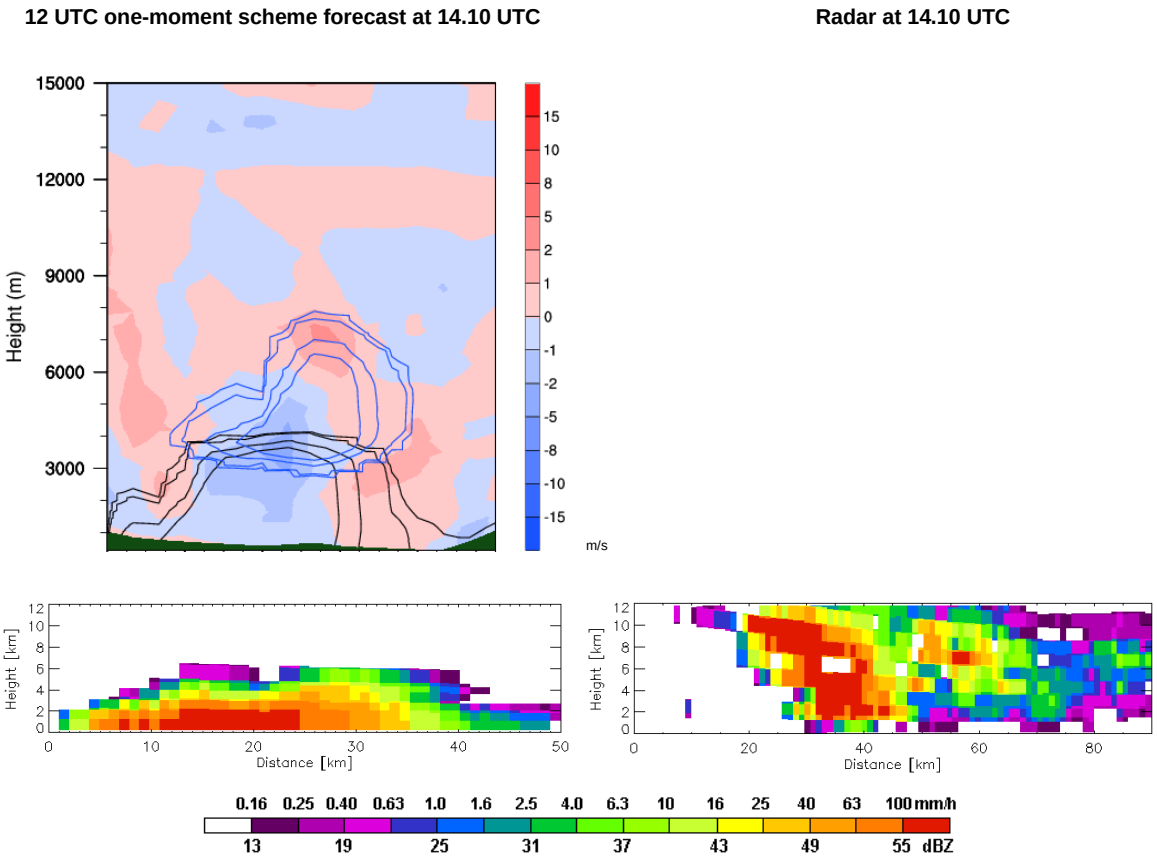

Figure 3.1.6: Top left panel: Vertical cross section of hydrometeor densities [kg/kg air] of the COSMO one-moment scheme 12 UTC forecast at 14.10 UTC with rain (black contour) and graupel (blue contour), along the same distance as in the bottom left panel near Berne. The dark green area is the topography. The scale of the contours is as follows: 0.00005, 0.0001, 0.0005, 0.001, 0.005, 0.01, 0.05, 0.1 [kg/kg air]. Bottom left panel: Vertical cross section of synthetic reflectivity [dBZ, mm/h] of the COSMO one-moment scheme 12 UTC forecast at 14.10 UTC near Berne. Bottom right panel: Vertical cross section of reflectivity [dBZ, mm/h] of the radar (OYC) at 14.10 UTC near Berne. The x-axis of the vertical cross sections of reflectivity shows the extension of the cross section [km].

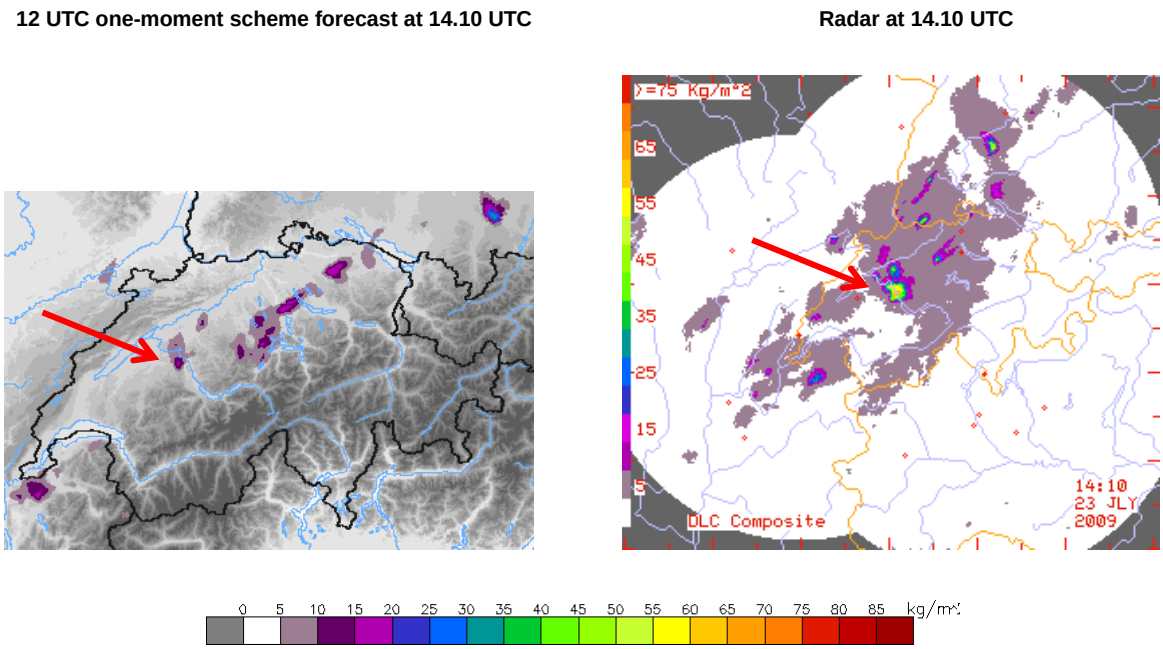

Figure 3.1.7: Left panel: VIL [kg/m²] of the COSMO one-moment scheme 12 UTC forecast at 14.10 UTC. Right panel: VIL [kg/m²] derived from radar data at 14.10 UTC. The midland cell is labeled with red arrows.

COSMO two-moment microphysical scheme 12 UTC forecast: data

The vertical structure and the VIL values of the COSMO two-moment scheme 12 UTC forecast can be seen in Figure 3.1.8 and Figure 3.1.9, respectively. Only the second midland cell is considered because the first cell did not show similar convective structures. High reflectivities above 55 dBZ are simulated from to ground to 4 km height. This high reflectivity core has a horizontal extent of approximately 20 km. The radar data shows values above 55 dBZ up to 11 km. This core has a horizontal extent of approximately 23 km. The vertical extent of the red core is approximately 4 km. The 45 dBZ values are simulates up to 6 km above the ground. The vertical cross section of hydrometeor densities of (Figure 3.1.8, top left panel) shows snow and graupel up to 11 km, hail up to 8 km and rain up to 7 km altitude. The vertical wind (Figure 3.1.8, top right panel) shows the hail cores (light blue contour) where the updrafts (red shaded colors) are simulated and where the rain contours (black) reach their maximum altitude. The up and down drafts are stronger in the COSMO two-moment scheme 12 UTC forecast as in the COSMO one-moment scheme forecast.

The simulated VIL of the COSMO two-moment scheme 12 UTC forecast at 15.10 UTC (Figure 3.1.9, left) shows maximum of about 25 kg/m². The radar derived maximum VIL (Figure 3.1.9, right) reaches values up to 70 kg/m².

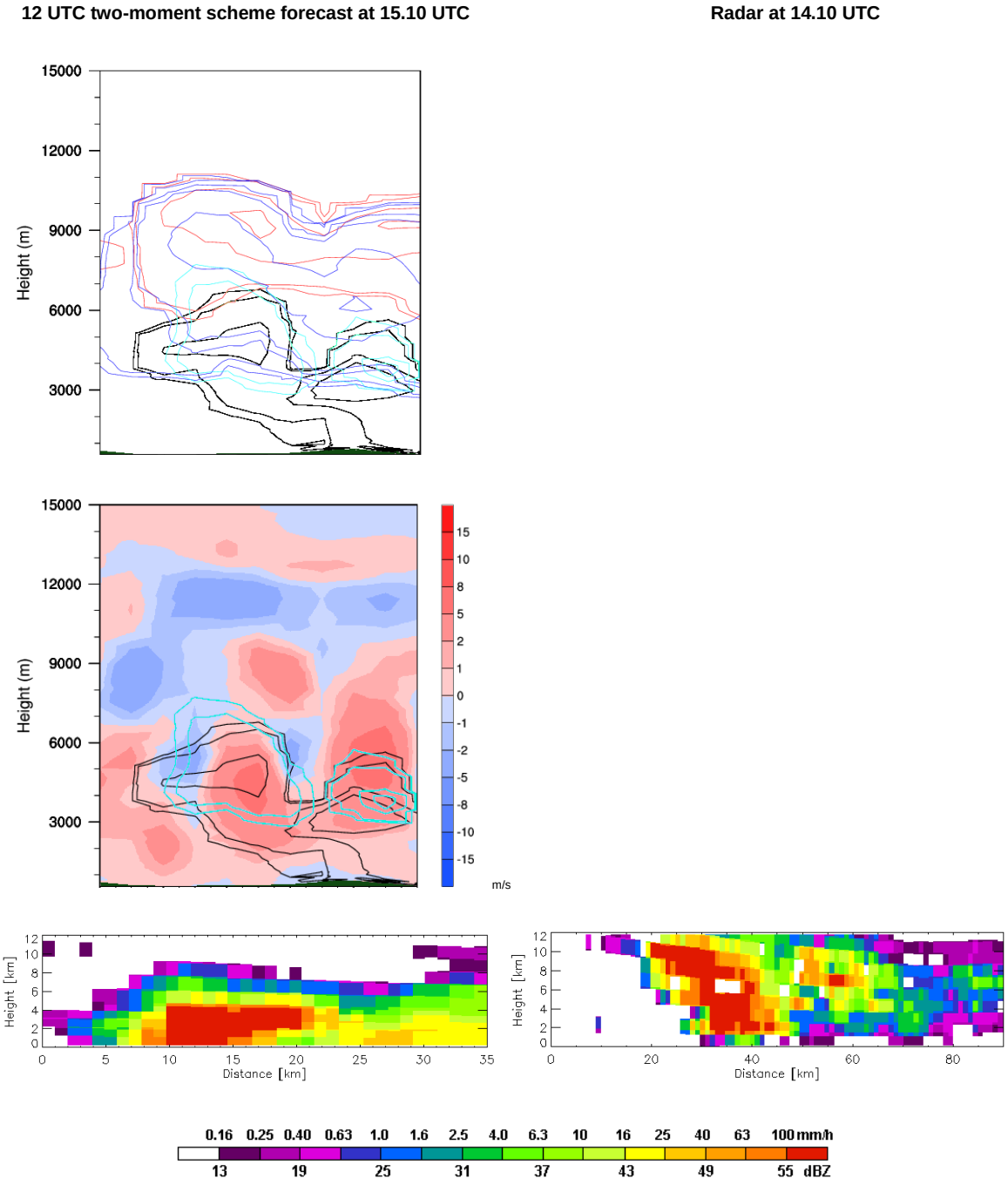

Figure 3.1.8: Top left panel: Vertical cross section of hydrometeor densities [kg/kg air] of the COSMO two-moment scheme 12 UTC forecast at 15.10 UTC with rain (black contour), snow (red contour), graupel (blue contour), and hail (cyan contour). Middle left panel: Vertical cross section of hydrometeor densities [kg/kg air] of the COSMO two-moment scheme 12 UTC forecast at 15.10 UTC with rain (black contour) and hail (cyan contour), as well as vertical winds [m/s] (shaded). Both vertical cross sections of hydrometeor densities are along the same distance as in the bottom left panel near Berne. The dark green area is the topography. The scale of the contours is as follows: 0.00005, 0.0001, 0.0005, 0.001, 0.005, 0.01, 0.05, 0.1 [kg/kg air]. Bottom left panel: Vertical cross section of synthetic reflectivity [dBZ, mm/h] of the COSMO two-moment scheme 12 UTC forecast at 15.10 UTC near Berne. Bottom right panel: Vertical cross section of reflectivity [dBZ, mm/h] of the radar (OYC) at 14.10 UTC near Berne. The x-axis of the vertical cross sections of reflectivity shows the extension of the cross section [km].

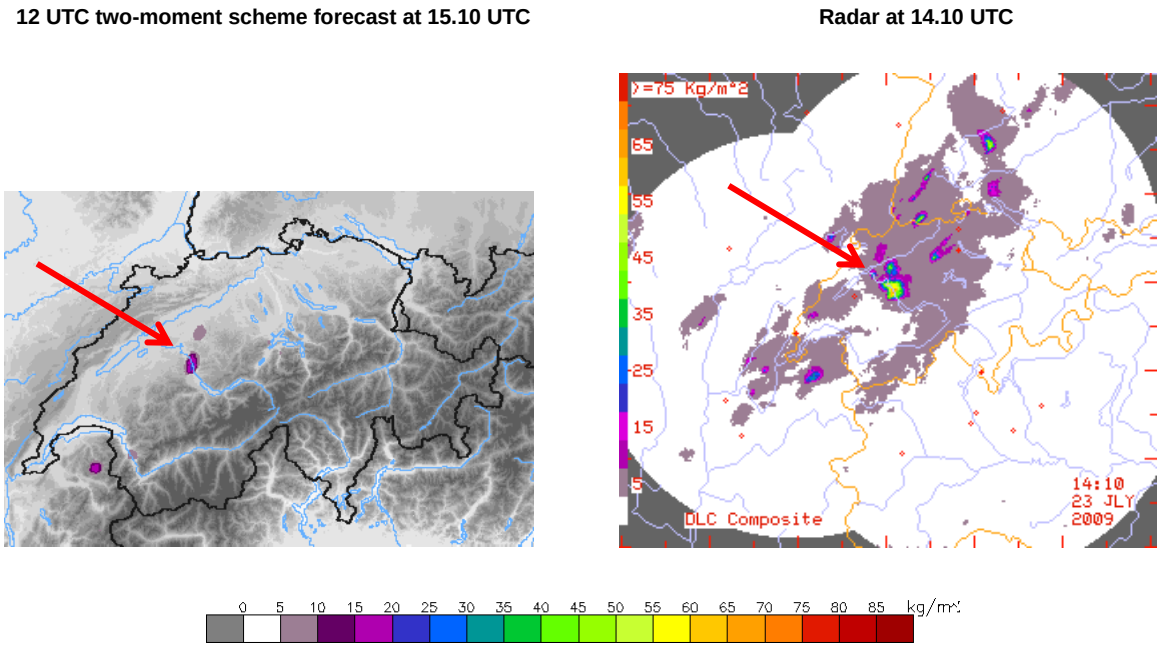

Figure 3.1.9: Left panel: VIL [kg/m²] of the COSMO two-moment scheme 12 UTC forecast at 15.10 UTC. Right panel: VIL [kg/m²] derived from radar data at 14.10 UTC. The midland cell is labeled with red arrows.

12 UTC forecasts, vertical structures and 3-dimensional reflectivities: discussion

The vertical cross sections of reflectivity of the COSMO one- and two-moment scheme 12 UTC forecasts show that the is capable to simulate high reflectivity cores with values above 55 dBZ. There are however distinctive differences between the model simulations and the radar data.

The radar shows maximum reflectivities between 2 and 11 km above the ground. Both model forecasts simulate maximum reflectivity cores much closer to the ground. The vertical extents of the maximum reflectivities of both simulations look however much lower than the vertical extend in the radar data. The COSMO two-moments scheme 12 UTC forecast simulates slightly better results in terms of the vertical extend of the 55 dBZ core as well as of the lower reflectivities.

These differences in the vertical extent between the two schemes can be explained with the different parameterizations of rain, snow, graupel and hail. The COSMO one-moment scheme includes an exponential size distribution of graupel, which probably tends to produce too small graupel particles and therefore, the simulated too small graupel particles generates too low synthetic reflectivities due to the D^6 dependency (see equation (3); Blahak 2012). In addition, a relatively low density of graupel (400kg/m³) is assumed (Blahak, 2012). These two reasons may at least in

parts explain the underestimation of the synthetic reflectivities of graupel and therefore the vertical extent of synthetic reflectivity values of the COSMO one-moment scheme.

Another remarkable feature of the one-moment forecast is the simulated high reflectivity core (red) close to the ground. Looking at the vertical cross section of the hydrometeor densities (Figure 3.1.6), it can be recognized that these high reflectivities are due to heavy precipitation. These high reflectivity values cannot be seen in the radar measurements. Because of the assumed particle size distribution of rain in the one-moment scheme, it is possible that for heavy precipitation events too many large rain drops with diameters larger than 5mm are simulated, which in reality break up into smaller droplets. This may lead to a systematic overestimation of simulated reflectivities in case of heavy rainfall (Blahak, 2012). Despite this possible systematic overestimation of simulated reflectivities for heavy rain, the model does not overestimate the amount of rain for this cell. From the 24h total precipitation plots (Figure 3.1.3) we know that the total precipitation amounts are to about fourth of the radar detected of the midland cell around Berne. Considering all the above, we can state that the one-moment scheme, which only simulates rain, snow and graupel as precipitating hydrometeors, cannot realistically describe the vertical (hydrometeor-) structure of the hailstorm in terms of reflectivities, and in our case probably overestimates the amount of the rain category close to the ground and underestimates the amount of snow and graupel (which are needed to describe the snow, graupel, and hail species). Due to the missing hail class and the special mass-size distribution of the one-moment scheme, the vertical structure and the synthetic radar based VIL content are different in comparison with radar data. The synthetic radar based VIL is underestimated by more than a factor of 3.

In the COSMO two-moment scheme 12 UTC forecast, reflectivities are simulated up to 9 km altitude. Even the graupel and snow classes lead to some reflectivities when using the RFO. This is not the case for the one-moment scheme. Further, a clear correlation of hail and rain with the updraft region of the COSMO two-moment scheme 12 UTC forecast is visible. The same is expected for real storms in nature.

In terms of the horizontal extent the differences between the model forecasts and the radar measurements are not as pronounced as the differences in the vertical.

The COSMO two-moment scheme 12 UTC forecast shows better VIL values and vertical structures as the one-moment scheme, but does not reach the same intensity in terms of surface precipitation and VIL as well as not in terms of the vertical structure, when compare them with the radar data. The reasons for that are unknown at this point. When considering the reflectivities in the vertical with the vertical cross section of hydrometeor densities, we still see an underestimation of reflectivities where the model only simulated graupel and snow. The low reflectivity values are what can be expected when considering graupel and snow properties in terms of their backscattering ability. Therefore, the COSMO two-moment scheme 12 UTC forecast seems to simulate more realistic reflectivities but is still not able to simulate what we observe in radar data.

3.1.2.4. Hail Detection Algorithms

COSMO one-moment microphysical scheme 12 UTC forecast: data

The synthetic daily maximum POH product of the COSMO one-moment scheme 12 UTC forecast (Figure 3.1.10, top left panel) displays a straight hail swath (as defined by the POH algorithm) from Geneva to the Lake of Constance with a short interruption around the area of Berne. This is due to the low altitude of the maximum reflectivities around Berne, whereas lower reflectivities in higher altitudes are simulated before and after the cell crosses Berne and therefore produces higher POH values. Another hail swath is visible from the Lake of Thun to the Lake of Constance. Values up to 100% probability are reached. On the right side of Figure 3.1.10 the corresponding radar derived daily maximum POH plot is shown. In general, higher POH values are detected in reality.

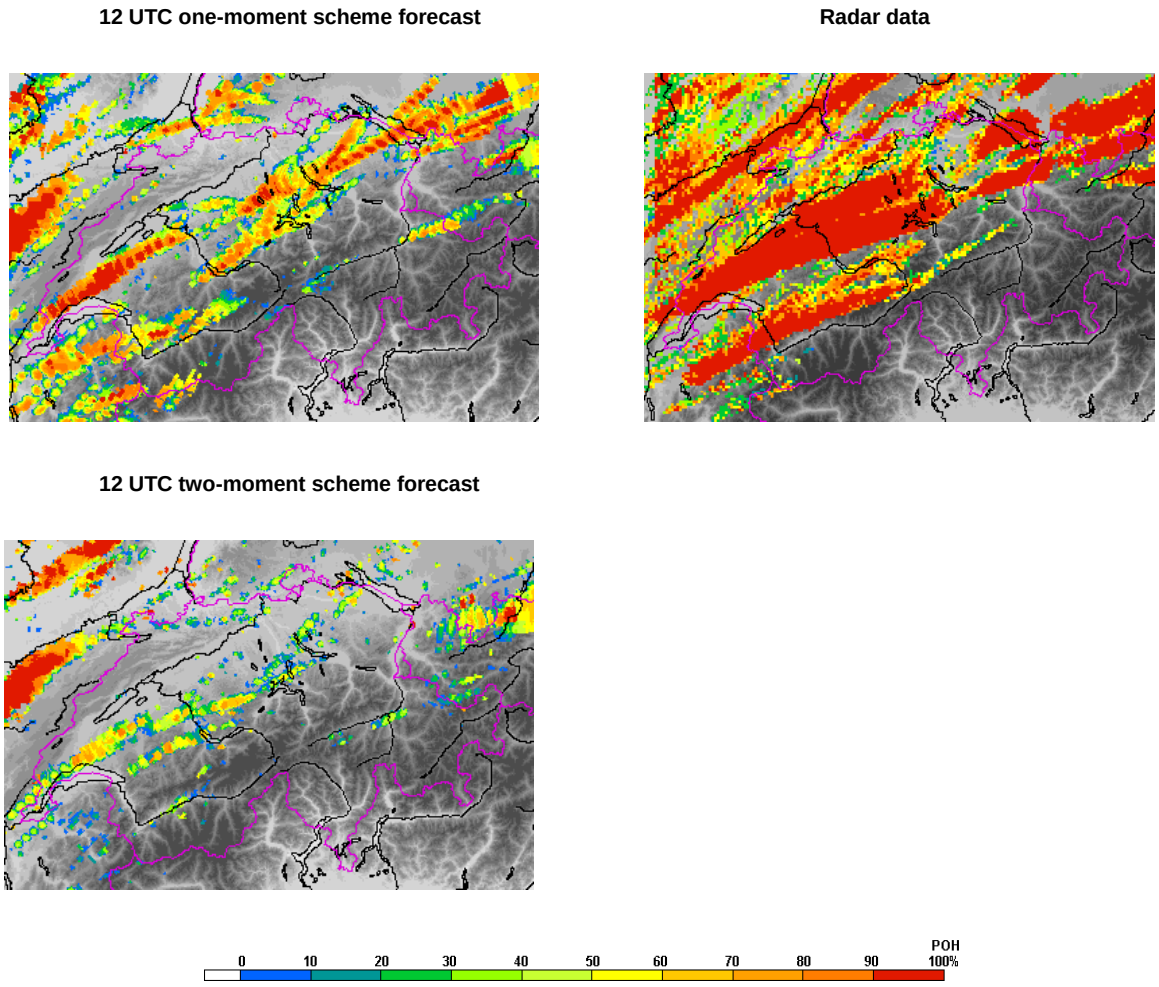

Figure 3.1.10: Top left panel: Synthetic daily maximum POH product [%] of July 23, 2009, of the COSMO one-moment scheme 12 UTC forecast. Bottom left panel: Synthetic daily maximum POH product [%] of July 23, 2009, of the COSMO two-moment scheme 12 UTC forecast. Top right panel: Daily maximum POH product [%] of the radar.

The Probability of Detection (POD) of the synthetic daily maximum POH product for the one-moment scheme 12 UTC forecast of July 23, 2009, is a first calculation and should give evidence about the quality of the synthetic POH product. A POD of around 90% was determined. The radar derived POD for the daily maximum POH product is 99% with a False Alarm Rate (FAR) of 11%. The FAR of the COSMO one-moment scheme 12 UTC forecast is of the same quantity. Figure 3.1.11 shows the synthetic daily maximum POH product of the COSMO one-moment scheme 12 UTC forecast (top) together with the ground truth verification data[2] in Google Earth and gives a good impression about the quality of the product.

The implemented MESHS algorithm for the COSMO one-moment scheme 12 UTC forecast does not show any MESHS values above 2 cm. The radar derived daily

[2] SHVDB09 (Swiss Hail Verification Data Base 2009)

maximum MESHS pot on the other hand shows two hail swaths, one from Geneva to Lucerne and another over the Alps of Valais and Bernese Oberland with MESHS values above 6 cm diameter (not shown).

COSMO two-moment microphysical scheme 12 UTC forecast: data

Figure 3.1.10 (bottom left panel) shows the daily maximum POH plot of the COSMO two-moment scheme 12 UTC forecast and the corresponding radar measurement (top right panel). A small hail swath (as defined by the POH algorithm) is visible from Geneva to Lucerne. The differences in terms of the geographical extension and the quantitative values between the simulation and the radar data are obvious. Maximum POH values below 90 % are simulated whereas in reality almost all values are above 90%.

No MESHS values above 2 cm are visible when considering the daily maximum MESHS plot of the COSMO two-moment scheme 12 UTC forecast (not shown).

The synthetic POD is determined as 55 %. The corresponding radar derived POD of the daily maximum POH plot of July 23, 2009 was determined as 99% with a FAR of 11 %. No FAR can be determined due to the small POH area, where ground truth observations can be found for every POH value. Figure 3.1.11 shows the synthetic daily maximum POH product of the COSMO two-moment scheme 12 UTC forecast (bottom) together with the ground truth verification data in Google Earth.

12 UTC one-moment scheme forecast

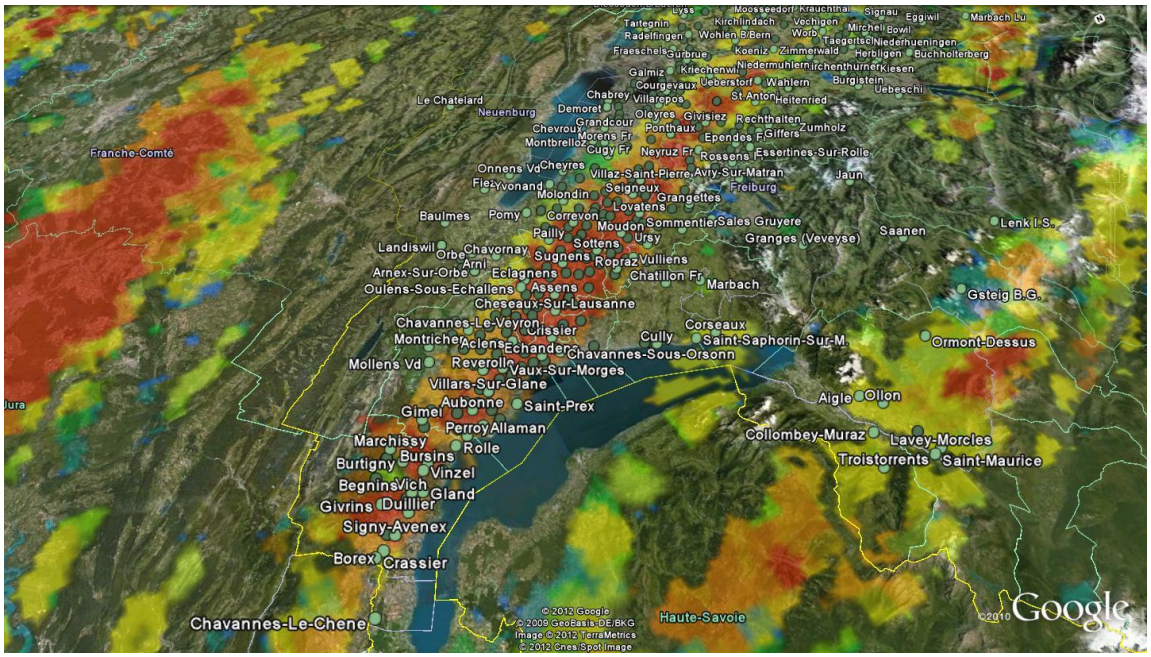

12 UTC two-moment scheme forecast

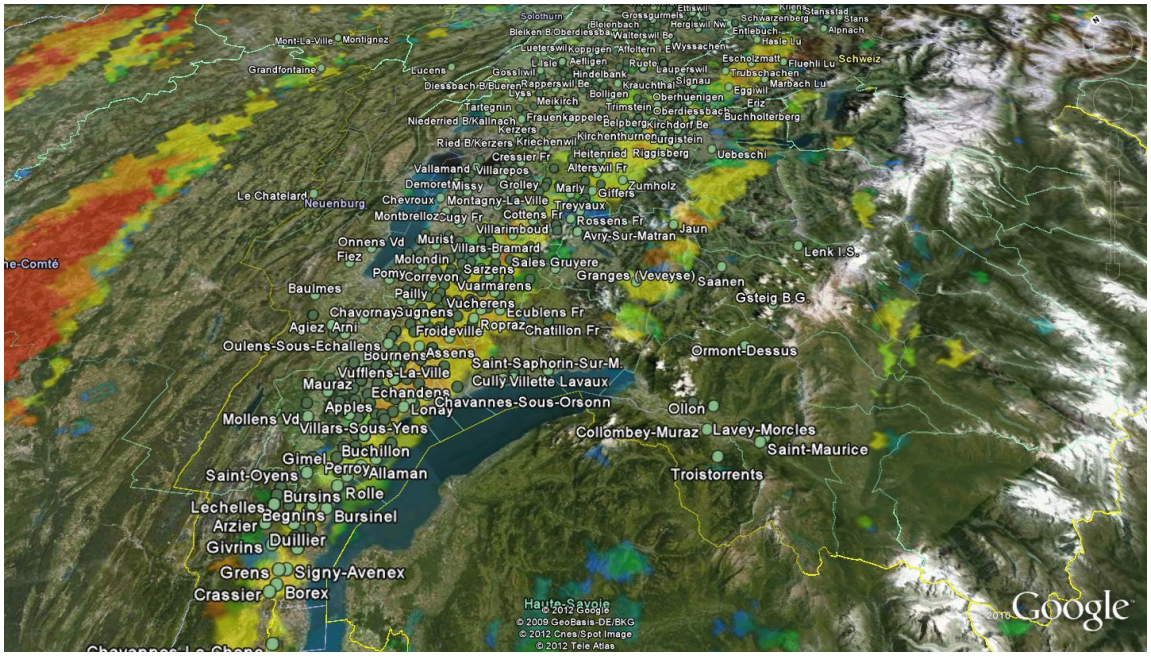

Figure 3.1.11: Synthetic daily maximum POH product (shaded) of the COSMO one-moment scheme 12 UTC forecast (top) and of the COSMO two-moment scheme 12 UTC forecast (bottom), with ground truth data (green circles) of the SHVDB09[3] of July 23, 2009, in Google Earth near the Lake of Geneva. The color shading shows the left side panels of Figure 3.1.10, adapted for Google Earth.

[3] Swiss Hail Verification Data Base 2009

12 UTC free forecasts, hail detection: discussion

The investigations with the applied POH and MESHS algorithm show that the one-moment scheme 12 UTC forecast is able to simulate hail (as defined by the POH algorithm) at least for some areas where hail was observed in reality. The POD is however not as high as for the corresponding radar derived POH product. The COSMO two-moment scheme was able to simulate POH values, but less than the one-moment scheme and with much lower probability values. The low POD value of the COSMO two-moment scheme approves this finding. The reasons for that are not clear. One reason might be that the zero degree height (H_0) is different in the two parameterization schemes and therefore different POH values are simulated. Another reason might be that the COSMO two-moment scheme does not simulate sufficient large graupel and snow particles and therefore lower reflectivities are simulated in the height. These lower reflectivities produces than lower POD values. For a concluding statement, more research is necessary.

Both schemes are not able to simulate any MESHS values above 2 cm in forecast mode. The reason for this is the fact that high reflectivity values ($\geq$ 51 dBZ) are simulated at high altitudes.

Together with the investigations above, the 12 UTC forecasts show some good results in terms of spatial and temporal simulation of the most severe convective cells, especially for the one-moment scheme. However, there are some clear limitations when considering the vertical structure of the hailstorms, such as the missing high reflectivity values at high altitudes, too high reflectivity values directly above the ground and too low simulated reflectivity-based VIL values. In general, the cells are mostly not intense enough and too short lived. In radar measurements, the cells are larger, more intense, and 'live' longer.

3.1.3. Analysis Cycles

The analyses of the COSMO one- and two-moment scheme are further investigated with the aim (or hope) that the LHN forces the model towards the right intensities of surface precipitation and we than can compare the cell characteristics of the analyses with the forecasts. Two time intervals are investigated. First, the time around 13.00 UTC, when the radar measured an intensification of the midland cell around Geneva, is investigated for both schemes. Second, the cells are analyzed

during its maximum intensity at 14.45 UTC, in order to see how the vertical structures look like when using the LHN in the one- and two-moment scheme.

In general, the surface precipitation plots of both analysis schemes (Figure 3.1.12) show different patterns in terms of the geographical extend and the amplitudes in comparison with the 12 UTC forecasts. While the amplitudes of the surface precipitation in both schemes reach similar values as seen in the radar data, the geographical extension of the heavy precipitation bands look different in both schemes. Swaths from Geneva to Lucerne (midland cell), as seen in the radar data, is totally missing in the 24h sum of precipitation plots in both analyses. Therefore, the time step at 13.00 UTC, when the midland cell was intensified in the radar data is investigated in order to find out why the model runs do not simulate this surface precipitation swath from Geneva to Lucerne when running them in the assimilation mode.

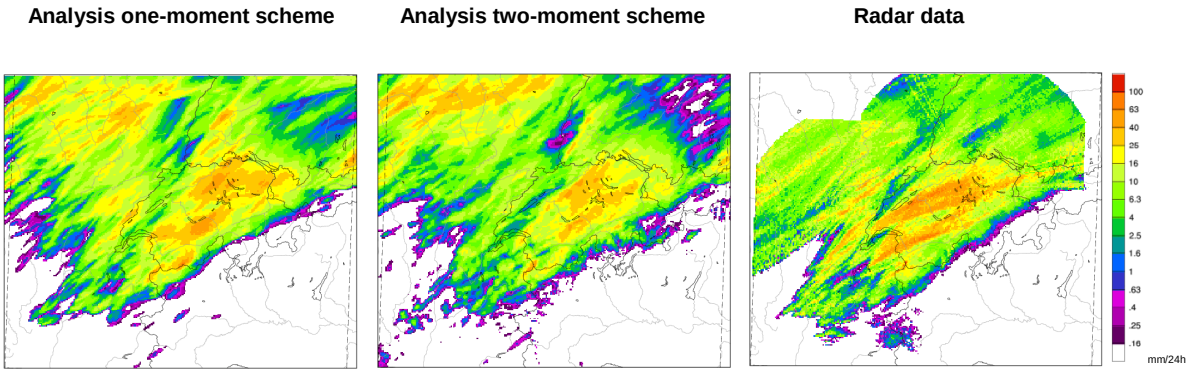

Figure 3.1.12: 24h precipitation sum (shaded) [mm/24h] of the COSMO one-moment analysis cycle (left), two-moment scheme analysis cycle (middle), and the radar measurements (PKC product, right) for July 23, 2009. Black solid lines are international borders and lakes, grey lines are rivers and coast lines, and the dashed lines indicate the radar domain.

3.1.3.1. Analyses Cycles during the Intensification Time Period around 13 UTC

Analysis cycle at 13 UTC of the COSMO one-moment scheme: data

Figure 3.1.13 shows the maximum reflectivities at 12.55 UTC of the COSMO one-moment scheme analysis cycle (top left panel) and the corresponding radar measurement (top right panel). In both plots, a cell is visible north of Geneva, slightly upstream of the La Dôle radar. The simulation (right) shows higher reflectivities below 55 dBZ, whereas the radar detected values up to 55 dBZ. The simulation overestimates the cell also in its geographical extension.

Figure 3.1.13 illustrates the midland cell 25 minutes later at 13.20 UTC of the COSMO one-moment scheme analysis cycle (bottom left panel) and the corresponding radar data (bottom right panel). While the cell reaches high maximum reflectivity values above 55 dBZ, the model simulates only weak reflectivities for this time step.

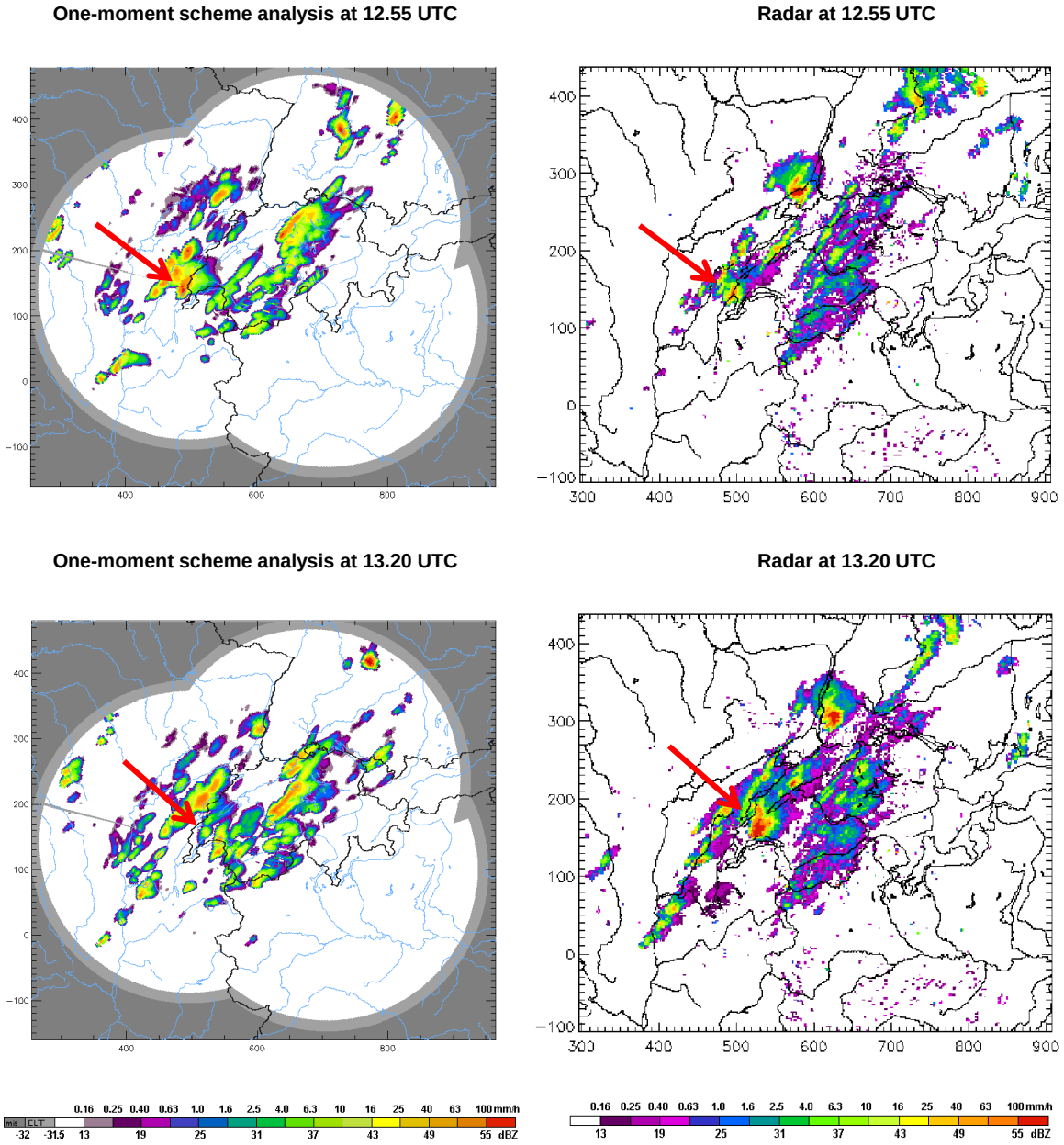

Figure 3.1.13: Maximum reflectivities (CZC product) [dBZ, mm/h] of the one-moment analysis cycle at 12.55 UTC (top left panel) and at 13.20 UTC (bottom left panel), as well as the corresponding radar derived maximum reflectivities (OMC product) at 12.55 UTC (top right panel) and at 13.20 UTC (bottom right panel). The midland cell is labeled with red arrows.

Vertical cross sections of hydrometeors of the one-moment scheme analysis cycle are depicted in Figure 3.1.14 and Figure 3.1.15 for the time period around 13.00 UTC when the midland cell was growing fast in the radar data. Figure 3.1.14 shows a vertical cross of hydrometeor densities (top left panel) in south-north direction near Geneva close to the La Dôle radar at 12.50 UTC. Graupel and snow are seen up to 12 km above sea level. Eye-catching are the sharp increases in the vertical extension of graupel and snow from 9 to 12 km. A similar increase is also seen at 13.10 UTC in Figure 3.1.15 from 5 to 8 km and from 8 to 9 km.

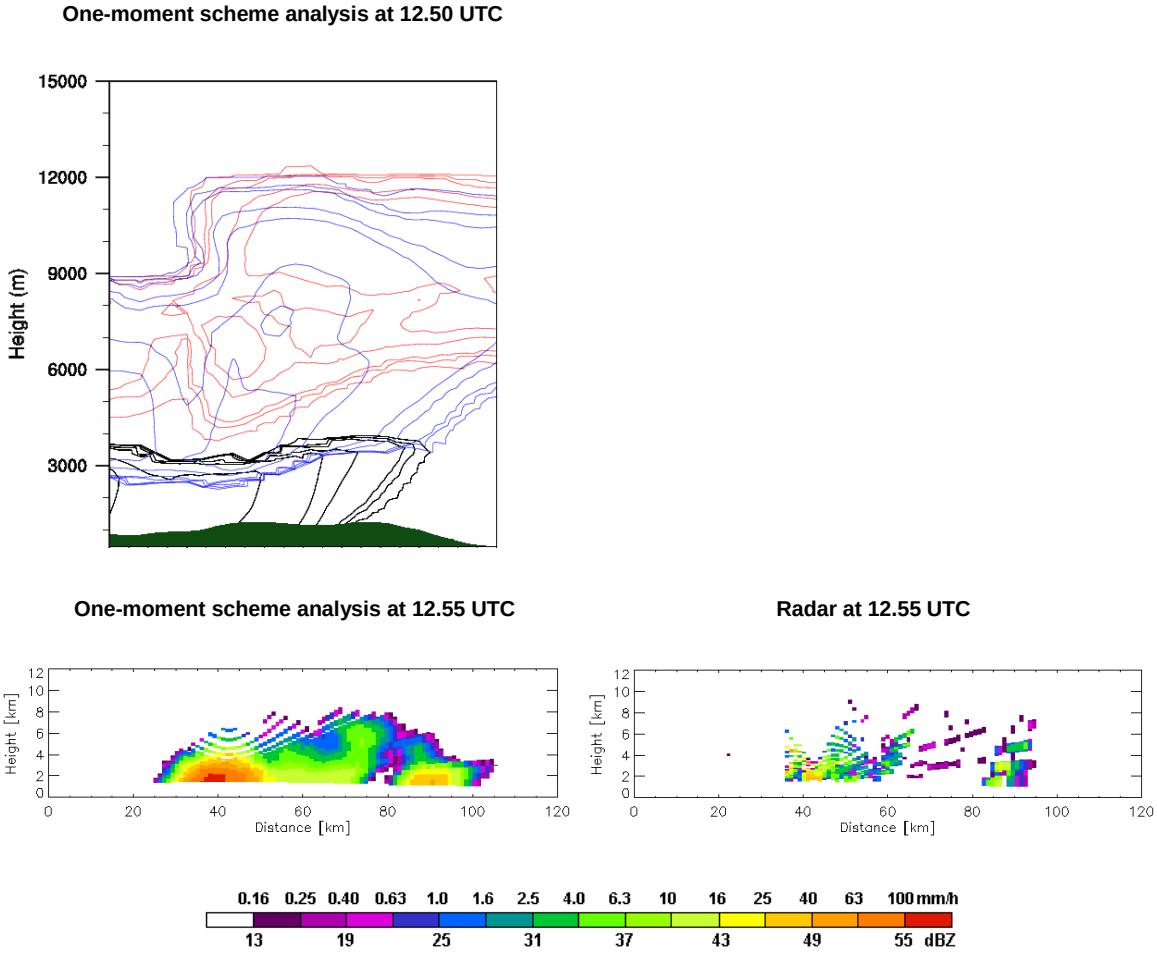

Figure 3.1.14: Top left panel: Vertical cross section of hydrometeor densities [kg/kg air] of the COSMO one-moment scheme analysis at 12.50 UTC with rain (black contour), graupel (blue contour), and snow (red contour), along the same distance as in the bottom left panel near Geneva close to the La Dôle radar. The dark green area is the topography. The scale of the contours is as follows: 0.00005, 0.0001, 0.0005, 0.001, 0.005, 0.01, 0.05, 0.1 [kg/kg air]. Bottom left panel: Vertical cross section of synthetic reflectivity [dBZ, mm/h] of the COSMO one-moment scheme analysis cycle at 12.55 UTC near Geneva close to the La Dôle radar. Bottom right panel: Vertical cross section of reflectivity [dBZ, mm/h] of the radar (OYC) at 12.55 UTC near Geneva close to the La Dôle radar. The x-axis of the vertical cross sections of reflectivity shows the extension of the cross section [km]. The La Dôle radar is approximately located at kilometer 40.

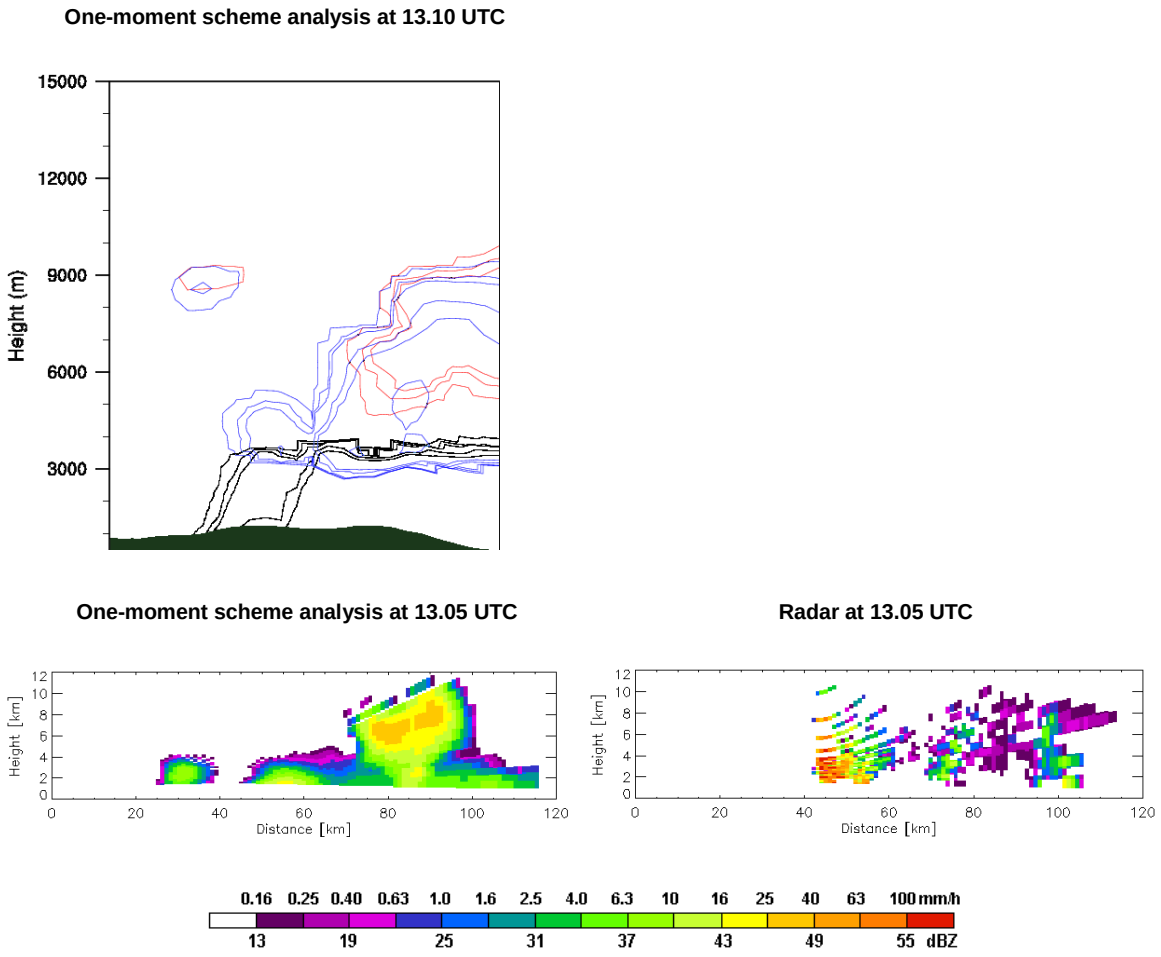

Figure 3.1.15: Top left panel: Vertical cross section of hydrometeor densities [kg/kg air] of the COSMO one-moment scheme analysis at 13.10 UTC with rain (black contour), graupel (blue contour), and snow (red contour), along the same distance as in the bottom left panel near Geneva close to the La Dôle radar. The dark green area is the topography. The scale of the contours is as follows: 0.00005, 0.0001, 0.0005, 0.001, 0.005, 0.01, 0.05, 0.1 [kg/kg air]. Bottom left panel: Vertical cross section of synthetic reflectivity [dBZ, mm/h] of the COSMO one-moment scheme analysis cycle at 13.05 UTC near Geneva close to the La Dôle radar. Bottom right panel: Vertical cross section of reflectivity [dBZ, mm/h] of the radar (OYC) at 13.05 UTC near Geneva close to the La Dôle radar. The x-axis of the vertical cross sections of reflectivity shows the extension of the cross section [km]. The La Dôle radar is approximately located at kilometer 40.

Figure 3.1.14 and Figure 3.1.15 show vertical cross sections for the midland cell north of Geneva. Because of slight displacements of the main cell between the radar measurements and the analysis cycle the time interval as well as the location has to be adapted for each cross section.

Figure 3.1.14 shows a vertical cross section of reflectivities of the La Dôle radar (bottom right panel) and synthetic reflectivities of the COSMO one-moment scheme analysis cycle (bottom left panel) at 12.55 UTC. The two plots look totally different. Apart from very few high-reflectivity pixels right above the radar, the La Dôle radar detected only weak reflectivities, whereas the synthetic product shows much more high-reflectivity pixels and a more realistic convective core. The missing reflectivity

values of the radar measurement are due to the location of the cell directly above the radar and therefore, the cell is not caught by the radar scan strategy. The model generates reflectivities above 46 dBZ (25 mm/h) up to 4 km above the ground. Above this height, much lower reflectivities are seen.

Figure 3.1.15 shows the vertical cross section of reflectivity of the La Dôle radar (bottom right panel) and of the analysis cycle (bottom left panel), respectively, at 13.05 UTC. Until 13.05 UTC, the cell moves along the vertical cross section line for both, model and radar data. In the analysis cycle, the midland cell gets weaker, high reflectivity values disappear altogether, and precipitation rates near the ground are at least one order of magnitude lower. At the same time, high precipitation rate values were detected above the La Dôle radar. The SHVDB09[4] shows that at this time hail was starting. This signal is totally missing in the COSMO generated reflectivities of the analysis cycle.

Analysis cycle at 13 UTC of the COSMO two-moment scheme: data

The COSMO two-moment scheme is investigated with the aim (or hope) that the LHN forces the model towards the right intensities of surface precipitation, we than can compare the cell characteristics of the analysis with the forecast and whether the same dissipation of the midland cell, as seen in the one-moment scheme, is seen in the two-moment scheme.

Maximum reflectivity plots of the COSMO two-moment scheme analysis cycle shows that the after 13.00 UTC the midland cell is not dissipated in terms of high reflectivity values. For the entire lifecycle from Geneva to Berne, high reflectivity values above 55 dBZ are visible (not shown).

Figure 3.1.16 shows the vertical cross section of hydrometeors of the COSMO two-moment scheme analysis cycle at 13.00 UTC. Graupel (blue contour) and snow (red contour) are simulated up to 13 km height. Between 3 km and approximately 7.5 km hail (cyan contour) is already simulated. When considering the same plots for the time beyond 13.00 UTC, the cell does not weaken in terms of the vertical extent, but in terms of the intensity (less contours).

[4] Swiss Hail Verification Data Base 2009

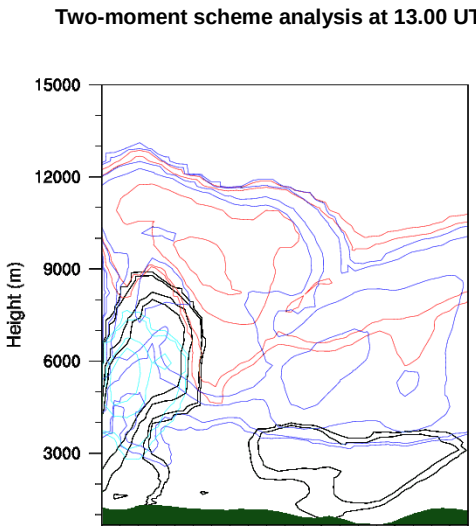

Figure 3.1.16: Vertical cross section of hydrometeor densities [kg/kg air] of the COSMO two-moment scheme analysis at 13.00 UTC with rain (black contour), snow (red contour), graupel (blue contour), and hail (cyan contour) near Geneva close to the La Dôle radar, along the same distance as in Figure 3.1.15 bottom left panel. The dark green area is the topography. The scale of the contours is as follows: 0.00005, 0.0001, 0.0005, 0.001, 0.005, 0.01, 0.05, 0.1 [kg/kg air].

Analysis cycles at 13 UTC of the COSMO analyses: discussion

The interpretation and comparison of the vertical structures of the COSMO one-moment and two-moment scheme analysis cycles at around 13.00 UTC suggests that the midland cell is suppressed when crossing over the La Dôle radar in the one-moment scheme but not in the two-moment scheme or at least not as much as in the one-moment scheme. Plots of the total precipitation amount differences (Figure 8.1.1, difference plots of the COSMO one-moment scheme) between the two parameterization schemes and the radar data from 13.00 UTC onwards confirm that the differences from the COSMO two-moment scheme analysis are around half of the amplitude as those of the COSMO one-moment scheme analysis. The reduction of the cell intensity and the vertical extent for the one-moment scheme analysis cycle can clearly be recognized when looking on the vertical cross sections of hydrometeors. The signal in the vertical cross sections of reflectivity of the radar data shows, that the cell was not detected directly above the La Dôle radar itself (Figure 3.1.14, bottom right panel). The simulated midland cell of the one-moment scheme seems to be overestimated before crossing the La Dôle radar (Figure 3.1.13, top left panel) and clearly suppressed five minutes later at 13.05 UTC (Figure 3.1.13, bottom left panel). When considering the differences plots between the simulations and the radar measurements (not shown), it seems to be obvious that the LHN forces

the model to reduce the intensity of the midland cell at the time when the cell is directly located over the La Dôle radar. Further investigations have shown, that the following two things plays an important role, for the poor performance of the one-moment analysis cycle in simulating the development of the cell in the vicinity of the La Dôle radar.

First, the model overestimates the intensity of the midland cell before 13.00 UTC. The same is the case for the two-moment analysis cycle but not that pronounced. Consequently, the LHN forces the simulation to reduce the surface precipitation rate by cooling the atmosphere and removing moisture. Second, the cell crosses directly above the La Dôle radar and therefore, the radar data do not show any reflectivities right above the radar due to the radar scan strategy. At the same time, the Albis radar shows only the reflectivity signals in high altitudes, what lead to lower corrected surface precipitation signals in the PKC products as measured with the La Dôle radar directly before. The second effect, which supports an underestimation of the effective surface precipitation by the radar (only around – 3 dBZ), is amplified due to radome attenuation when heavy precipitation hits the radar. Due to underestimation of the surface precipitation by the radar, the LHN forces the model to reduce the intensities even more. Putting both effects together, the LHN suppresses the midland cell too strongly and the cell (or the LHN, for that matter) needs more than hour to re-ingest the cell into the model after crossing the La Dôle radar.

The high total precipitation amounts of the radar (Figure 3.1.12, right panel) directly upstream of Geneva are not caused due to the midland cell but due to another cell which moved along the Jura mountains in France already before. The midland cell has its maximum intensities after crossing the La Dôle radar. It is a typical case where the time of the amplification in reality comes together at the location where the radar at this location does not detect any precipitation due to its scan strategy. The distance to the Albis radar is in this extreme case too far to capture the entire precipitation and to calculate the correct surface precipitation (PKC product). It might be that the radar assimilation quality function leads to an underestimation of the surface precipitation of extreme convective cases. In order to reduce such negative effects, this phenomenon should be investigated in more detail in future.

Therefore, it is surprising that the COSMO two-moment scheme analysis cycle does not show the signal of the suppressing as much as the one-moment scheme. That could be (as speculation) due to the better simulation of the vertical structure as seen in Figure 3.1.16. As speculation it can be note that the two-moment scheme needs more time to react to the forcing of the LHN due to the more sophisticated number-size and mass-size distribution of the hydrometeors and the additional hail category. Therefore, the model needs longer to lose the hydrometeor mass and to reduce the vertical extent. The five to ten minutes while the midland cell crosses the radar shadow over the La Dôle radar seems to be not enough to close down the cell. We only observe a temporal reduction of the maximum reflectivities.

Another speculative reason might be that due to the lower overestimation of the surface precipitation upstream of the La Dôle radar, the LHN does not force the model to less surface precipitation as it is done in the COSMO one-moment scheme analysis and therefore, the model does not react as pronounced as in the one-moment scheme.

3.1.3.2. Analyses Cycles at Maximum Intensity 14.45 UTC

The maximum reflectivities of the COSMO one- and two-moment scheme analyses can be seen in Figure 3.1.17 (left side panels). In both analyses the maximum intensity is simulated at 14.45 UTC near Lucerne and is in good agreement with the radar measurements in terms of time and space, which is of course a (wanted) consequence of the LHN. Vertical cross sections for the analyses of the COSMO one- and two-moment scheme are investigated for the time and location of maximum intensity.

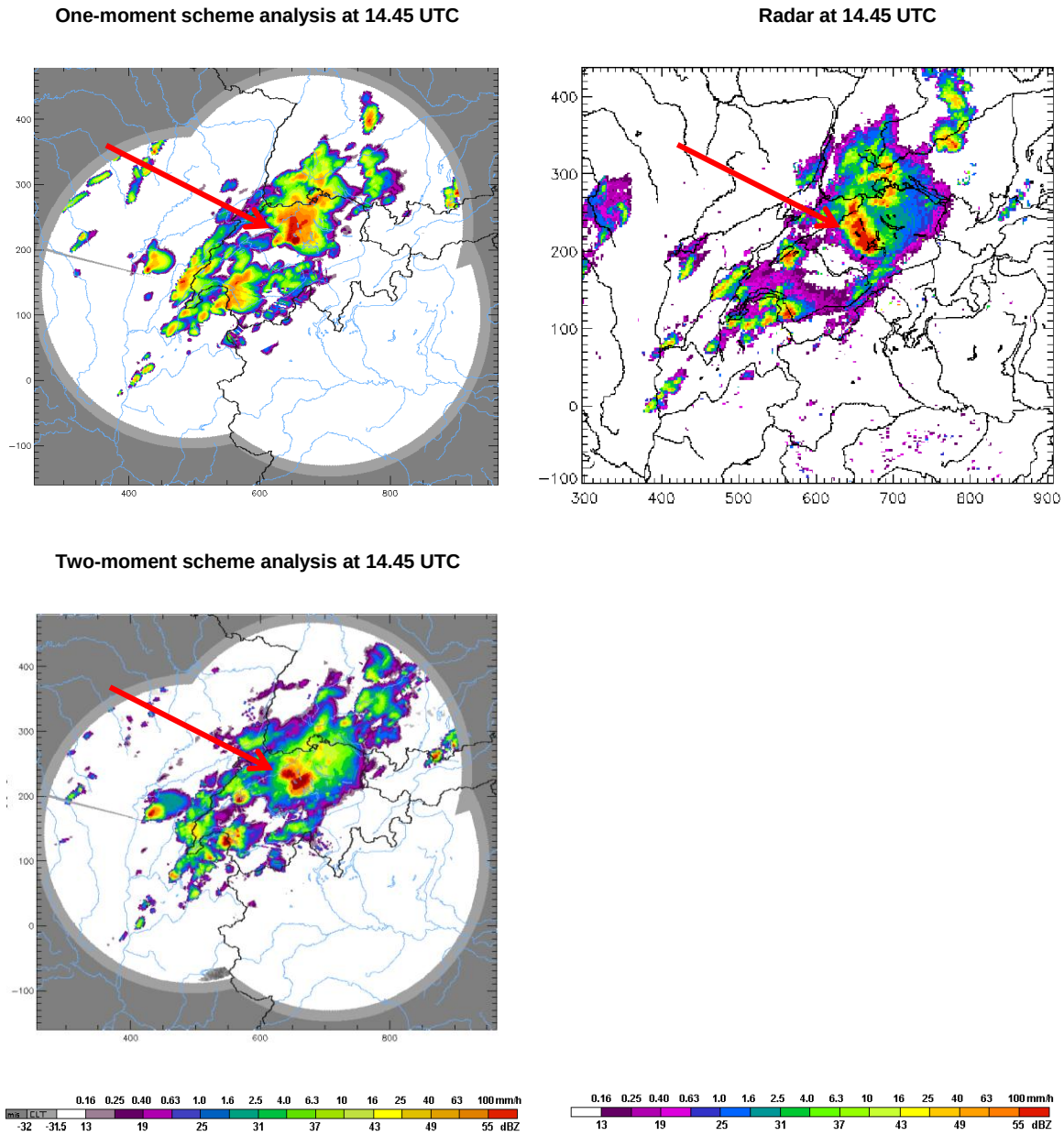

Figure 3.1.17: Maximum reflectivities (CZC product) [dBZ, mm/h] of the one-moment scheme analysis at 14.45 UTC (top left panel) and of the two-moment scheme analysis at 14.45 UTC (bottom left panel), as well as the corresponding radar derived maximum reflectivities (OMC product) at 14.45 UTC (top right panel). The midland cell is labeled with red arrows.

Vertical structures of the COSMO one-moment scheme analysis cycle at 14.45 UTC: data

Figure 3.1.18 shows the vertical cross sections of reflectivity (bottom left panel) and hydrometeor densities (top left panel), respectively, at 14.45 UTC of the COSMO one-moment scheme analysis cycle. High reflectivity values above 55 dBZ are simulated up to 5 km altitude. The 49 dBZ values are simulated up to 12 km height or even higher. A two core structure is visible but only the left core has reflectivities

above 55 dBZ. The corresponding radar measurement (bottom right panel) shows high reflectivity values above 55 dBZ up to 8 km with maximum altitudes for the 49 dBZ values above 12 km. Considering the hydrometeor density plot, rain is simulated up to approximately 7 km altitude (super-cooled water). Snow and graupel are simulated up to 15 km height.

The VIL of the COSMO one-moment scheme analysis cycle at 14.45 UTC (Figure 3.1.20, top left panel) shows maximum values up to 45 kg/m^2, whereas the radar derived VIL (Figure 3.1.20, bottom middle panel) shows maximum quantities of 60 kg/m^2. The area of values ≥ 5 kg/m^2 in the radar data is larger than the area in the analysis at 14.50 UTC

Vertical structures of the COSMO two-moment scheme analysis cycle at 14.45 UTC: data

Comparing the vertical cross section of reflectivities of the COSMO two-moment scheme analysis cycle at 14.45 UTC (Figure 3.1.19, bottom left panel), when the cell reaches the maximum intensity, and the corresponding radar derived reflectivities (Figure 3.1.19, bottom right panel) with each other, similar structures can be recognized. The COSMO two-moment scheme analysis cycle simulates high reflectivity values up to approximately 10 km altitude. The radar data shows the same quantity up to 8 km above the ground. Red and orange pixels are simulated where hail occurs when considering the vertical cross section of hydrometeors densities (Figure 3.1.19, top left panel). The hydrometeor density plot shows simulated rain up to 9 km, hail up to 11 km, and snow and graupel up to 14 km.

Maximum VIL values of 56 kg/m^2 are simulated with the forced model (Figure 3.1.20, top right panel) whereas 60 kg/m^2 were measured by the radar (Figure 3.1.20, bottom middle panel). The area of values between 5 and 10 kg/m^2 is smaller in the analysis cycle than in the radar data.

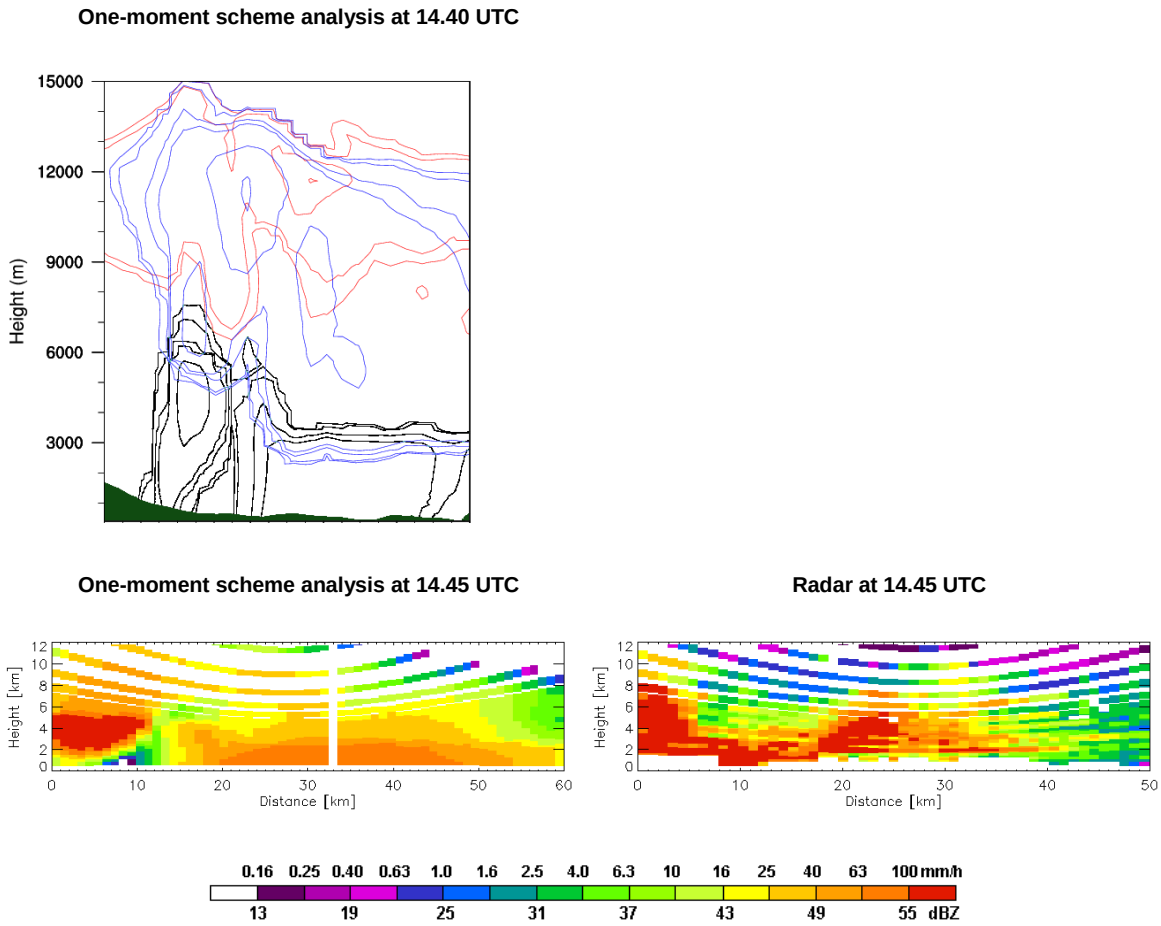

Figure 3.1.18: Top left panel: Vertical cross section of hydrometeor densities [kg/kg air] of the COSMO one-moment scheme analysis at 14.40 UTC with rain (black contour), graupel (blue contour), and snow (red contour), along the same distance as in the bottom left panel near Lucerne. The dark green area is the topography. The scale of the contours is as follows: 0.00005, 0.0001, 0.0005, 0.001, 0.005, 0.01, 0.05, 0.1 [kg/kg air]. Bottom left panel: Vertical cross section of synthetic reflectivity [dBZ, mm/h] of the COSMO one-moment scheme analysis cycle at 14.45 UTC near Lucerne. Bottom right panel: Vertical cross section of reflectivity [dBZ, mm/h] of the radar (OYC) at 14.45 UTC near Lucerne. The x-axis of the vertical cross sections of reflectivity shows the extension of the cross section [km].

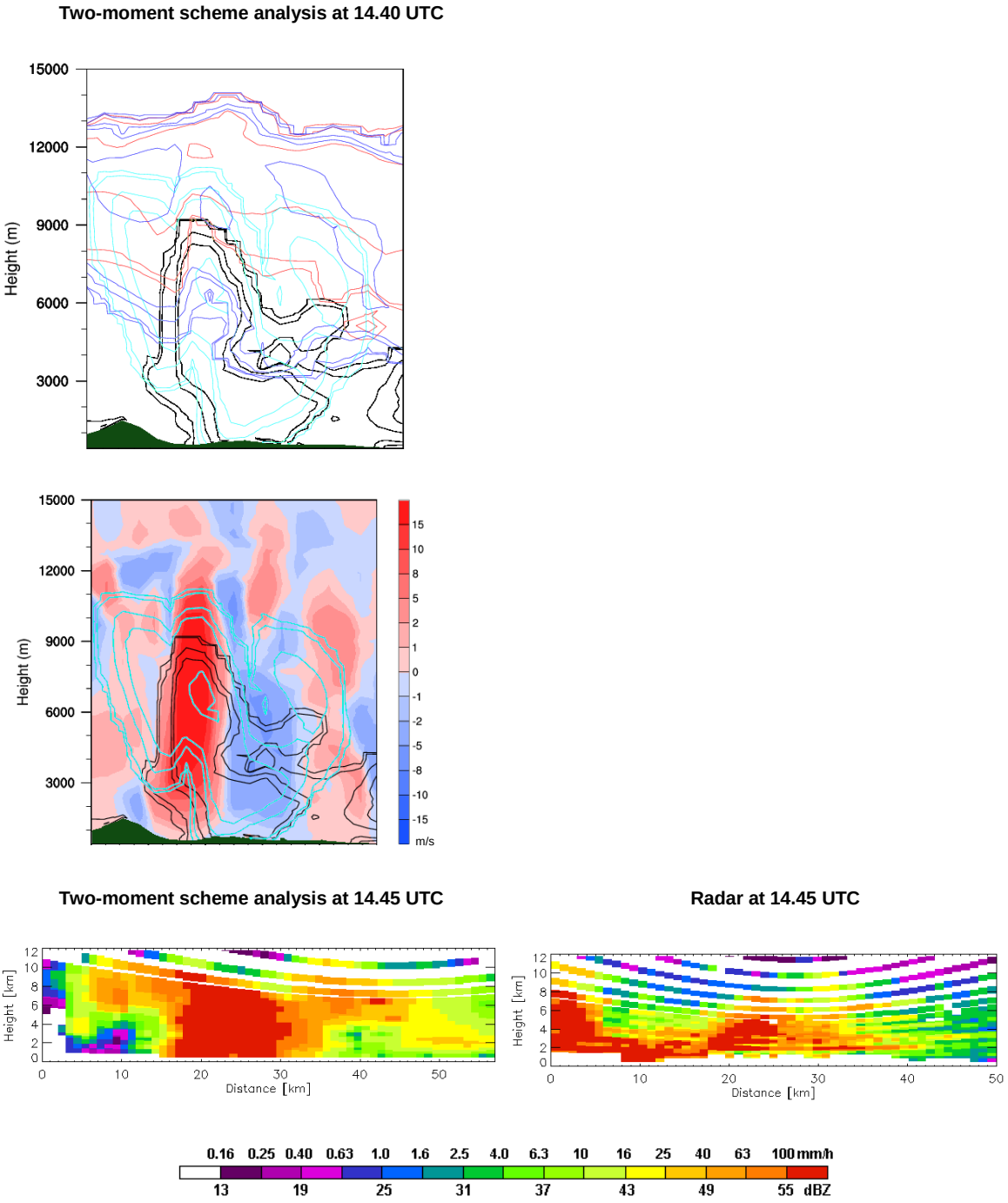

Figure 3.1.19: Top left panel: Vertical cross section of hydrometeor densities [kg/kg air] of the COSMO two-moment scheme analysis at 14.40 UTC with rain (black contour), snow (red contour), graupel (blue contour), and hail (cyan contour). Middle left panel: Vertical cross section of hydrometeor densities [kg/kg air] of the COSMO two-moment scheme analysis at 14.40 UTC with rain (black contour) and hail (cyan contour), as well as vertical winds [m/s] (shaded). Both vertical cross sections of hydrometeor densities are approximately along the same distance as in the bottom left panel near Lucerne. The dark green area is the topography. The scale of the contours is as follows: 0.00005, 0.0001, 0.0005, 0.001, 0.005, 0.01, 0.05, 0.1 [kg/kg air]. Bottom left panel: Vertical cross section of synthetic reflectivity [dBZ, mm/h] of the COSMO two-moment scheme analysis at 14.45 UTC near Lucerne. Bottom right panel: Vertical cross section of reflectivity [dBZ, mm/h] of the radar (OYC) at 14.45 UTC near Lucerne. The x-axis of the vertical cross sections of reflectivity shows the extension of the cross section [km].

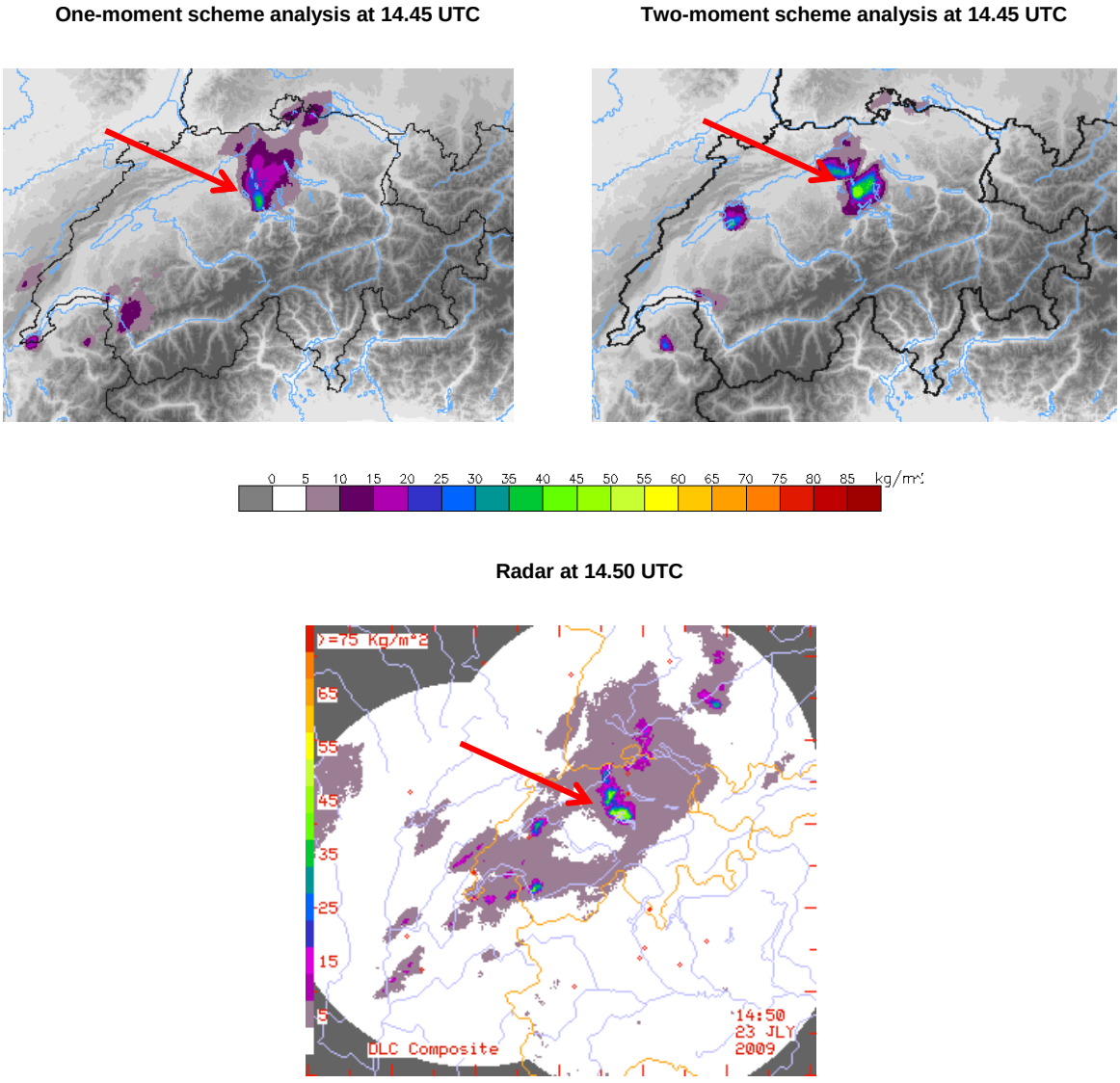

Figure 3.1.20: Top left panel: VIL [kg/m²] of the COSMO one-moment scheme analysis at 14.45 UTC. Top right panel: VIL [kg/m²] of the COSMO two-moment scheme analysis at 14.45 UTC. Bottom panel: VIL [kg/m²] derived from radar data at 14.50 UTC. The midland cell is labeled with red arrows.

Vertical structures of the COSMO one-moment scheme analysis cycle at 14.45 UTC: discussion

The COSMO one-moment scheme analysis cycle shows in general better vertical structures in terms of the extent as well as in terms of the maximum reflectivities for the time of maximum reflectivities when comparing it with the 12 UTC forecast. In comparison with the 12 UTC forecast, where the vertical extent of reflectivities reaches values up to 6 km, the COSMO one-moment scheme analysis simulates more reflectivities up to 12 km, or even above (Figure 3.1.18, bottom left panel). This might be due to the temperature forcing of the LHN. The general reflectivity pattern corresponds well with the radar measurement (Figure 3.1.18, bottom right panel)

and the VIL values are higher than the values of the 12 UTC forecast, but still slightly too low (45kg/m^2 instead of 60 kg/m^2). There are however several substantial differences. The highest reflectivity values are due to the rain when considering the hydrometeor density plot (Figure 3.1.18, top left panel). We know from the 24h total surface precipitation plots (Figure 3.1.12) that the simulated precipitation amounts agree with the radar data. Hence, the LHN is successful in forcing the model to produce sufficient precipitation amounts. But the vertical extent of high reflectivity values above 55 dBZ is not as high as in the radar data and only one red core is visible. Therefore, it seems that the COSMO one-moment scheme predicts the right total precipitation amount but with a wrong hydrometeor distribution in the vertical and hence with a wrong distribution of maximal reflectivities in the vertical.

As already discussed for the COSMO one-moment scheme 12 UTC forecast, the reasons have to be prospected in the way how the one-moment scheme tries to simulate the vertical structure as seen in reality. The one-moment scheme analysis tries to simulate more or less correct surface precipitation amounts (with the forcing of the LHN) and replaces the hail class trough other hydrometeors.

Vertical structures of the COSMO two-moment scheme analysis cycle: discussion

The differences between the two-moment scheme 12 UTC forecast with the COSMO two-moment scheme analysis cycle are impressive in terms of the vertical structure and the quantitative VIL values. The latter reaches with 56 kg/m^2 (Figure 3.1.20, top right panel) similar values than the radar derived VIL with 60 kg/m^2 (Figure 3.1.20, bottom middle panel). In terms of the vertical structure, the high reflectivity values above 55 dBZ have a higher vertical extend than measured by the radar. The vertical winds (Figure 3.1.19, middle left panel) are in good agreement with the hydrometeor density contours of rain and hail. Both reach their highest altitudes where the updrafts are strongest (red shaded areas). It can be recognized that two hail cores (cyan contours) exists where the updraft regions are. Between, a downdraft region (blue shaded areas) is simulated and exactly at these location, the vertical extend of the hail is lowest. Within this updraft regions, hail and rain are lifted in extraordinary altitudes (extraordinary when comparing the altitudes with the forecast or with the one-moment scheme, but probably realistic when compare with the nature). The hail and rain reach the ground within the downdraft region. The red reflectivity core is a result of the two hail cores with its precipitation region in

the middle. The two higher reflectivity cores between 6 and 12 km above the ground to the left and right of the red core could be hail in suspense (as mentioned in the figure caption, the vertical cross section of reflectivity and the vertical cross section of hydrometeor density are not exactly of the same length).

The LHN seems to work quite well for the COSMO two-moment scheme in this case. Although the synthetic radar reflectivities do not look like the radar derived reflectivities in detail, some structures such as the vertical extend of the high reflectivities is quite well simulated.

COSMO analyses hail detection algorithms: data

The daily maximum POH products of the two COSMO schemes analyses reflect the illustrated improvements in the vertical structure. In comparison with the 12 UTC forecasts (Figure 3.1.10, top left and bottom left panel), the POH swaths of the analyses (Figure 3.1.21) look broader and have in general higher probabilities. As described in chapter 3.1.3.1 the midland cell nearly dissolves in the one-moment scheme analysis after crossing the La Dôle radar near Geneva. Therefore, no hail swath (as defined by the POH algorithm) is simulated from approximately Geneva to the Lake of Neuchatel in the one-moment scheme. Clear visible, around the region of Berne, is a right-turn in the one-moment scheme. The COSMO two-moment scheme shows less interruption between Geneva and the Lake of Neuchatel as well as less turn against south at Berne.

Figure 3.1.22 illustrates the daily maximum MESHS output of the COSMO two-moment scheme analysis cycle (left) and the radar derived daily maximum MESHS output (right). Apart from a few pixels on the lower and of the MESHS scale at the area where the most intense reflectivities are simulated, no hail (as defined by MESHS) is simulated in the COSMO one-moment scheme analysis cycle and is therefore not shown.

The COSMO two-moment scheme simulates a hail swath (as defined by the MESHS algorithm) from the Lake of Neuchatel to the Lake of Zurich with maximum MESHS values larger than 6 cm. Swaths close to the Lake of Constance are missing.

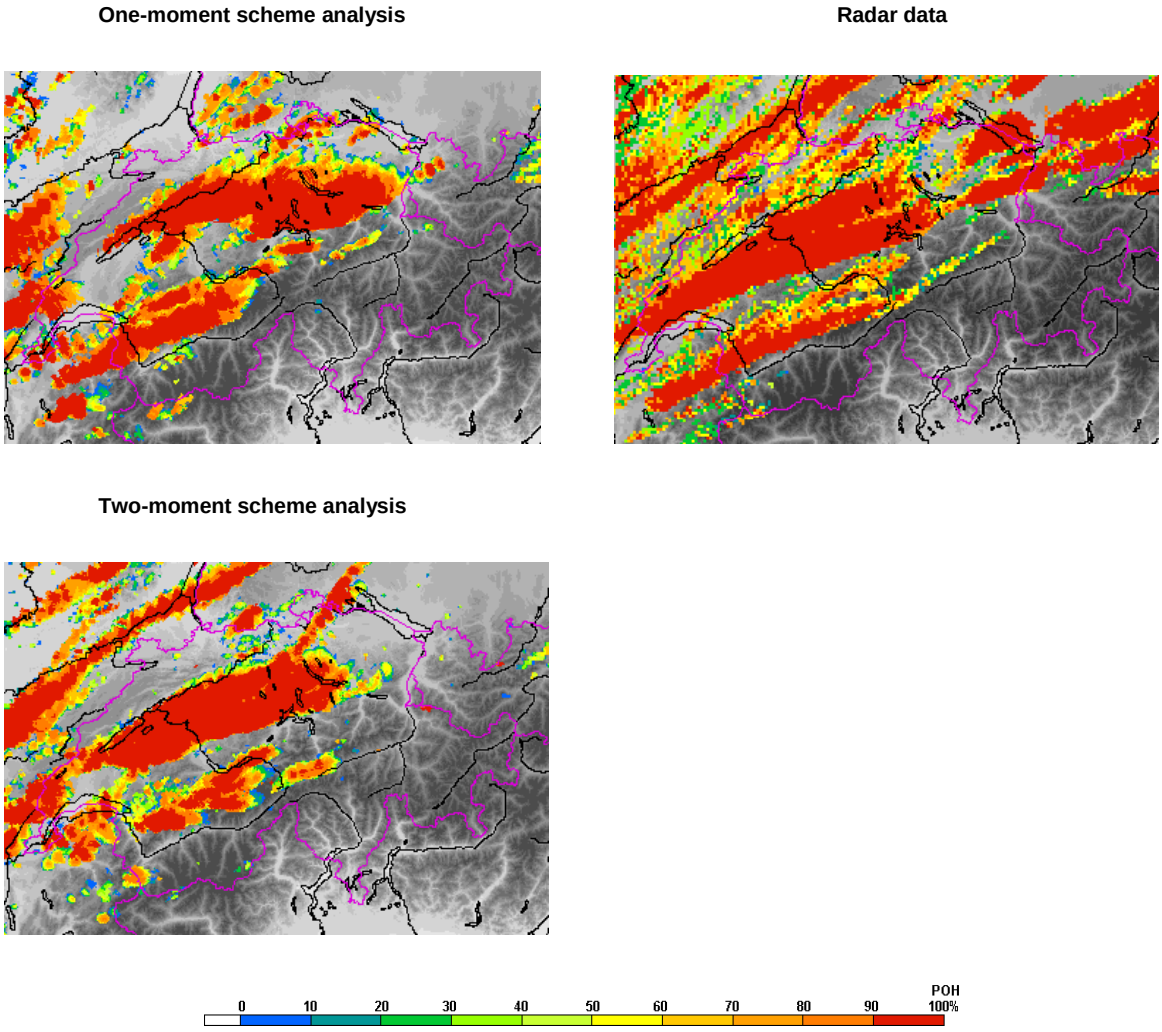

Figure 3.1.21: Top left panel: Synthetic daily maximum POH product [%] of July 23, 2009, of the COSMO one-moment scheme analysis. Bottom left panel: Synthetic daily maximum POH product [%] of July 23, 2009, of the COSMO two-moment scheme analysis. Top right panel: Daily maximum POH product [%] of the radar of July 23, 2009.

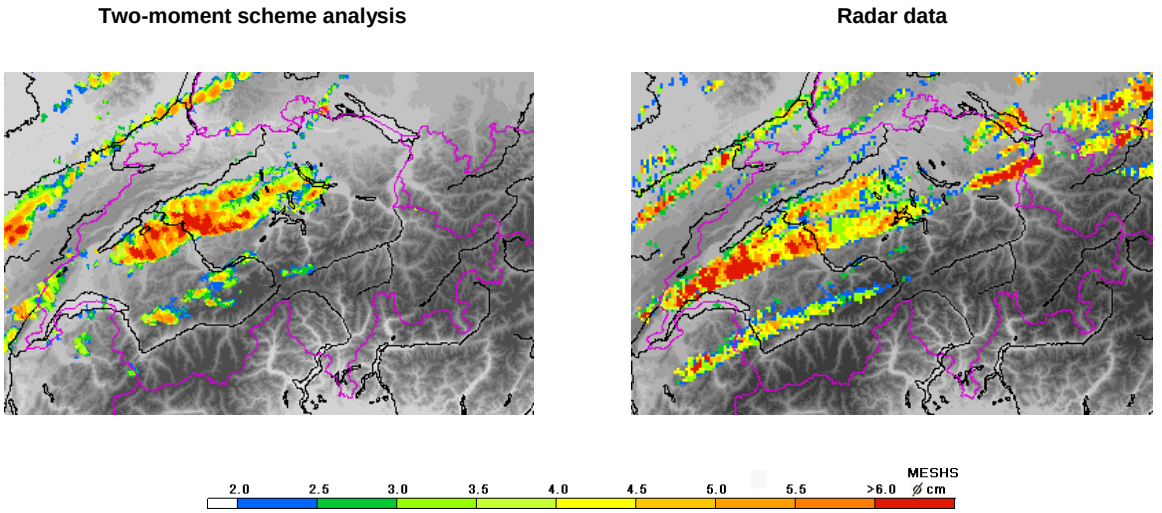

Figure 3.1.22: Synthetic daily maximum MESHS plot [cm] of the COSMO two-moment scheme analysis cycle (left panel) and the corresponding radar derived MESHS plot [cm] of July 23, 2009.

COSMO analyses hail detection algorithms: discussion

The synthetic daily maximum POH products of the two COSMO schemes analyses cycles in general corresponds well with the radar derived daily maximum POH plot. The turn towards the south can be interpreted as the result of the LHN forcing. While the model tends to simulate the cell too far against north, the LHN force the cell after a certain point against the south. The result is a turn of the cell against the south. This same can be observed when considering the 10min surface precipitation plots (not shown). After the cell crosses the La Dôle radar near Geneva, the COSMO two-moment scheme seems to model the high reflectivity values above 45 dBZ, which are used in order to calculate the POHs, closer to the reality as the one-moment scheme. The interruption between Geneva and the Lake of Neuchatel is not as pronounced as in the one-moment scheme.

The investigations of the COSMO one-moment scheme with the MESHS algorithm point out, that neither the analysis nor the forecast are capable to simulate the 51 dBZ values at a sufficient altitude. The general underestimation of the vertical extent of high reflectivity values can be confirmed.

The COSMO two-moment scheme analysis cycle shows that with the help of the LHN forcing realistic MESHS values can be simulated. This is in agreement with the investigations of the vertical structure (chapter 3.1.3.2), where high reflectivities above 55 dBZ are simulated up to 10 km altitude. Finally, it can said that while the COSMO two-moment scheme 12 UTC forecast is not able to simulate the vertical structure and therefore MESHS values in a sufficient way, the COSMO two-moment scheme analysis cycle generates realistic MESHS values. The simulated MESHS products are impressive in comparison with the forecast or the one-moment scheme. From that perspective, it might be, at least for this case, that the convection does not develop enough when using the COSMO two-moment scheme in an operational forecast mode. Further research is needed to understand why the model does not fully develop the vertical reflectivity structures in the forecasts, as can be observed in the analysis.

3.2. May 11, 2010

On the afternoon and evening of May 11, 2010, thunderstorms with hail and strong wind gusts moved from west to east in the northeastern part as well as in Central Switzerland. The total damage to crops in the Cantons of Aargau, Bern, Lucerne, Vaude, Zug, Zurich, and Baselland amounted to 2.6 Mio Swiss Francs (Schweizer Hagel[5]).

3.2.1. Synoptic Situation and Measurements

The synoptic situation was dominated by a weak surface pressure gradient from Scandinavia to the western Mediterranean. A surface low moved from France northwards to Germany. During the afternoon, a cold front moved across northern Switzerland. The humid and unstable air ahead of the cold front offered a favorable environment for a shortwave upper-level trough to trigger strong pre-frontal convection. Previously, foehn had been observed in the alpine valleys (Müller and Stoll, 2010).

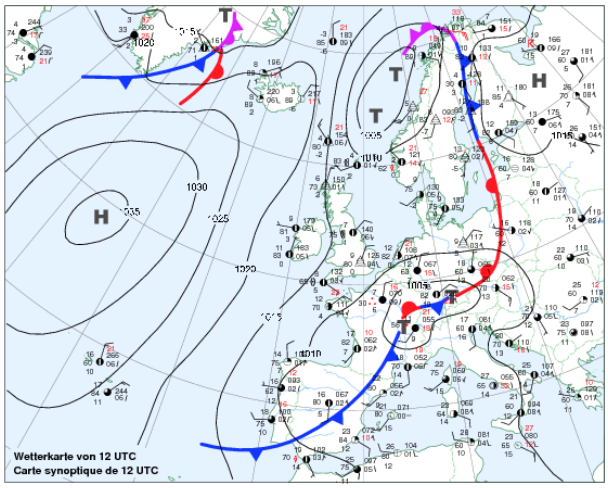

Figure 3.2.1: Synoptic weather chart of Europe at May 11, 2010. Blue signatures are surface cold fronts whereas red signatures are surface warm fronts. Purple signatures are occlusions. Black lines show the pressure [hPa] at the ground (source: MeteoSwiss).

A first strong cell, which was initiated over France, moved over the northwestern part of Switzerland. This cell intensified over the Jura mountains at 11.30 UTC and hit Basel as hailstorm with hail sizes of around 2 cm diameter one hour later at 12.30 UTC (Figure 3.2.2, left). Precipitation sums of 7.6 mm/10min were measured

[5] Information of the management (private communication)

by the SwissMetNet[6] station at Basel from 12.30 to 12.40 UTC. Henceforth, this cell is called the Basel cell.

A second intense cell formed over the Fribourg Alps around 11.30 UTC which then intensified and further moved to the east. From this cell and along the approaching cold front, a thunderstorm line with three separated cells formed over the area of the Emmental-Entlebuch starting at 13.00 UTC. The cells moved eastward to Lucerne, the Lake of Zurich, Zurich Oberland, the Lake of Constance, and to the Allgäu (Germany) as squall with maximum intensity between 13.45 and 16.15 UTC, thereby producing hail and strong wind gusts. Figure 3.2.2 (right) shows the squall line at 14.00 UTC. Precipitation amounts of 13.7 mm/10min were measured by the SwissMetNet station at Lucerne for the time period when the cell crossed the station (14.30 – 14.40 UTC). Henceforth, this squall line cell is called the Lucerne cell.

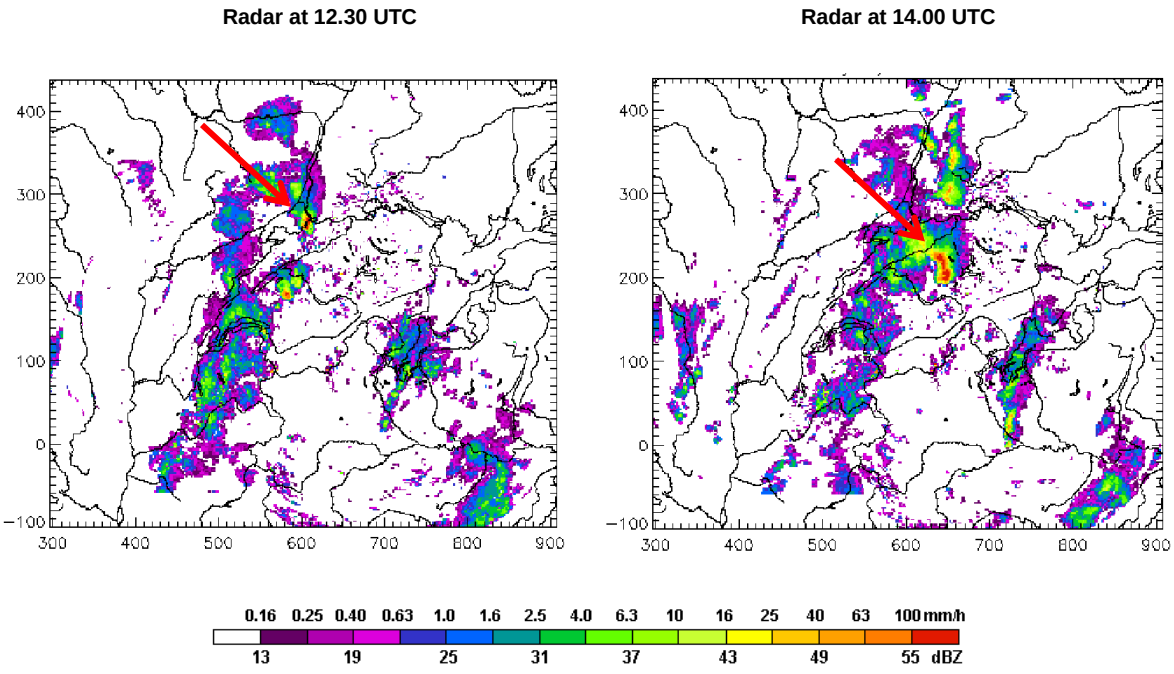

Figure 3.2.2: Precipitation [mm/h] (OMC product) at 12.30 UTC on May 11, 2010 (left), and at 14.00 UTC (right). The red arrow on the left side shows the location of the Basel cell, whereas the red arrow on the right side shows the location of the Lucerne cell during the moment of highest intensity.

3.2.2. 09 UTC Forecast

We first look at the 09 UTC forecast, which assimilates radar data until 09.00 UTC. The Basel as well as the Lucerne cell were not present in the radar data and therefore, the model has to simulate the entire convective lifecycle by itself. The 12

[6] SwissMetNet stands for the network of ground-based automatic weather stations operated by MeteoSwiss.

UTC forecast already include 30 minutes of radar assimilation that contains the initial phase of the Basel cell and therefore the model has not to simulate the entire convective lifecycle by itself. For this reason the 09 UTC forecast is investigated first.

3.2.2.1. Total Precipitation Sums

COSMO one-moment microphysical scheme 09 UTC forecast: data

The comparison of the 24h precipitation sum of the COSMO one-moment scheme 09 UTC forecasts with the radar derived data show clear differences in terms of quantitative values (e.g., Zurich cell up to 100 mm/24h in the radar observation and up to 40 mm/24h in the model run) as well as geographical distribution, where the swath of the radar is broader by approximately 10 km (Figure 3.2.3). For the 09 UTC free forecast, a small swath with higher precipitation sums is visible from the region of Emmental-Entlebuch to the Lake of Constance for the 09 UTC free forecast. The same behavior can be seen for the region of Basel. Further investigations of the 1h precipitation sums or even the 10min precipitation sums show a delay of the cells between one and two and a half hours (not shown). The geographical displacement is quite small. Both cells are close to the surface precipitation sums swaths measured by the radar.

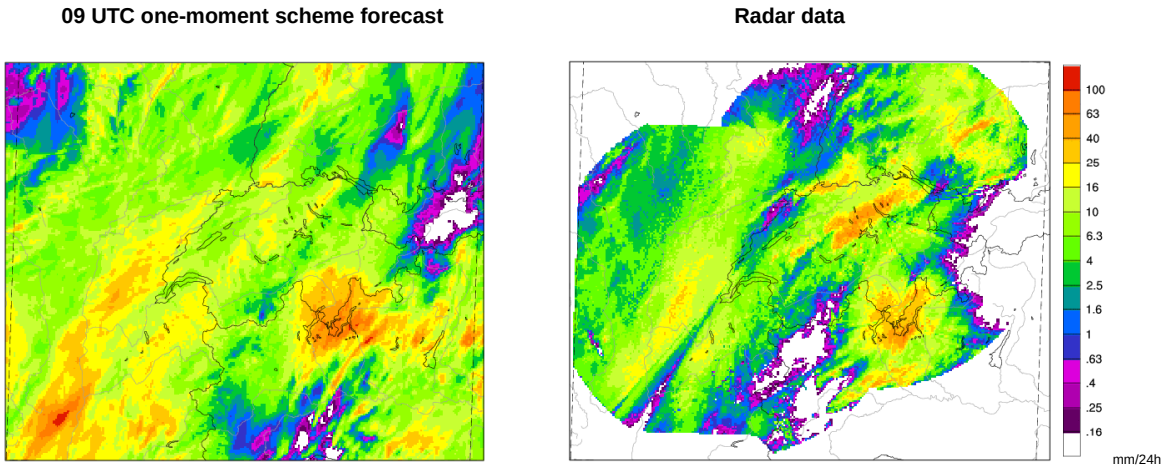

Figure 3.2.3: 24h precipitation sum (shaded) [mm/24h] of the COSMO one-moment 09 UTC forecast (left) and the radar measurements (PKC product, right) for May 11, 2010. Black solid lines are international borders and lakes, grey lines are rivers and coast lines, and the dashed lines indicate the radar domain.

COSMO two-moment microphysical scheme 09 UTC forecast: data

The total precipitation sum of the COSMO two-moment 09 UTC forecast shows a no precipitation signal of the Basel and Lucerne cells (Figure 3.2.4). The two thunderstorm cells cannot be identified in the hourly precipitation sums or even in the 10min precipitation sums.

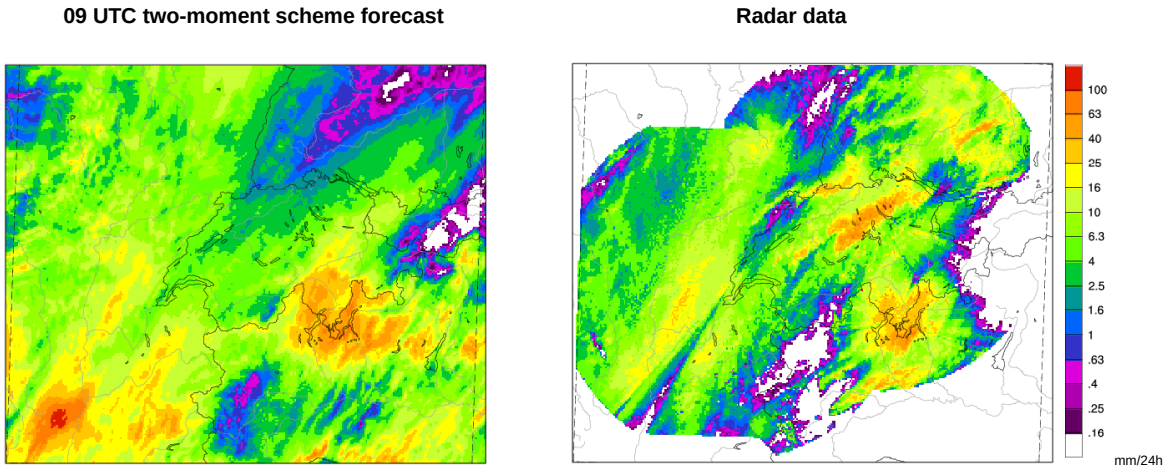

Figure 3.2.4: 24h precipitation sum (shaded) [mm/24h] of the COSMO two-moment 09 UTC forecast (left) and the radar measurements (PKC product, right) for May 11, 2010. Black solid lines are international borders and lakes, grey lines are rivers and coast lines, and the dashed lines indicate the radar domain.

09 UTC forecasts total precipitation sums: discussion

The data of the one-moment 09 UTC forecast show that the Basel cell as well as the Lucerne cell are predicted, but the model underestimates both in terms of the surface precipitation amounts. The two-moment 09 UTC forecast shows no cell when considering the surface precipitation amounts. It is possible that the two strong cells are not that pronounced in both schemes due to smoothing effects when plotting 24h surface precipitation sums. But even the 10min sums indicate no cell with the COSMO two-moment scheme. In the one-moment scheme forecast, at least small swaths with higher precipitation values are seen, but the maximum precipitation values are only about half the ones detected by the radar. In terms of the geographical occurrence, those simulated swaths are positioned at the right place. Therefore, high maximum reflectivity values can be expected with the one-moment scheme for these locations.

3.2.2.2. Maximum Reflectivities

COSMO one-moment microphysical scheme 09 UTC forecast: data

The radar derived maximum reflectivities show first values above 55 dBZ for the Basel cell at 09.55 UTC over France with lower values already before. The corresponding one-moment 09 UTC free forecast simulates values above 55 dBZ for the Basel cell at 12.25 UTC for the same location as measured with the radar. After that, the simulated cell intensifies over the Jura mountains and hits Basel at 14.55 UTC (Figure 3.2.5, top left panel). In reality, the cell was detected by radar over Basel at 12.45 UTC (Figure 3.2.5, top right panel). The geographical extension of values above 55 dBZ for the simulated cell over Basel corresponds well with the radar measurements. Later on, the cell moves to the east and dissipates in the same way as observed in radar data (not shown).

For the simulated Lucerne cell first small high reflectivity cores are located in the Fribourg Alps. In agreement with the radar derived maximum reflectivities. First values above 55 dBZ are detected for the simulated cell at 15.10 UTC over the Emmental while the radar detected such values already at 12.20 UTC for the area of the Fribourg Alps and again later at 13.10 UTC over the Emmental. After 15.10 UTC, the simulated Lucerne cell is getting weaker in terms of maximum reflectivities, and intensifies again after crossing the Lake of Zurich at 16.40 UTC. Maximum reflectivity values are simulated around 17.15 UTC over the region of Zurich Oberland, Winterthur, and Frauenfeld. Radar derived maximum reflectivities show high values from Emmental-Entlebuch to the Lake of Constance for the entire period. The simulated cell dissipates after crossing the Lake of Constance. This is in agreement with the radar measurements. Figure 3.2.5 (bottom left panel) shows the maximum reflectivities at 17.15 UTC for the 09 UTC one-moment scheme forecast and the corresponding radar measurements at 15.30 UTC (bottom right panel).

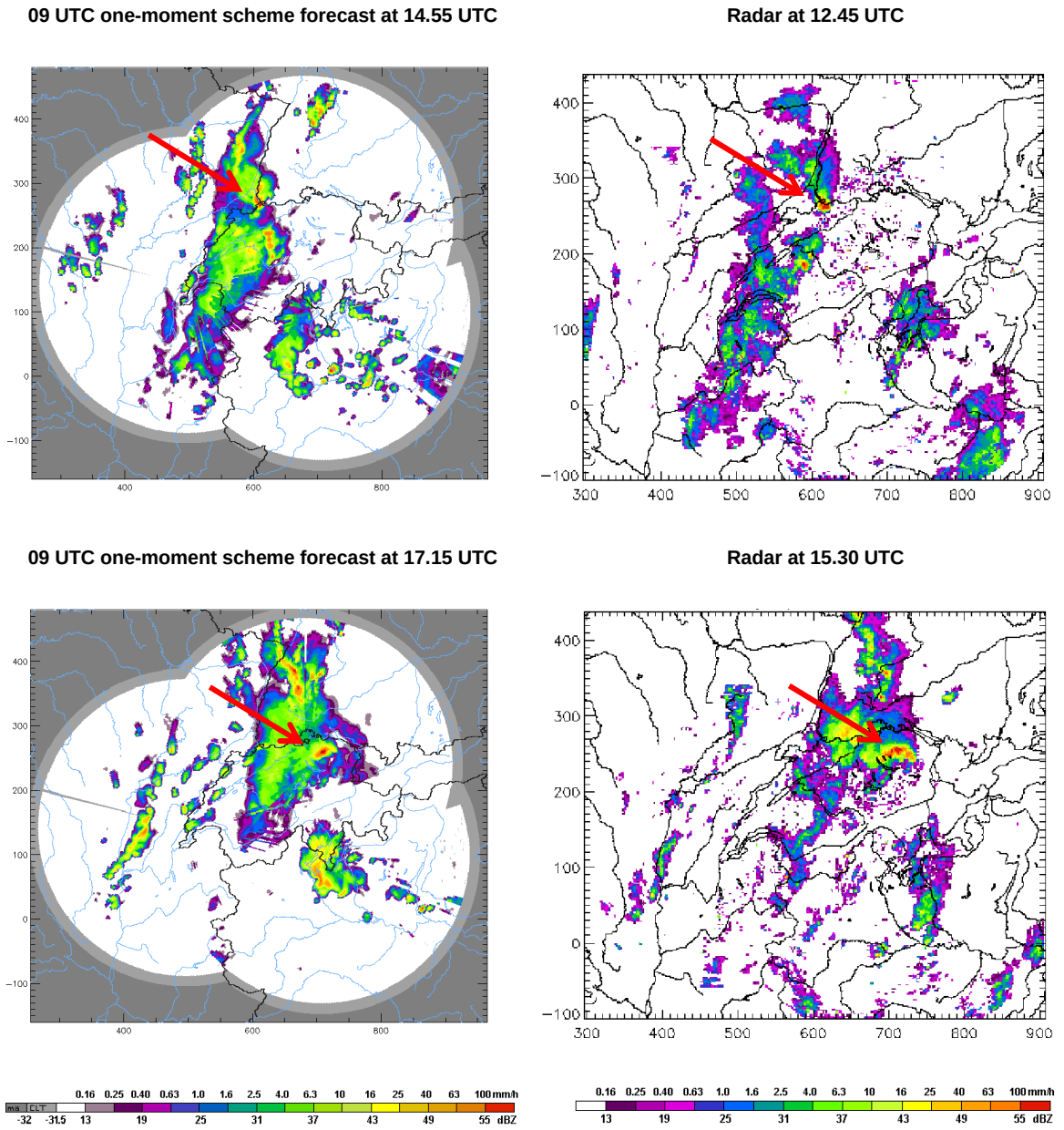

Figure 3.2.5: Maximum reflectivities (CZC product) [dBZ, mm/h] of the one-moment analysis cycle at 14.55 UTC (top left panel) and at 17.15 UTC (bottom left panel), as well as the corresponding radar derived maximum reflectivities (OMC product) at 12.45 UTC (top right panel) and at 15.30 UTC (bottom right panel). The Basel cell (top panels) is labeled with red arrows as well as the Lucerne cell (bottom panels).

COSMO two-moment microphysical scheme 09 UTC forecast: data

Maximum reflectivity data of the COSMO two-moment 09 UTC forecast show a different picture in terms of convection. No cell is visible which could possibly be matched with the Basel cell for the entire day. The same is true for the Lucerne cell. Only at 18.30 UTC, maximum reflectivities above 55 dBZ occurred for the duration of more than 5 minutes over the Toggenburg.

09 UTC forecasts maximum reflectivities: discussion

The Basel cell is simulated by the COSMO one-moment scheme in good agreement with the radar measurements. Apart from a temporal delay of approximately 2.5 hours, maximum reflectivities above 55 dBZ are simulated in good agreement with radar measurement. The breakup of the cell is simulated as observed with the radar data. No comparable cell is simulated with the COSMO two-moment scheme.

The Lucerne cell is only simulated with the COSMO one-moment scheme. The one-moment scheme triggers the cell in the right position. The cell was 'alive' for the entire period from the initiation to the breakup. Although the cell weakens between Lucerne and the Lake of Zurich, the one-moment scheme model re-intensifies the cell. The maximum simulated reflectivities are in good agreement with the radar data in terms of quantitative values. The geographical distribution looks more like a single cell than a line structure as seen in the radar measurements.

The COSMO two-moment scheme 09 UTC forecast shows only one intense cell moving over the Toggenburg. Based on the origin and life cycle of this cell, it cannot be interpreted as a displaced Basel or Lucerne cell.

For this case, the COSMO one-moment scheme is able to simulate realistic convection in terms maximum reflectivities. This is in agreement with the investigations of the total precipitation sums above (Figure 3.2.3, left panel), where swaths with higher ground precipitation rates are seen. The missing ground precipitation swaths of the two-moment scheme can be explained with the missing cells.

While maximum reflectivity gives a 2-dimensional view only, further investigations of the vertical structure for the time when most intense reflectivity values are simulated should give a better insight, how the COSMO one-moment scheme simulates convection in the vertical. Therefore the focus is based on the Lucerne cell due to more intense reflectivities and the better simulation of the entire life cycle. The two-moment scheme is not considered for any further investigations due to missing convective cells.

3.2.2.3. Vertical Structures and 3-dimensional Reflectivities

COSMO one-moment microphysical scheme 09 UTC forecast: data

Figure 3.2.6 shows the vertical cross section of reflectivity for the COSMO one-moment 09 UTC forecast at 17.15 UTC (bottom left panel) and the corresponding radar measurement at 15.30 UTC (bottom right panel). For the one-moment forecast, reflectivity values above 55 dBZ are simulated in between approximately 0.5 km and 1.5 km above ground. Values between 43 and 46 dBZ (yellow; 16 and 25 mm/h, respectively) can be seen up to 6 km above ground. The horizontal size of the cell is approximately 13 km when considering the category between 46 and 49 dBZ (light orange; 25 and 40mm/h, respectively). No reflectivities are simulated higher than 9 km above ground. Radar measurements show reflectivity values above 55 dBZ in between 4 km and 9 km above ground. The yellow category as well as the orange category reach same heights as the red category. The horizontal size of the entire cell system is approximately 10 km when considering the light orange (46-49 dBZ) category as well.

The vertical cross section of hydrometeors densities of the COSMO one-moment 09 UTC forecast (Figure 3.2.6, top left panel) shows rain up to 4 km above ground (black contours). Graupel (blue contours) is simulated from 2 km to 10 km height, whereas snow (red contours) reaches heights up to 11 km.

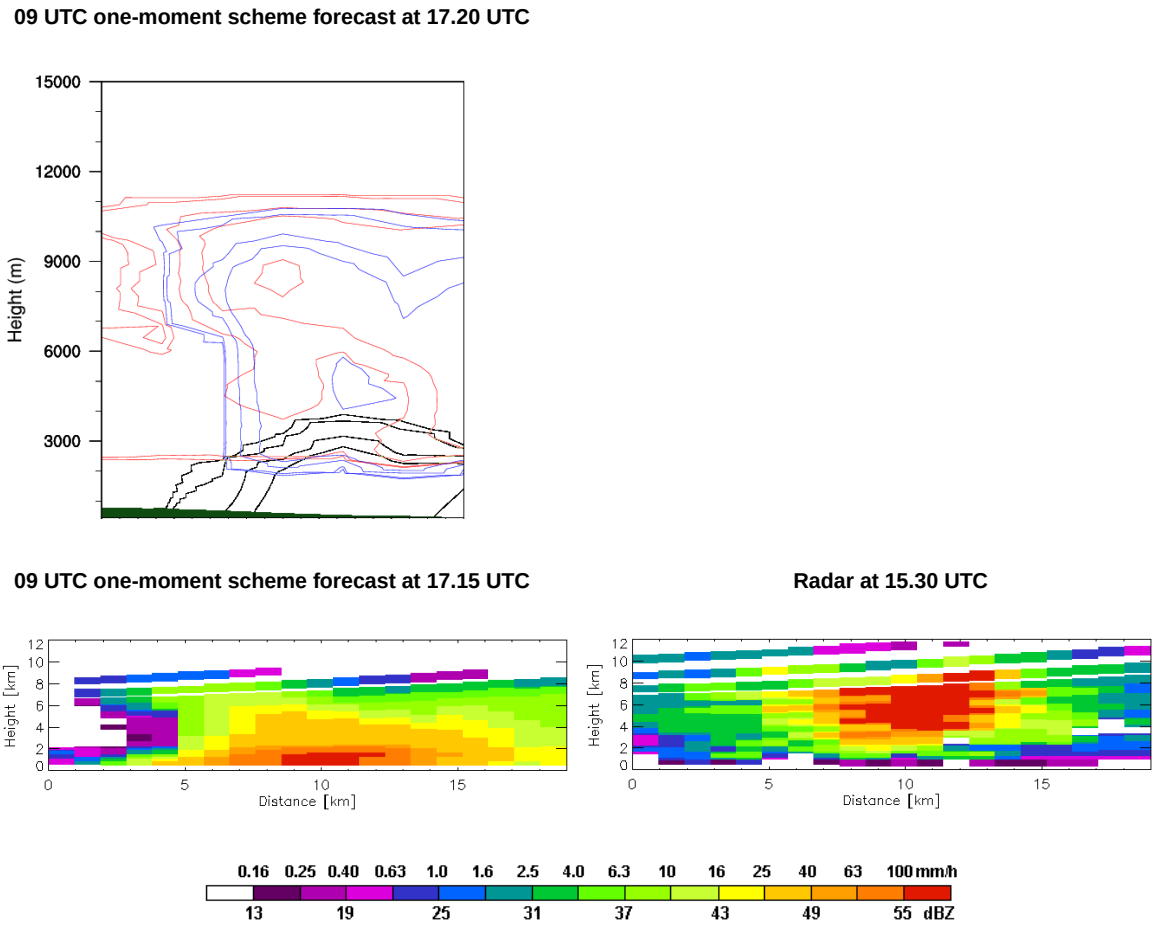

Figure 3.2.6: Top left panel: Vertical cross section of hydrometeor densities [kg/kg air] of the COSMO one-moment scheme 09 UTC forecast (Lucerne cell) at 17.20 UTC with rain (black contour), graupel (blue contour), and snow (red contour), along the same distance as in the bottom left panel near Winterthur. The dark green area is the topography. The scale of the contours is as follows: 0.00005, 0.0001, 0.0005, 0.001, 0.005, 0.01, 0.05, 0.1 [kg/kg air]. Bottom left panel: Vertical cross section of synthetic reflectivity [dBZ, mm/h] of the COSMO one-moment scheme 09 UTC forecast (Lucerne cell) at 17.15 UTC near Winterthur. Bottom right panel: Vertical cross section of reflectivity [dBZ, mm/h] of the radar (OYC, Lucerne cell) at 15.30 UTC near Winterthur. The x-axis of the vertical cross sections of reflectivity shows the extension of the cross section [km].

Figure 3.2.7 shows the VIL of the COSMO one-moment scheme 09 UTC forecast simulation (right panel) and the corresponding radar derived measurements (left panel). In the radar measurement, VIL values up to 45 kg/m^2 can be seen with large areas with values between 5 and 10 kg/m^2. The simulated radar forward operator VIL output shows maximum values up to 20 kg/m^2 for the same location as seen by the radar. Only two cores with a small geographical extension are visible in the COSMO one-moment scheme 09 UTC forecast simulation.

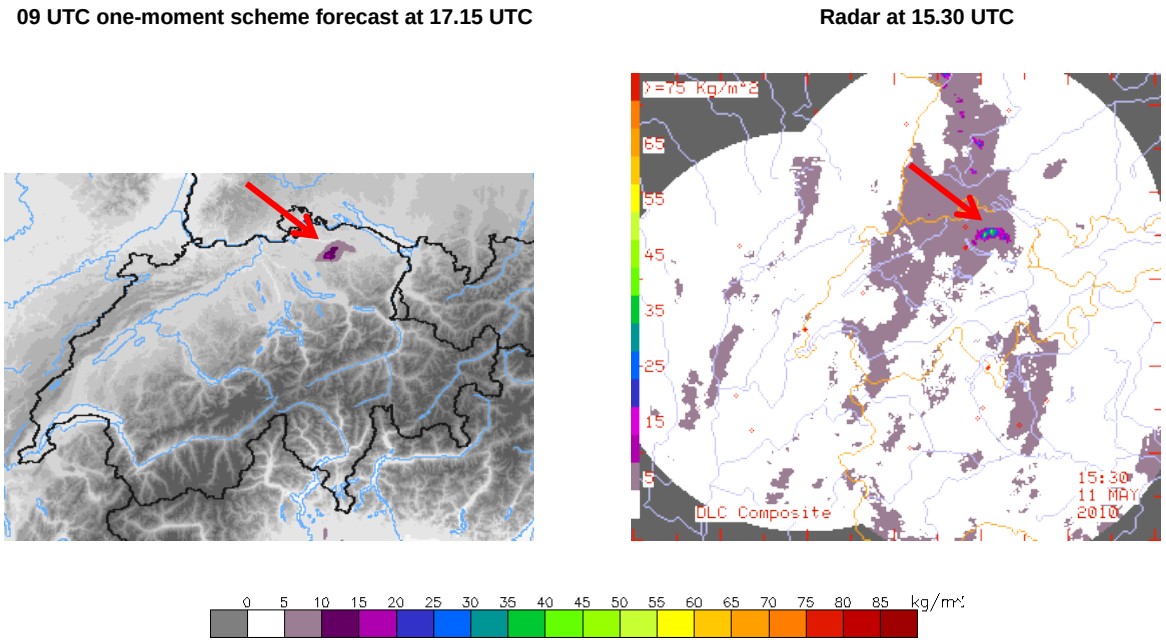

Figure 3.2.7: Left panel: VIL [kg/m²] of the COSMO one-moment scheme 09 UTC forecast at 17.15 UTC. Right panel: VIL [kg/m²] derived from radar data at 15.30 UTC. The Lucerne cell is labeled with red arrows.

09 UTC forecasts vertical structures and 3-dimensional reflectivities: discussion

The vertical cross section of reflectivity of the one-moment scheme 09 UTC forecast shows that the radar forward operator is able to simulate high reflectivity values above 55 dBZ. There are however distinct differences between the model simulation and the radar data.

While the radar data shows maximum reflectivities above 55 dBZ between 4 and 9 km above ground, the model forecast's highest reflectivity values are much closer to the ground, and does not produce any reflectivities beyond 40 dBZ above 4km. At this height, the model simulates snow and graupel, only (see Figure 3.2.6, top left panel). The interpretations of the specific synthetic reflectivity structures such as low synthetic reflectivities due to graupel and high synthetic reflectivities near the ground are the same as already mentioned in the first case (see 3.1.2.3, 12 UTC forecasts, vertical structures and 3-dimensional reflectivities: discussion).

In terms of the spatial extent the simulation is in good agreement with the radar data.

The simulated VIL is lower than the corresponding radar measured VIL (Figure 3.2.7). Due to the wrong size-mass distribution of the one-moment scheme, the synthetic radar reflectivities are underestimated. Therefore, not only the vertical

structure looks different in terms of the reflectivities, the simulated VIL displays much lower quantities as well.

The assumed particle size distribution of rain in the one-moment scheme might also simulate too many large rain drops with diameters larger than 5 mm. In reality, they would break up in smaller droplets. The resulting systematic overestimation may lead to an overestimation of reflectivity values (Blahak, 2012). In terms of reflectivity it can be conclude that the COSMO one-moment scheme simulates too much rain near the ground with too low reflectivities from 4 to 9 km above the ground. It might be that the standards to the COSMO one-moment scheme, to simulate a fully development hailstorm structure, are too high due to the extreme case of a strong hail cell and therefore the outcome of the model is obviously a too low precipitation rates as sum of all hydrometeors.

The COSMO two-moment scheme which explicitly simulates hail and therefore might simulate strong convection more realistically unfortunately does not trigger any convective cores. At least for this case the COSMO two-moment scheme is not capable to simulate (vertical structures of) a hail storm when using it in forecast mode.

3.2.2.4. Hail Detection Algorithms

COSMO one-moment microphysical scheme 09 UTC forecast: data

The investigations of the Probability of Hail (POH) for the COSMO one-moment 09 UTC forecast at 17.15 UTC shows a hail cell (as defined by the POH algorithm) at the location of maximal intensity (Figure 3.2.8, left panel). Maximum probability values of 80% are simulated. The corresponding radar derived POH is shown on the right side. Probability values up to 100% were detected. In terms of the geographical extension, the radar derived POH values cover a larger region.

The synthetic daily maximum POH plot of the COSMO one-moment scheme 09 UTC forecast (Figure 3.2.9, left panel) shows a hail swath (as defined by the POH algorithm) from Zurich to the Lake of Constance, with maximum probabilities over the Zurich Oberland where the cell intensifies. There, values of 100% are simulated for the entire time period. Another high POH swath is simulated for the northern part of Switzerland close to Basel, with probability values up to 100%. The

corresponding radar derived daily maximum POH plot (Figure 3.2.9, right panel) shows a broader hail swaths in terms of the geographical extension for the Lucerne cell, as well as more high POH values. The main POH swath starts at Emmental-Entlebuch and ends at the Lake of Constance. Another POH swath is visible over Basel.

The implementation of the radar-based Maximum Expected Severe Hail Size (MESHS) algorithm for the COSMO one-moment scheme 09 UTC forecast shows no simulated hail size values for the Lucerne cell when considering the daily maximum MESHS plot and only a few values for the Basel cell with largest expected diameters of 4.5 cm (not shown). The radar derived daily maximum MESHS product on the other hand shows a MESHS swath for the Lucerne cell with expected hail sizes > 6 cm and a MESHS swath over Basel with maximum expected hail sizes > 6 cm as well (not shown).

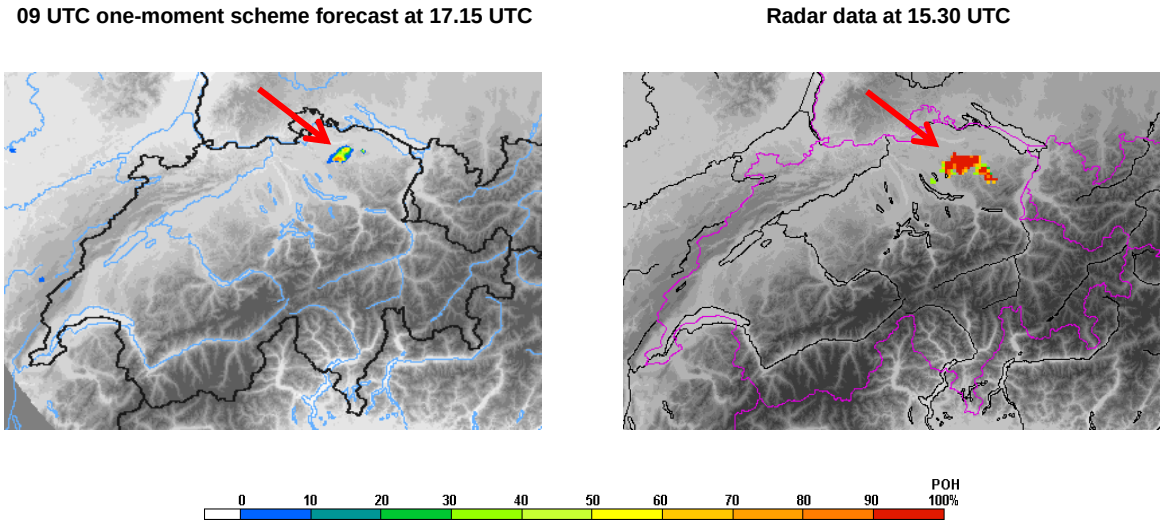

Figure 3.2.8: Left panel: Synthetic POH product [%] of May 11, 2010, of the COSMO one-moment scheme 09 UTC forecast at 17.15 UTC. Right panel: POH product [%] of the radar of May 11, 2010 at 15.30 UTC. The Lucerne cell is labeled with red arrows.

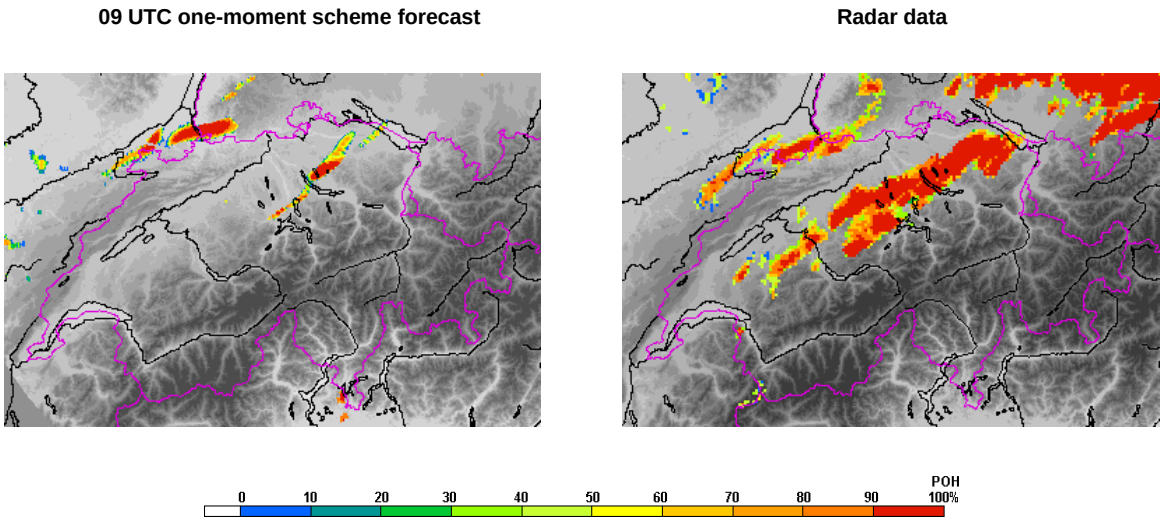

Figure 3.2.9: Left panel: Synthetic daily maximum POH product [%] of May 11, 2010, of the COSMO one-moment scheme 09 UTC forecast. Right panel: Daily maximum POH product [%] of the radar of May 11, 2010.

The verification of the simulated daily maximum POH product of the COSMO one-moment scheme 09 UTC forecast with the method used in Betschart and Hering (2012) and the corresponding SHVDB10[7] results in a Probability of Detection (POD) of approximately 40 % (Table 3.1). The False Alarm Rate (FAR) cannot be determined with the method in Betschart and Hering (2012) and is therefore not available. The corresponding scores for the radar derived daily maximum POH product for the same day are a POD of 96% and a FAR of 6%. Figure 3.2.10 shows the COSMO one-moment scheme 09 UTC forecast in Google Earth with the corresponding hail observations of the SHVDB10.

Table 3.1: POD of the simulated daily maximum POH product of the one-moment scheme 09 UTC forecast on May 11, 2010, using the SHVDB10. Only POH values within the boarder of Switzerland are considered.

Date	number of ground-truth reports	POD POH
11.05.2010	136	0.42

[7] Swiss Hail Verification Data Base 2010

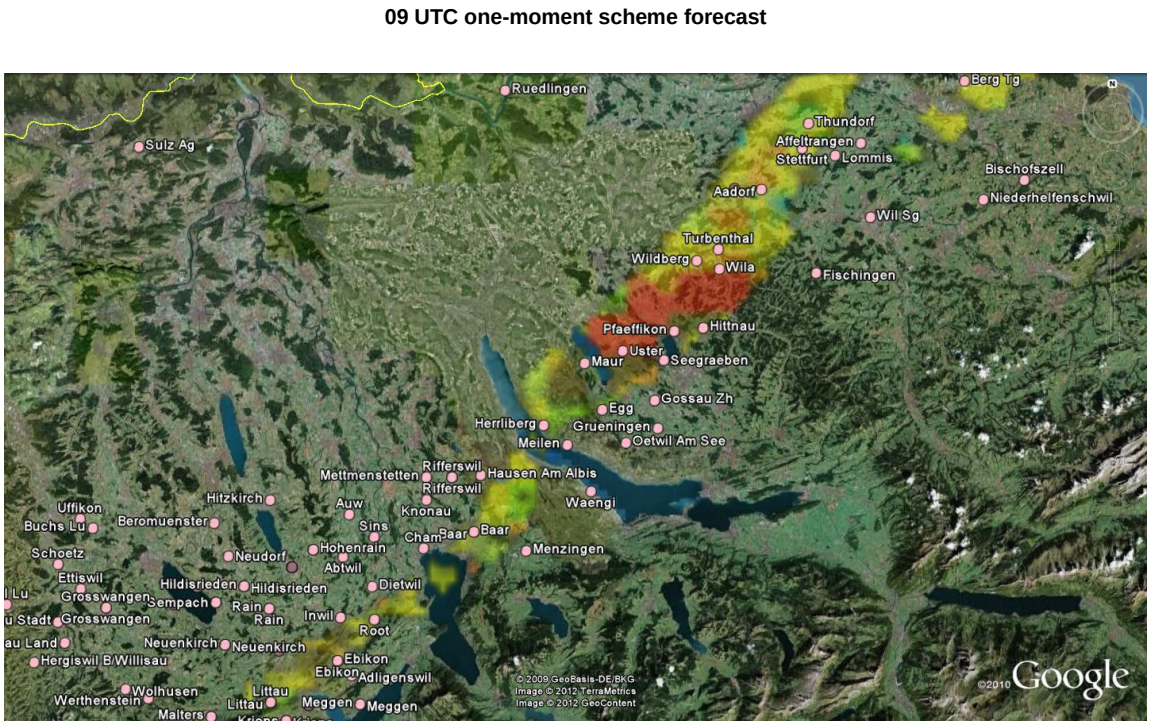

Figure 3.2.10: Synthetic daily maximum POH product (shaded) of the COSMO one-moment scheme 09 UTC forecast, with ground truth data (rose circles) of the SHVDB10[8] of May 11, 2010, in Google Earth near the Lake of Zurich. The color shading shows the left side panels of Figure 3.2.9, adapted for Google Earth.

09 UTC free forecast, hail detection: discussion

The implementation of the radar-based hail detection algorithms for the COSMO one-moment scheme 09 UTC forecast shows two things. First, the forecast simulates hail (as defined by the POH algorithm: difference between 45 contour height (yellow color) and zero degree height) at least for a part of the regions where hail was measured by radar and hail observations were made in correct manner. The POD is however not as high as for the corresponding radar derived POH product. Second, the forecast was not capable to simulate MESHS values within the simulation domain in a sufficient way. This is in agreement with the investigations of the vertical structures. Due to the fact, that high reflectivity values (≥ 51 dBZ) are not simulated for high altitudes, the MESHS cannot be simulated correctly. In general, the POH swaths are too small in terms of their geographical extension. With the investigations on the vertical structure of the simulations above, it seems that the model simulates the hailstorms of this case at the right position, when disregarding the temporal displacement/delay of the cell, but the cell cores themselves are not as strong/vertically extended as they were measured by the radar.

[8] Swiss Hail Verification Data Base 2010

3.2.3. 12 UTC Forecast

COSMO 12 UTC forecast one-moment scheme

The 12 UTC forecast simulates high total precipitation amounts above 40mm/24h from the Emmental-Entlebuch to the Lake of Lucerne, the Lake of Zurich, and the Lake of Constance. No high precipitation values can be found over the Region of Basel (not shown).

In terms of maximum reflectivities there is a Basel cell simulated but with lower maximum reflectivities (up to 55 dBZ) than seen in the 09 UTC forecast (above 55 dBZ). The temporal delay is about 1 hour and therefore closer to the reality then the corresponding 09 UTC forecast (delay of 2:30 h).

The Lucerne cell is trigged at Emmental-Entlebuch. First reflectivities above 55 dBZ, as seen in the radar measurements, are detected at 13.45 UTC and therefore much closer to the radar (13.10 UTC) than in the case of the 09 UTC forecast (15.10 UTC). Parallel a second cell develops north of the Mount Napf and moves further to Schaffhausen, which is not seen in the radar measurements. The Lucerne cell moves along the same path than the corresponding Lucerne cell of the 09 UTC forecast. The maximum intensity is reached at 15.05 UTC to the east of the lake of Zug.

Vertical cross sections of the Lucerne cell during its maximum intensity shows similar structures as seen for the 09 UTC forecast. Likewise, the simulated daily maximum POH product displays similar results as the 09 UTC forecast. No hail (as defined by the MESHS algorithm) is simulated with the synthetic daily maximum MESHS output of the 12 UTC one-moment scheme forecast, again similar to the 09 UTC forecast.

COSMO 12 UTC forecast two-moment scheme

The 12 UTC forecast with the COSMO two-moment scheme does not display any kind of convection or even high reflectivities when using the COSMO RFO. Therefore, no additional information can be won by investigating this forecast.

3.2.4. Analyses Cycles

The analyses of the COSMO one-moment scheme and two-moment scheme are investigated in order to learn how deep convection is simulated, when the LHN forces the model towards observed surface precipitation values.

Analysis cycle of the COSMO one-moment scheme: intro

Considering the COSMO one-moment scheme analysis cycle, no higher total precipitation values above 6.3 mm/24h are visible for the Basel cell (Figure 3.2.11, left panel), where the radar detected values up to 63mm/24h . This is in agreement when considering the maximum reflectivities. Although the LHN should force the model to simulate more precipitation for the Basel cell, only maximum reflectivity values up to 52 dBZ are simulated and the cell is positioned too far north and is therefore worse than the positioning of in the 09 UTC forecast.

For the Lucerne cell, higher total precipitation amplitudes are visible for a swath from Lucerne to the Lake of Zurich (Figure 3.2.11, left panel). Afterwards, the swath is interrupted and two areas with higher precipitation values are seen at Zurich Oberland and close to the Lake of Constance. If considering the maximum reflectivity products for the Lucerne cell, the genesis agrees quite well with the radar measurements. Maximum reflectivities above 55 dBZ are shown at 14.20 UTC over the area of the Lake of Sempach and the Lakes of Hallwil and Baldegg, when the cell reaches maximum intensity (Figure 3.2.12, top left). After crossing the Lake of Zurich, the signal of maximum reflectivity does not agree that well with the radar data. As it is observed in the total precipitation plots (Figure 3.2.11, left panel), the Lucerne cell tends to dissipate in the simulation whereas the cell moves further with the same intensities in the radar data (Figure 3.2.11, right panel).

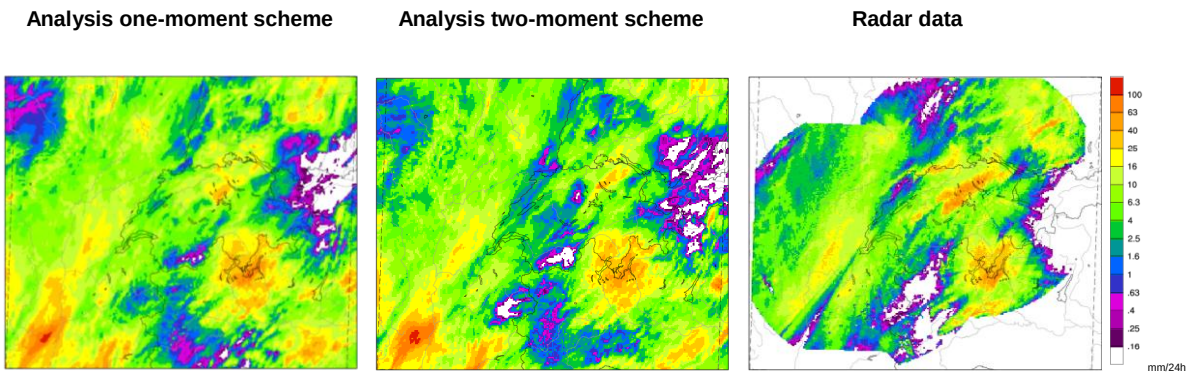

Figure 3.2.11: 24h precipitation sum (shaded) [mm/24h] of the COSMO one-moment analysis cycle (left), two-moment scheme analysis cycle (middle), and the radar measurements (PKC product, right) for May 11, 2010. Black solid lines are international borders and lakes, grey lines are rivers and coast lines, and the dashed lines indicate the radar domain.

Analysis cycle of the COSMO two-moment scheme: intro

In the COSMO two-moment scheme analysis cycle total precipitation plots (Figure 3.2.11, middle), a swath with high precipitation values up to 100 mm/24h can be recognized from Zug to the Lake of Constance. Similar maximum precipitation values were detected by the radar measurements (Figure 3.2.11, right), but the length of the swath from Zug to the Lake of Constance is shorter than measured by the radar (Emmental-Entlebuch to the Lake of Constance). In terms of maximum reflectivity no high values are seen for the Basel cell (not shown). The Lucerne cell starts intensifying at 14.00 UTC over the area of the Lake of Sempach and the Lakes of Hallwil and Baldegg. This is quite close to the radar data which shows intensification at 13.10 UTC over the Emmental (not shown). The cell intensifies very quickly and reaches its maximum intensities at 15.00 UTC over Zurich as seen in Figure 3.2.12 (top left panel). Afterwards, the cell dissipates within one hour.

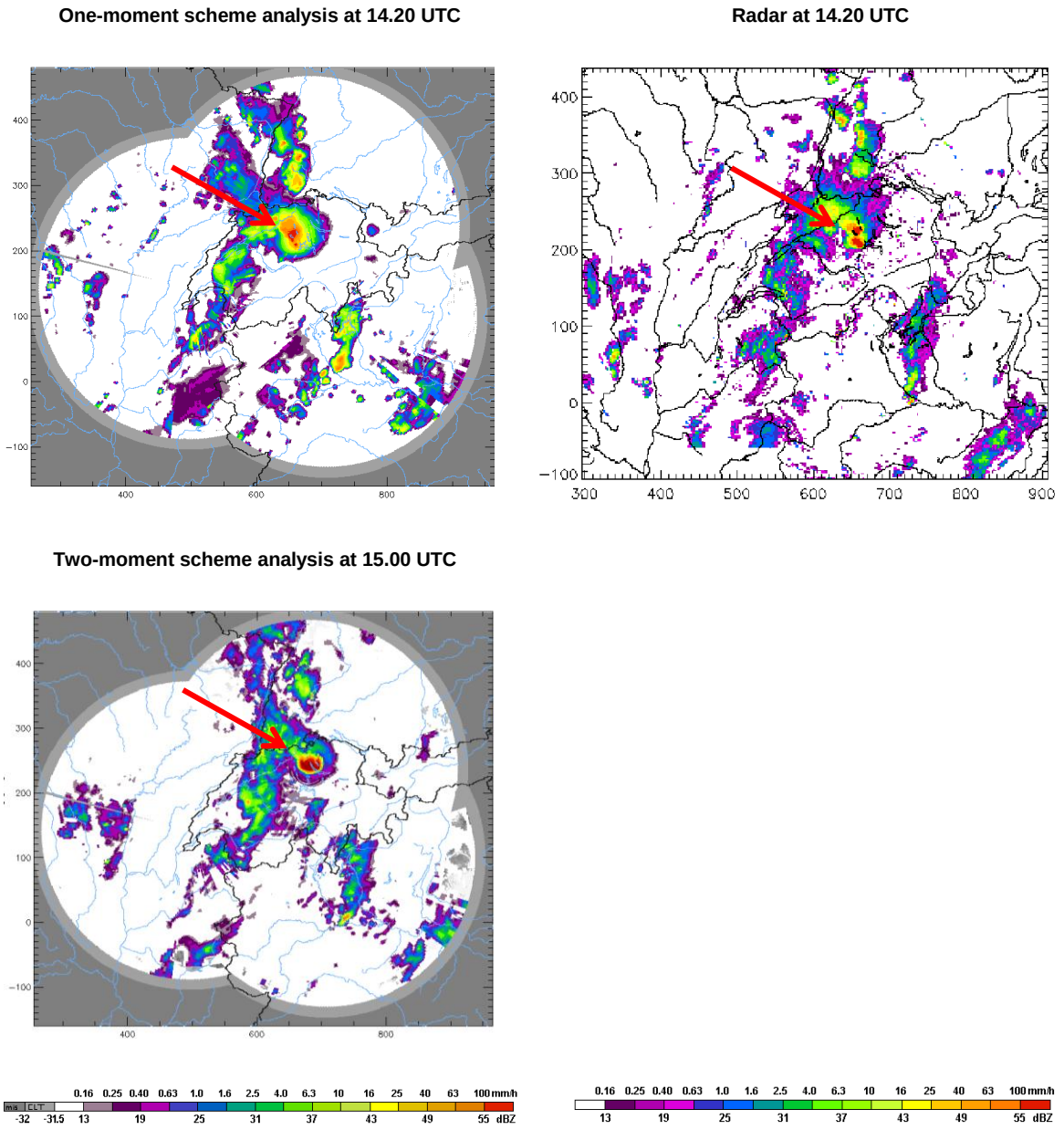

Figure 3.2.12: Maximum reflectivities (CZC product) [dBZ, mm/h] of the one-moment scheme analysis at 14.20 UTC (top left panel) and of the two-moment scheme analysis at 15.00 UTC (bottom left panel), as well as the corresponding radar derived maximum reflectivities (OMC product) at 14.20 UTC (top right panel). The Lucerne cell is labeled with red arrows.

Vertical cross sections of the analysis cycles: data

In order to compare the vertical structures of the COSMO one- and two-moment analysis cycles and for a comparison with the 09 and 12 UTC forecasts, vertical cross sections are made for the time when the maximum intensities occurred. For the one-moment scheme analysis cycles this is at 14.20 UTC (Figure 3.2.13) and for the two-moment scheme at 15.00 UTC (Figure 3.2.14).

Figure 3.2.13 shows the vertical cross section of reflectivity (bottom left panel) and hydrometeors densities (top left panel) in south-north direction for the COSMO one-moment scheme analysis cycle at 14.20 UTC. Figure 3.2.14 shows the vertical cross section of reflectivity of the COSMO two-moment analysis cycle at 15.00 UTC (bottom left panel) and the vertical cross section of hydrometeor densities (top and middle left panel), respectively. As reference the vertical cross section of radar reflectivity is shown on the bottom left panel of Figure 3.2.13 and Figure 3.2.14, respectively.

The vertical cross section of reflectivity of the COSMO one-moment scheme analysis cycle shows high reflectivity values above 55 dBZ near the ground from approximately 0.5 km to 1.5 km. Values between 43 and 46 dBZ (16-25 mm/h, respectively) can be recognized up to 10 km above the ground. Clearly visible is the left inclined tube of values between 46 and 49 dBZ (25-40 mm/h, respectively) up to approximately 8 km. When looking at the one-moment analysis cycle vertical cross section of hydrometeors (Figure 3.2.13, top right panel), graupel (blue contours) and snow (red contours) are visible up to 13 km above the ground. The most intense graupel values are between approximately 5 and 11 km height. Rain is only visible below 3 km height.

The vertical cross section of reflectivity of the COSMO two-moment scheme analysis cycle shows high reflectivity values above 55 dBZ from the ground up to approximately 10 km height as left inclined tube. If considering the two-moment analysis cycle vertical cross section of hydrometeor densities (Figure 3.2.14, middle left panel), graupel and snow can be seen up to approximately 13 km. The most intense zone is due to hail (cyan contours) and the dimension in the vertical is from the ground to approximately 11.5 km height.

Both, the one-moment scheme analysis cycle as well as the two-moment scheme analysis cycle show the same horizontal extent between 9 and 12 km above the ground (ambos) in terms of reflectivities. In the one-moment scheme analysis cycle, the structure on the left side of the plot after 9 km height is mainly generated due to snow whereas the same structure is simulated with graupel and snow in the two-moment scheme analysis cycle.

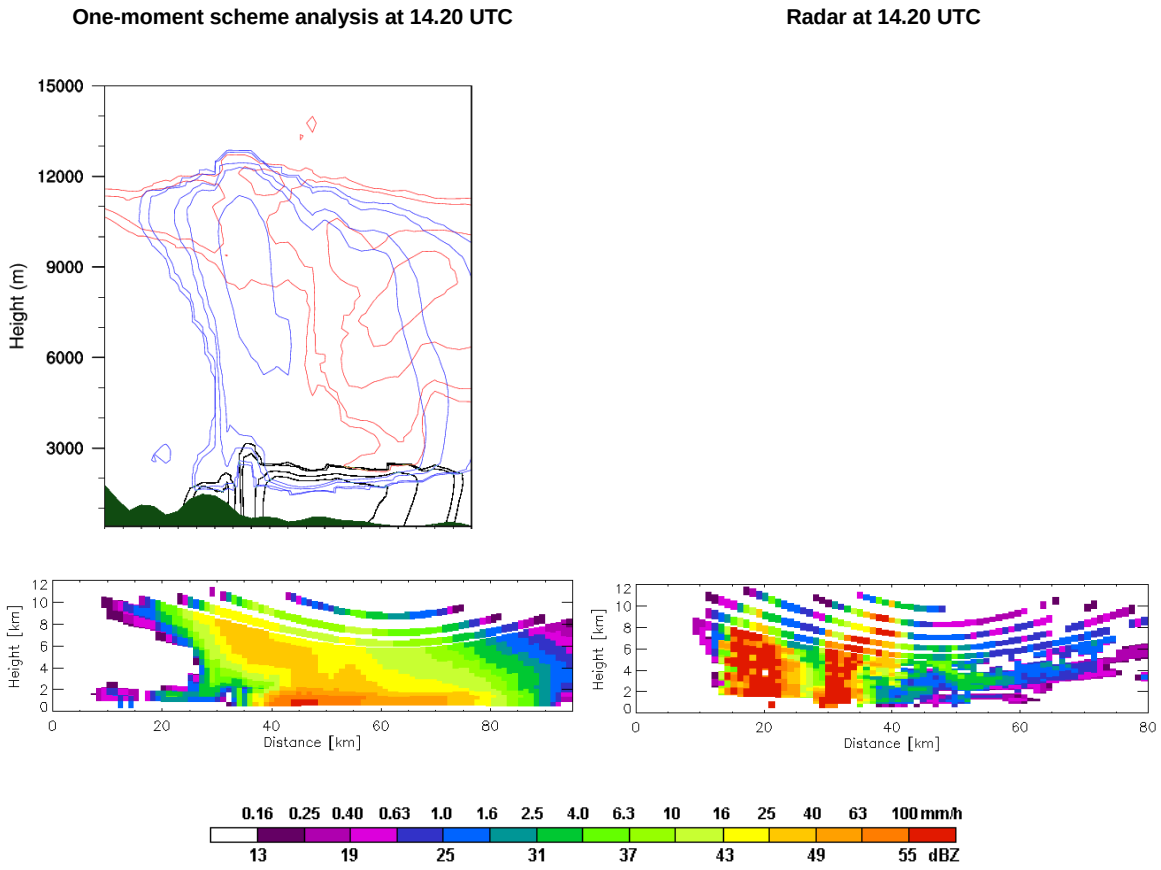

Figure 3.2.13: Top left panel: Vertical cross section of hydrometeor densities [kg/kg air] of the COSMO one-moment scheme analysis at 14.20 UTC with rain (black contour), graupel (blue contour), and snow (red contour), along the same distance as in the bottom left panel near Zurich. The dark green area is the topography. The scale of the contours is as follows: 0.00005, 0.0001, 0.0005, 0.001, 0.005, 0.01, 0.05, 0.1 [kg/kg air]. Bottom left panel: Vertical cross section of synthetic reflectivity [dBZ, mm/h] of the COSMO one-moment scheme analysis at 14.20 UTC near Zurich. Bottom right panel: Vertical cross section of reflectivity [dBZ, mm/h] of the radar (OYC) at 14.20 UTC near Zurich. The x-axis of the vertical cross sections of reflectivity shows the extension of the cross section [km].

Figure 3.2.14 (middle left panel) shows the up- (red shaded areas) and downdraft (blue shaded areas) regions of the COSMO two-moment scheme analysis cycle together with rain (black contours) and hail (cyan contours). It is clearly visible that hail is simulated where the updrafts are strongest. The same is valid for rain, which is simulated up to 7000 m above the ground. This is approximately 5000 m (or 2.5 times) higher than the corresponding COSMO one-moment scheme (Figure 3.2.13, top left panel).

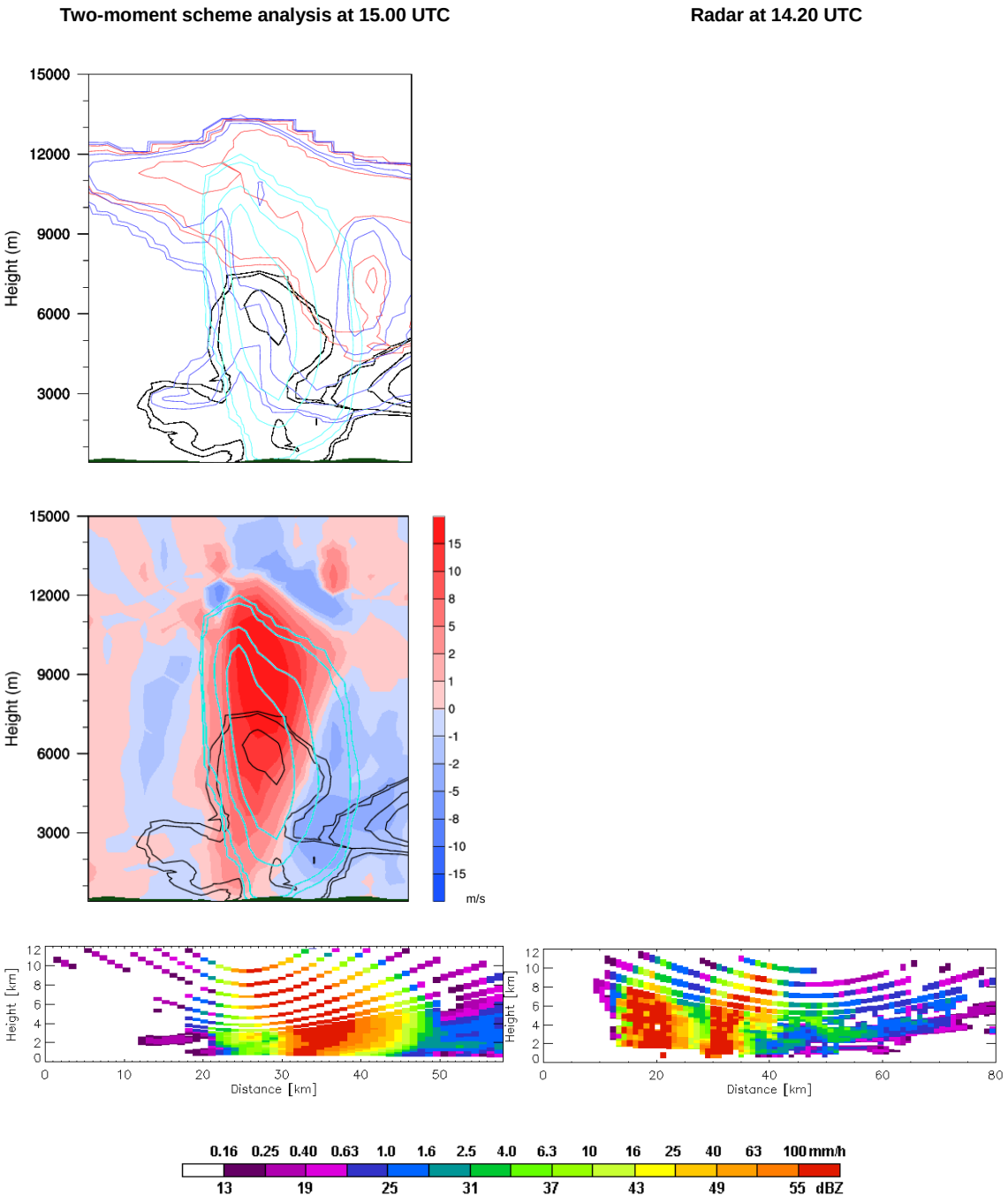

Figure 3.2.14: Top left panel: Vertical cross section of hydrometeor densities [kg/kg air] of the COSMO two-moment scheme analysis at 15.00 UTC with rain (black contour), snow (red contour), graupel (blue contour), and hail (cyan contour). Middle left panel: Vertical cross section of hydrometeor densities [kg/kg air] of the COSMO two-moment scheme analysis at 15.00 UTC with rain (black contour) and hail (cyan contour), as well as vertical winds [m/s] (shaded). Both vertical cross sections of hydrometeor densities are approximately along the same distance as in the bottom left panel near Zurich. The dark green area is the topography. The scale of the contours is as follows: 0.00005, 0.0001, 0.0005, 0.001, 0.005, 0.01, 0.05, 0.1 [kg/kg air]. Bottom left panel: Vertical cross section of synthetic reflectivity [dBZ, mm/h] of the COSMO two-moment scheme analysis at 15.00 UTC near Zurich. Bottom right panel: Vertical cross section of reflectivity [dBZ, mm/h] of the radar (OYC) at 14.20 UTC near Zurich. The x-axis of the vertical cross sections of reflectivity shows the extension of the cross section [km].

Figure 3.2.15 shows the VIL of the COSMO one-moment scheme analysis cycle (top left panel) and the corresponding two-moment scheme analysis cycle (top right panel). The analysis with the one-moment scheme reaches maximum VIL values of 35 kg/m². The analysis cycle of the two-moment scheme shows values up to 50 kg/m². The corresponding radar derived VIL (bottom middle panel) presents values up to 55 kg/m².

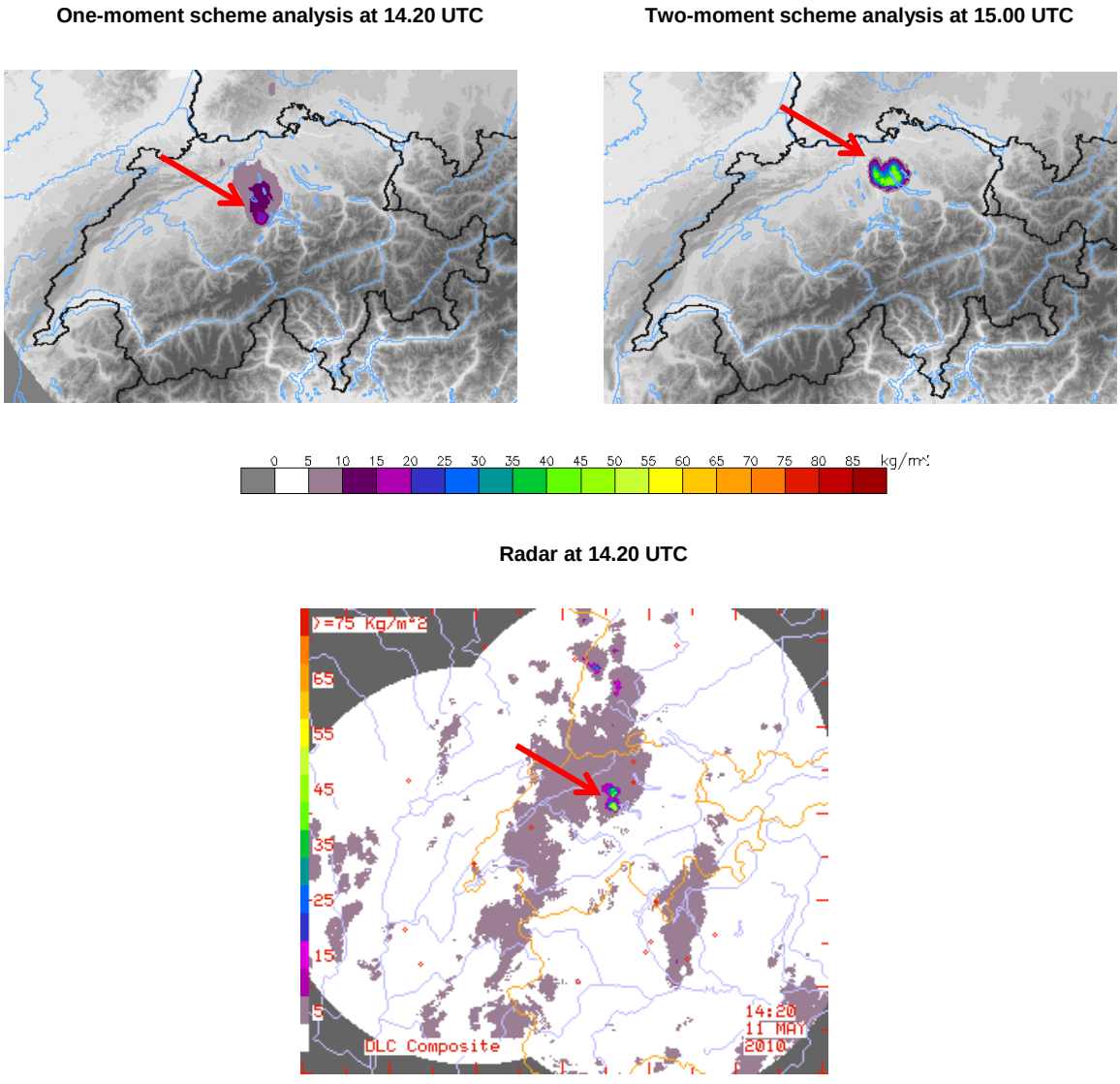

Figure 3.2.15: Top left panel: VIL [kg/m²] of the COSMO one-moment scheme analysis at 14.20 UTC. Top right panel: VIL [kg/m²] of the COSMO two-moment scheme analysis at 15.00 UTC. Bottom panel: VIL [kg/m²] derived from radar data at 14.20 UTC. The Lucerne cell is labeled with red arrows.

Vertical cross sections of the COSMO one-moment scheme analysis cycle: discussion

The COSMO one-moment scheme shows similar patterns and structures in the corresponding 09 UTC and 12 UTC forecasts, when considering the vertical. High reflectivity values are still only visible close to the ground and therefore different

than the radar measurements. Slightly better results are seen when considering the vertical extent in comparison with the forecast. Yellow values (43-46 dBZ, 16-25 mm/h) up to 10 km can be seen whereas the forecasts show the same amplitudes just up to 6 km.

Maximum vertical integrated liquid values are with 35 kg/m^2 higher than those of the forecasts (20 kg/m^2) but still underestimated when considering the radar derived maximum VIL values of 55 kg/m^2.

Vertical cross sections of the COSMO two-moment scheme analysis cycle: discussion

In comparison with the results of the 09 UTC forecasts and 12 UTC forecasts, the COSMO two-moment scheme analysis cycle looks totally different. The LHN forces the COSMO two-moment scheme towards more precipitation at the ground. The result of this forcing can be recognized in the vertical cross section plots (Figure 3.2.14) and the vertically integrated liquid plot (Figure 3.2.15). While we cannot see any convective structures in the forecasts, the analysis shows structures which are close to the reality. Reflectivity values equal or above 55 dBZ are simulated up to 10 km height and are in comparison with the approximately 1,5 km much higher than simulated high reflectivity values in the one-moment scheme runs (forecasts and analysis). A rough interpretation of the reflectivities in the vertical of the two-moment scheme analysis cycle with the corresponding vertical cross section of hydrometeors indicates that the high reflectivities (above 55 dBZ) are the result of the additional hail class. The reflectivities are a bit overestimated in comparison with the radar data (Figure 3.2.14, bottom left panel), but this cannot be confirmed with the surface precipitation products, where similar values are reached as in the radar measurements.

Clearly visible is the simulation of rain up to approximately 8 km height (Figure 3.2.14, top left panel). The corresponding vertical winds (Figure 3.2.14, middle left panel) show a pronounced updraft region where the rain is simulated at higher altitudes. It seems that the model is able to simulate more supercooled water in higher altitudes than in the forecasts or even in comparison with the one-moment scheme. The plot shows further that the region of hail and therefore the region of reflectivities above 55 dBZ correspond with the main updraft region.

The differences of the vertical structure of the COSMO two-moment scheme, compared with the forecasts, can also be seen when considering the VIL plots. The simulation shows maximum values up 50 kg/m^2 and is therefore very close to the radar derived maximum VIL values with 55 kg/m^2.

It can be that the analyses are closer to the reality in terms of vertical structure and the precipitation amounts, the two-moment scheme even more. Although the LHN is not specifically adapted for the two-moment scheme, good results are reached for this case.

COSMO analyses hail detection algorithms: data

The daily maximum POH plots of both analyses (not shown) show similar data in terms of POH values. With both schemes, POH up to 100 % are simulated for the regions of maximum intensities. In comparison with the forecasts, the hail (as defined by the POH algorithm) swaths are a bit broader in terms of the geographical extension.

Figure 3.2.16 displays the COSMO two-moment scheme daily maximum MESHS plot of the analysis cycle (left panel) and the corresponding radar derived daily maximum MESHS (the daily maximum MESHS output of the one-moment scheme analysis cycle shows no MESHS values within Switzerland (not shown)). The two-moment analysis cycle shows a strong signal with values above 6.0 cm around the area of Zurich. The radar derived daily maximum MEHS figure shows values above 6.0 cm as well but not as pronounced as for the two-moment scheme.

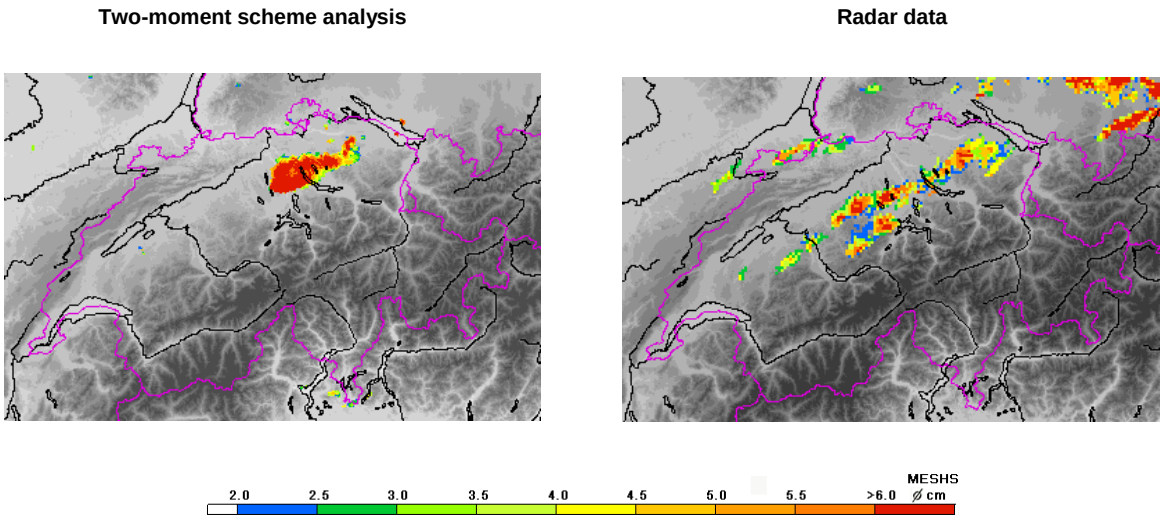

Figure 3.2.16: Left panel: Synthetic daily maximum MESHS product [cm] of May 11, 2010, of the COSMO one-moment scheme analysis. Right panel: Daily maximum MESHS product [cm] of the radar of May 11, 2010.

COSMO analyses hail detection algorithms: discussion

Whereas the daily maximum POH plots shows more or less what is also seen in the forecast runs, the daily maximum MESHS figure of the two-moment scheme analysis cycle (Figure 3.2.16, left panel) shows some calculated hail sizes, whereas the COSMO one-moment scheme does not show any values when considering the analysis cycle.

The analyses above show that the one-moment scheme is not able to simulate reflectivity values above 50 dBZ for higher altitudes, neither in the forecasts nor in the analysis cycle, whereas the two-moment scheme is able to simulate MESHS values, but only when the model is forced with the radar assimilation (LHN). Therefore it can be conclude that the two-moment scheme does not work for this case as forecast, but it shows impressively results in terms of the vertical structure and the ability to simulate hail (as defined by the MESHS algorithm) for the analysis cycle when using the LHN. It has to be investigated in future, why the COSMO two-moment scheme fails to trigger convection in the forecast mode.

3.3. July 22, 2010

On the afternoon of July 22, 2010, a single thunderstorm cell with hail and strong wind gusts moved from Thun to Lucerne, Einsiedeln, Linth valley, Appenzell, and to Germany. In total, cost of several million CHF were caused on crops, buildings, and cars in the Cantons of Lucerne, Zug, Schwyz, Zurich, Glarus, St. Gallen, and both Appenzells.

3.3.1. Synoptic Situation and Measurements

The synoptic situation was dominated by a shallow pressure distribution over Europe. A trough was situated over Great Britain and a cold front approached Switzerland in the afternoon. Embedded in the approaching cold front, an intense thunderstorm was triggered near Thun in the Bernese Oberland at 11.30 UTC. Later on, the cell hit Lucerne at 13.50 UTC. Maximum gusts of 103 km/h were measured at the SwissMetNet station at Lucerne. At 14.30 UTC the cell reached Einsiedeln. There, hail stones with golf ball size (3-4 cm) were observed while the SwissMetNet station at Wallensee measured a total precipitation sum of 31.8mm/30min.

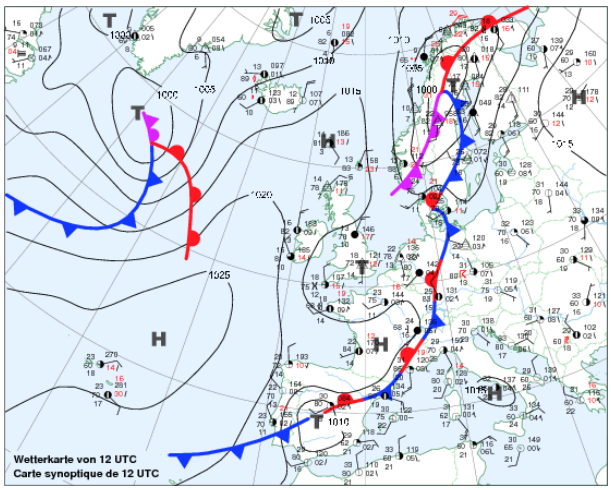

Figure 3.3.1: Synoptic weather chart of Europe at July 22, 2010. Blue signatures are surface cold fronts whereas red signatures are surface warm fronts. Purple signatures are occlusions. Black lines show the pressure [hPa] at the ground (source: MeteoSwiss).

3.3.2. Summary and Special Findings

The case study of July 22, 2010, shows in many ways what has already been found for the first two cases. Therefore, not every single detail will be discussed again, as has been done in the other cases. Only the main findings and some special features will be pointed out in this sub-chapter.

COSMO one-moment scheme

Considering the COSMO one-moment scheme, the above introduced hail cell can be recognized in the 09 UTC forecast, in the 12 UTC forecast as well as in the analysis cycle, in the surface precipitation plots as well as in the maximum reflectivity plots. While the radar detected maximum rain amounts up to 80 mm/24h, 63 mm/24h and 40 mm/24h are simulated in the 09 UTC forecast and 12 UTC forecast, respectively. The COSMO one-moment scheme analysis simulates maximum rain rates up to 63 mm/24h. In general, the cell swath in terms of precipitation and reflectivity is broader in the analysis cycle as in the forecasts. This is in agreement with the other cases, where the COSMO one-moment scheme analyses are more realistic in terms of the geographical extension than the forecasts. Considering maximum reflectivities, quantities above 55 dBZ are simulated for all runs (09 UTC, 12 UTC, and analysis). The weaknesses of the COSMO one-moment scheme are clearly visible when considering the vertical structure of reflectivity or synthetic VIL values. The vertical extent of reflectivities is too small in comparison with the radar measurements but best in the analysis cycle. While the radar derived maximum VIL values are up to 60 kg/m^2, the COSMO one-moment scheme analysis cycle simulates maximum VIL values up to 25 kg/m^2. The difficulties in simulating high reflectivities in the upper troposphere and therefore realistic VIL values are the same as seen in the other cases. The reasons for this are most probably the fact that the one-moment microphysics scheme needs to simulate the hailstorm without a proper hail class (more under 3.1 and 3.2).

The synthetic daily maximum POH plot of the COSMO one-moment scheme analysis

Figure 8.1.2, appendix A) shows a small hail swath for the region of the Lake of Lucerne to the north-eastern part of Switzerland with maximum POH quantities of 70%. The radar derived daily maximum POH plot shows mainly values around 100% probability of hail. No POH values are simulated for the COSMO one-moment scheme forecasts. As already has been seen in the other two cases, no MESHS values above 2cm are simulated in the daily maximum MESHS plot of the COSMO one-moment scheme forecasts and analysis cycle of this case.

None the less, the COSMO one-moment scheme simulates respectable quantities in terms of total surface precipitation in both, the forecasts and the analysis, but

generally underestimates it although the LHN should force the model to more realistic surface precipitation. It has to be kept in mind that this case, as well as the other cases, is extreme in terms of atmospheric conditions. Therefore, it is not surprising that the COSMO one-moment scheme, which has been tuned for more common situations, has some problems in simulating extreme hailstorms.

As conclusion for this case it can be said that the COSMO one-moment scheme shows similar results, properties, and structures as have been seen in the other cases.

COSMO two-moment scheme

More surprising results are found for the runs of the COSMO two-moment scheme. As already known from the case study of May 11, 2010, neither the 09 UTC forecast nor the 12 UTC forecast simulate any convective structures in terms of reflectivities or surface precipitation. It seems that the model is not able to trigger and maintain convection in the forecast mode when using the two-moment scheme in operational mode. But contrary to the case of May 11, 2010, even the COSMO two-moment scheme analysis cycle does not show any convection or high reflectivity cores, neither when considering the surface precipitation plots nor in the maximum reflectivity plots. Consequently, no similar structures as measured by the radar can be found when producing vertical cross sections, daily maximum POH and MESHS products.

The reasons for this behavior are unclear. The cell of July 22, 2010 was smaller in terms of the geographical extent than the cells in the other two cases. Considering the results of the other cases, the two-moment scheme seems to need more time to develop deep convection. This might be due to more sophisticated chain, which has to be passing through, until reaching hail and a full mature convective structure. For a better understanding of this behavior, more research is needed.

4. Summary, Conclusions and Outlook

This study presents a qualitative validation of COSMO-2 simulations of three recently observed hailstorms in Switzerland. The operational COSMO one-moment microphysical scheme as well as a new COSMO two-moment microphysical scheme were investigated. Synthetic radar reflectivities were simulated with a new COSMO radar forward operator and compared to radar derived reflectivities of the operational Swiss radar network. A number of 2-dimensional radar products, vertical cross sections, and radar-based hail detection products were investigated in order to see how realistic COSMO-2 simulates hail events over Switzerland and to describe the main differences between the COSMO one-moment and two-moment microphysical schemes in modeling convective storms. The results presented in this study are only valid for the three case studies, and the findings need to be confirmed statistically for a larger sample of hailstorms in a follow-up study.

The main results and answers to the sub questions formulated in chapter 1 can be summarized as follows:

- In forecast mode, the COSMO one-moment scheme simulates higher surface precipitation amounts than the COSMO two-moment scheme for the July 23, 2009 case. For the other two cases, the COSMO two-moment scheme does not simulate any convective cells. All forecasts of the COSMO one-moment scheme, as well as the COSMO two-moment scheme underestimate the amount of surface precipitation and the geographical extent. In analysis mode, the COSMO two-moment scheme simulates more realistic surface precipitation quantities than the one-moment microphysical scheme, except for the July 22, 2010, case, where it does not simulate a convective cell at all.

- The synthetic maximum reflectivities in general agree quite well with the radar data in forecasts and analyses, provided the model simulated convective cells, which is not always the case for the COSMO two-moment scheme.

- Integrated quantities such as the radar-based VIL are too low in the forecasts for both COSMO microphysical schemes. In analysis mode, the COSMO one-moment scheme generates more realistic VIL values than in the forecasts but still underestimates the values as observed by the radar.

  The COSMO two-moment scheme simulates VIL values well, except for the July 22, 2010, case, where it does not simulate a convective cell at all. The vertical structure of the synthetic reflectivities of the COSMO one-moment scheme show an overestimation of high reflectivities above 55 dBZ close to the ground due to simulated high hydrometeor densities of rain. The reason for that is probably an overestimation of large rain drops with diameters larger than 5 mm. The vertical extend of reflectivities was in general too low in comparison with the radar. A possible reason for underestimating synthetic reflectivities in the height might be a wrong mass-size distribution of the graupel class. The dependency of the radar on changes in the hydrometeor diameters (D^6 in the radar equation (3)) pronounces small changes in the mass-size distribution of graupel even more.

  The COSMO two-moment scheme shows better results in terms of the vertical reflectivity structure. High reflectivity values above 55 dBZ are simulated with higher vertical extend in the analyses of the case July 23, 2009 and May 11, 2010. But the reflectivities close to the ground are too high. This could be due to the same reason as for the COSMO one-moment scheme. Investigations of the vertical winds of the COSMO two-moment scheme show that rain is simulated to much higher altitudes and hail occurs preferentially in the areas of strongest updrafts. Highest precipitation rates are simulated in both schemes where the downdrafts exist. It would be interesting for a follow-up study to find out whether the downdrafts are a consequence of the evaporation of precipitation in dry air layers or not.

- Simulated synthetic daily maximum POH plots in general show an underestimation of hail (as defined by the POH algorithm) in terms of the geographical extent in both schemes (analyses and forecasts), whereas the maximum POH values are simulated realistically. As for MESHS, only the COSMO two-moment scheme analysis simulations contain realistic MESHS

quantities for two out of three cases, but with an underestimation of the geographical extent as well.

Besides these findings, also additional results were found:

- The COSMO two-moment scheme analyses of the two more extreme case studies (July 23, 2009 and May 11, 2010) show that the LHN mechanism seems to work quite well and forces the model runs towards strong convection and realistic vertical reflectivity structures, but it does not work as expected for the strong and small scale single cell storm of July 22, 2010. Especially the fact that the cell was the only one of this day is different to the other cases where many cells developed and were partially connected with each other. For the two successful cases, the COSMO two-moment analysis simulates realistic and impressive reflectivity structures in good agreement with radar data. But the limitations of the COSMO two-moment scheme are clear: Due to unknown reasons and with only one exception, no convective cell is simulated in forecast mode.

- The case of July 23, 2009, exposes the disastrous effect of radar assimilation when the cell amplifies close to the radar. The cell of the COSMO one-moment scheme analysis dissipates completely due to the LHN forcing while the cell in reality won on power. The COSMO two-moment scheme analysis reacts not that sensitive on the LHN forcing as the COSMO one-moment scheme. It possibly might that the more realistic vertical structure of the COSMO two-moment scheme analysis hydrometeor densities and their more realistic synthetic reflectivities do not dissipate that fast when the LHN forces the model towards less surface precipitation. Another reason might be the weaker precipitation signal upstream of the La Dôle radar in comparison with the one-moment scheme analysis. The LHN then does not that strong force the simulation towards less surface precipitation. In combination, the cell does not fully dissipate in the COSMO two-moment scheme analysis mode.

To answer the main question of this study, how realistic the COSMO-2 model simulates hail events over Switzerland and what the main differences between the COSMO one-moment scheme and the COSMO two-moment scheme are, the following statements can be made:

- In forecast mode, the COSMO-2 model only simulates realistic convective storms using the COSMO one-moment scheme. The amplitudes of the total surface precipitation sums are lower than in reality and smaller in terms of the geographical extent. High synthetic reflectivities are reached (≥ 55 dBZ) where the hydrometeor densities of rain are highest. The vertical extent of these reflectivities is too low in general. Radar based VIL simulations show underestimation of the entire liquid in the vertical. Synthetic POH values are simulated with the COSMO one-moment scheme forecast at locations where in reality hail was observed. The geographical extent of the synthetic POH values are however too small. With the exception of the July 23, 2009 case, the COSMO two-moment scheme does not simulate any strong convective cells in the forecast mode. The results of the July 23, 2009 case, show at least that the vertical extent of reflectivities and hydrometeor densities as well as synthetic VIL are slightly better than the COSMO one-moment scheme. The reasons why the COSMO two-moment scheme does not work in forecast mode with more reliability are unknown and need further research.

- In analysis mode, the COSMO one-moment scheme simulates in every case study more realistic convection than in the forecast simulations. Total surface precipitation sums are higher than in the forecast mode in terms their amplitudes and geographical extension but still smaller than the radar measured total precipitation sums. Better results are reached in terms of the vertical structure of maximum reflectivities and a higher vertical extend of reflectivity values. VIL values as well as synthetic POH values of the analyses come closer to the reality than in the forecast mode but have still some limitations. High precipitation values have to be simulated with only three hydrometeor classes, there are rain, snow and graupel. Therefore, the results are realistic in terms of the surface precipitation amounts but not in terms of the vertical structure. The COSMO two-moment scheme analysis however does not simulate reliable convection for one of the three cases. The

reasons why the COSMO two-moment scheme does not simulate realistic convective cells for the case of July 22, 2010 like the COSMO one-moment scheme does when using it in the analysis mode with the LHN forcing, are unknown. For the two cases of July 23, 2009 and May 11, 2010 where hail cells are generated in the COSMO two-moment scheme analysis, impressively realistic results are reached in terms of the total precipitation amounts, the vertical structure, the vertical extend, and synthetic radar-based VIL values, as well as synthetic POH values when compare them with the radar derived measurements. Updrafts are simulated where rain is lifted the most and hail reaches its maximum densities within the cells. Therefore, the COSMO two-moment scheme seems to be promising in terms of its potential in simulating strong hailstorms, provided the convective cell is triggered and can be maintained by the model.

- For both schemes, maximum synthetic reflectivities (≥ 55 dBZ) are simulated close to the ground. Investigations with hydrometeor densities show that this is due to high precipitation values of the rain class. In reality, high reflectivity values are detected at higher altitudes due to hail, graupel and rain. It seems that the COSMO-2 model setups of both schemes tend to simulate convection in terms of the surface precipitation and not in terms of the vertical structure and therefore, maximum synthetic reflectivities values are simulated too close to the ground. Total surface precipitation amounts are therefore better simulated as the vertical structure of convective cells itself.

Surprisingly good results are found for the COSMO one-moment scheme in terms of hail predictions when applying the radar-based POH algorithm. Hail (as defined by the POH algorithm) is simulated at the right position. From a more applied forecasting perspective, the application of this algorithm might improve the information on whether and where hail can be expected within the next hours and may hence help to close the gap between forecasting and nowcasting without any additional effort since the tools are already available. MEHS values are only simulated for the analysis of the COSMO two-moment scheme of July 23, 2009. For all other cases, no MESHS values are simulated.

As mentioned above, further research in many areas of this topic is still necessary. First, it has to be investigated why the COSMO two-moment scheme nearly never triggers any convection in forecast mode. On the other hand, it seems to be promising to improve the COSMO one-moment scheme towards better synthetic reflectivities when using the COSMO RFO.

Further research is needed on the mass-size distribution of the graupel class in order to simulate more graupels with large diameters and therefore higher synthetic reflectivities due to the D^6 dependency of the radar reflectivities. One possible approach could be to do some sensitivity studies with different mass-size distributions (e.g., exponential distribution against gamma distribution etc.).

In order to make more general conclusions about the capability of the model to simulate strong hailstorms, a more statistical-based approach could be applied in the future. This study has shown that the COSMO radar forward operator works and can be used to compare model data directly with radar reflectivities. One procedure could therefore be to count high reflectivity pixels above a certain threshold in both model simulations as well as radar measurements to get more quantitative values about the storm size and its intensity.

Finally, better results in simulating extreme hailstorms can probably only be achieved with higher spatial resolution, since the relevant processes governing intensive hailstorms are still poorly resolved at 2.2 km mesh-size.

5. List of Figures

6. List of Tables

7. References

Baldauf, M., Seifert, A., Förstner, J., Majewski, D. and Raschendorfer, M. (2011) 'Operational Convective-Scale Numerical Weather Prediction with the COSMO Model: Descripition and Sensitivities', *Monthly Weather Review*, pp. 3887-3905.

Bertram, I., Seifert, A. and Beheng, K.D. (2004) 'The evolution of liquid/ice content of a mid-latitude convective storm derived from radar data and results from a cloud-resolving model', *Meteorologische Zeitschrift*, vol. 13, pp. 221-232.

Betschart, M. and Hering, A. (2012) 'Automatic Hail Detection at MeteoSwiss - Verification of the radar-based hail detection algorithms POH, MESHS and HAIL', *Arbeitsberichte der MeteoSchweiz* , vol. 238, pp. 1-59.

Blahak, U. (2007) 'RADAR_MIE_LM and RADAR MIELIB - Calculation of Radar Reflectivity from Model Output.', *Internal report, Institut for Meteorologie und Klimaforschung, Universität/Forschungszentrum Karlsruhe, Germany.*

Blahak, U. (2008a) 'An Approximation to the Effective Beam Weighting Function for Scanning Meteorological Radars with an Axsymmetric Antenna Pattern', *Journal of Atmospheric and Oceanic Technology*, vol. 25, pp. 1182-1196.

Blahak, U. (2008b) 'Towards a Better Representation of High Density Ice Particles in a State-of-the-Art Two-Moment Bulk Microphysical Scheme', *15th International Conference on Clouds and Precipitation.*

Blahak, U. (2012) 'Personal communication'.

Blahak, U., Epperlein, D. and Zeng, Y. (2011) 'Radar forward operator for data assimilation and model verification for the COSMO-model ', *35th Conference on Radar Meteorology*, 26-30 September, pp. 1-9.

Chevallier, F. and Bauer, P. (2003) 'Model rain and clouds over oceans: Comparison with SSM/I observations', *Monthly Weather Review*, vol. 131, pp. 1240-1255.

Doms, G., Förstner, E., Heise, H.J., Herzog, D., Mironov, M., Raschendorfer, T., Reinhardt, B., Ritter, R., Schrodin, R., Schulz, J.P. and Vogel, G. (2011b) 'A Description of the Nonhydrostatic Regional COSMO Model - Part II: Physical

Prameterization', *Consortium for Small-Scale Modelling, Deutscher Wetterdienst (DWD).*

Doms, G., Schättler, U. and Baldauf, M. (2011a) 'A Description of the Nonhydrostatic Regional COSMO-Model - Part I: Dynamics and Numerics', *Consortium for Small-Scale Modelling, Deutscher Wetterdienst (DWD).*

Droegmeier, K.K., Smith, J.D., Businger, S. and Doswell, C. (2000) 'Hydrological aspects of weather prediction and flood', *Bulletin of the American Meteorological Society*, vol. 81, pp. 2665-2680.

Ebert, E.E., Damrath, U., Wergen, W. and Baldwin, M.E. (2003) 'The WGNE assessment of short-term quantitative precipitation', *Bulletin of the American Meteorological Society*, vol. 84, pp. 481-492.

Emanuel, K. (2005) *Divine Wind*, Oxford: Oxford University Press.

Federer, B., Waldvogel, A..S.W., Schiesser, H.H., Hampel, F., Schweingruber, M., Stahel, W., Bader, J., Mezeix, J.F., Doras, N., d'Aubigny, G., DerMegreditchian, G. and Vento, D. (1986) 'Main results of Grossversuch IV', *Journal of Cliamte and Applied Meteorology*, vol. 25, pp. 917-957.

Ferrier, B.S. (1994) 'A double-moment multiple-phase four class bulk ice scheme. Part I: Description', *Journal of Atmospheric Sciences*, vol. 51, pp. 249-280.

Frei, C. and Schär, C. (1998) 'A Precipitation Climatology of the Alps from high-resolution Rain-Gauge Observations', *International Journal of Climatology* , vol. 18, pp. 873-900.

Germann, U. (1999) 'Radome attenuation - a serious limiting factor for quantitative radar measurements?', *Meteorologische Zeitschrift*, vol. 8, pp. 85-90.

Germann, U., Galli, G., Boscacci, M. and Bolliger, M. (2006) 'Radar precipitation measurements in a mountainous region', *Quarterly Journal of the Royal Meteorological Society*, vol. 132, pp. 1669-1692.

Germann, U. and Joss, J. (2004) 'Operational Measurement of Precipitation in Mountainous Terrain', in Meischner, P. (ed.) *Weather Radar - Principles and Advanced Applications* , Springer Verlag.

Greene, D.R. and Clark, R.A. (1972) 'Vertically integrated liquid: A new analysis tool', *Monthly Weather Review*, vol. 100, pp. 548-552.

Hering, A.M. (2010) 'TRT (Thunderstorm Radar Tracking) documentation.', *Internal Documentation: MeteoSwiss*, pp. 1-5.

Hering, A.M., Morel, C., Galli, G., Sénési, S., Ambrosetti, P. and Boscacci, M. (2004) 'Nowcasting thunderstorms in the Alpine region using a radar based adaptive thresholding scheme', *Proc. ERAD Conference 2004*, pp. 206-2011.

Holleman, I. (2001) 'Hail detection using single-polarization radar.', *Scientific Report, KNMI WR-2001-01*, pp. 1-72.

Houze, R.A.J. (1993) *Cloud dynamics*, San Diego: Academic Press.

Illingworth, A.J. and Coauthors (2007) 'Cloudnet: Continuous evaluation of cloud profiles in seven operational models using groundbased', *Bulletin of the American Meteorological Society*, vol. 88, pp. 883-898.

Johnson, J.T., MacKeen, P.L., Witt, A., Mitchell, E.D.W., Stumpf, G., Eilts, M. and Thomas, K.W. (1998) 'The Storm Cell Identification and Tracking Algorithm: An Enhanced WSR-88D Algorithm', *Weather and Forecasting*, vol. 13, pp. 263-276.

Jones, C.D. and Macpherson, B. (1997) 'A Latent Heat Nudging Scheme for the Assimilation of Precipitation Data into an Operational Mesoscale Model', *Meteorological Applications*, vol. 4, pp. 269-277.

Joss, J., Schädler, B., Galli, G., Cavalli, R., Boscacci, M., Held, E., Della Bruna, G., Kappenberger, G., Nespor, V. and Spiess, R. (1997) 'Operational use of radar precipitation measurements in Switzerland', *MeteoSwiss*, pp. 1-121.

Keil, C., Tafferner, A. and Mannstein, H. (2003) 'Evaluating highresolution model forecasts of European winter storms by use of satellite and radar observations.', *Weather and Forecasting*, vol. 18, pp. 732-747.

Kunz, M., Sander, J. and Kottmeier, C. (2009) 'Recent trends of thunderstorm and hailstorm frequency and their relation to atmospheric characteristics in southwest Germany', *International Journal of Climatology*, pp. 2283-2297.

Leuenberger, D. (2005) 'High-Resolution Radar Rainfall Assimilation: Exploratory Studies with Latent Heat Nudging', *Dissertation ETH Zürich No. 15884*.

Lin, Y.L. (2007) *Mesoscale Dynamics*, Cambridge: Cambridge University Press.

Marshall, J.S. and Palmer, K. (1948) 'The distribution of raindrops with size', *Journal of Meteorology* , vol. 5, pp. 165-166.

Meyers, M.P., Walko, R.L., Harrington, J.Y. and Cotton, W.R. (1997) 'New RAMS cloud microphysics parameterization. Part II: The two-moment scheme', *Atmospheric Research*, vol. 45, pp. 3-39.

Müller, E. and Stoll, M. (2010) 'Erste verbreitete Hagelgewitter dieses Jahres', *MeteoSchweiz: Aktuelles Wettergeschehen*, pp. 1-5.

Noppel, H., Blahak, U., Seifert, U. and Beheng, K.D. (2010) 'Simulations of a hailstorm and the impact of CCN using an advanced two-moment cloud microphysical scheme', *Atmospheric Research*, vol. 96, no. 2-3, pp. 286-301.

Noppel, H., Seifert, A., Beheng, K.D. and Blahak, U. (2006) 'A two-moment cloud microphysics scheme with two process-separated modes of graupel', *AMS Conference on Cloud Physics, 10. - 14.07.2006*, vol. 10.

Pfeifer, M., Craig, G.C., Hagen, M. and Keil, C. (2008) 'A Polarimetric Radar Forward Operator for Model Evaluation', *Journal of Applied Meteorology and Climatology*, vol. 47, pp. 3202-3220.

Reisner, J., Rasmussen, R.M. and Bruintjes, R.T. (1998) 'Explicit forecasting of supercooled liquid water in winter storms using the MM5 mesoscale model', *Quarterly Journal of the Royal Meteorological Society*, vol. 124, pp. 1071-1107.

Rinehart, R.E. (2010) *Radar for Meteorologists*, 5th edition, Rinehart Publications.

Salamin, C., Voisard, C., Konantz, B., Stoll, M. and Z'graggen, L. (2009) 'Nach Föhn starke Gewitter am 23.07.2009', *MeteoSchweiz: Aktuelles Wettergeschehen*, pp. 1-7.

Schättler, U., Doms, G. and Schraff, C. (2011) 'A Descripiton of the Nonhydrostatic Regional COSMO-Model - Part VII: User's Guide', *Consortium for Small-Scale Modelling, Deutscher Wetterdienst (DWD)*.

Schiesser, H.H. (2003) 'Extremereignisse und Klimaänderung: Wissensstand und Empfehlung des OcCC.', *OcCC*, pp. 65-68.

Schiesser, H.H., Houze, R.A. and Huntriesser, H. (1994) 'The Mesoscale Structure of Severe Precipitation Systems in Switzerland', *Monthly Weather Review*, vol. 123, pp. 2070-2097.

Schraff, C. and Hess, R. (2003) 'A Description of the Nonhydrostatic Regional Model LM: Part III: Data Assimilation', *Consortium for Small Scale Modelling - Deutschwer Wetterdienst (DWD)*, pp. 1-85.

Schweizer Hagel (2009) '23. Juli 2009: Ein verheerender Hageltag', *Hagel Info*, pp. 2-12.

Seifert, A. and Beheng, K.D. (2006a) 'A two-moment cloud microphysics prameterization for mixed-phase clouds. Part1: Model description', *Meteorology and Atmospheric Physics*, vol. 92, pp. 45-66.

Seifert, A. and Beheng, K.D. (2006b) 'A two-moment cloud microphysics parameterization for mixed-phase clouds. Part2: Maritime vs. continental deep convective storms', *Meteorology and Atmospheric Physics*, vol. 92, pp. 67-82.

Stephan, K. and Schraff, C. (2008) 'Improvements of the operational latent heat nudging scheme used in COSMO-DE at DWD', *COSMO Newsletter*, vol. 9, pp. 7-11.

Tao, W.K., Simpson, J., Baker, D., Braun, S., Chou, M.D., Ferrier, B., Johnson, D., Khain, A., Lang, S., Lynn, B., Shie, C.L., Starr, D., Sui, C.H., Wang, Y. and Wetzel, P. (2003) 'Microphysics, radiation and surface processes in the Goddard Cumulus Ensemble (GCE) model.', *Meteorology and Atmospheric Physics*, vol. 82, pp. 97-137.

Treloar, A.B.A. (1998) 'Vertically integrated radar reflectivity as an indicator of hail size in greater sidney region of Australia', *American Meteorological Society, 19th Conference on Severe Local Storms*, pp. 48-51.

Uijlenhoet, R. (2001) 'Raindrop size distributions and radar reflectivity-rain rate relationships for radar hydrology', *Hydrology and Earth System Sciences*, vol. 5, pp. 615-627.

Waldvogel, A., Federer, B. and Grimm, P. (1979) 'Criteria for the detection of hai cells', *Journal of Applied Meteorology*, vol. 18, pp. 1521-1525.

Wallace, J.M. and Hobbs, P.V. (2006) *Atmospheric Sciene - An Introduction Survey,* , 2nd edition, Amsterdam: Elsevier Academic Press.

Weusthoff, T., Ament, F., Arpagaus, M. and Rotach, M.W. (2010) 'Assessing the Benefits of Convection-Permitting Models by Neighborhood Verification: Examples from MAP D-PHASE', *Monthly Weather Review*, vol. 138, pp. 3418-3433.

Willemse, S. (1995) 'A statistical analysis and climatological interpretation of hailstorms in Switzerland', *Swiss Federal Institute of Technology (ETH), Diss. ETH No. 11137*.

Witt, A., Eilts, M.D., Stumpf, G.J., Johnson, J.T., Mitchell, E.D. and Thomas, K.W. (1998) 'An enhanced hail detection algorithm for the wsr-88d', *Weahter and Forecasting*, vol. 13, pp. 286-303.

Wüest, M. (2011) 'Mesoscale atmospheric systems - observation and modelling: the radar principle', *ETH Zurich, lecture notes*.

8. Appendix A

8.1. Additional Figures

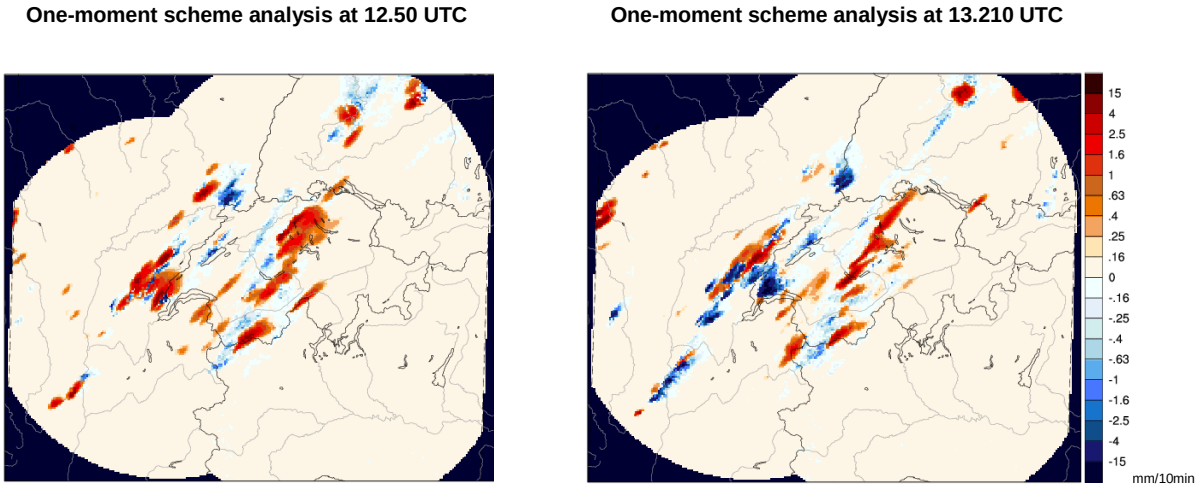

Figure 8.1.1: Differences [mm/10min] between the radar data and the COSMO one-moment scheme analysis of July 23, 2009, of the 10 min total surface precipitation sum at 12.50 UTC (left) and 13.10 UTC (right). Red colors (shaded) are areas where the COSMO one-moment scheme overestimates the 10 min total precipitation sums and blue colors (shaded) are underestimated areas, respectively.

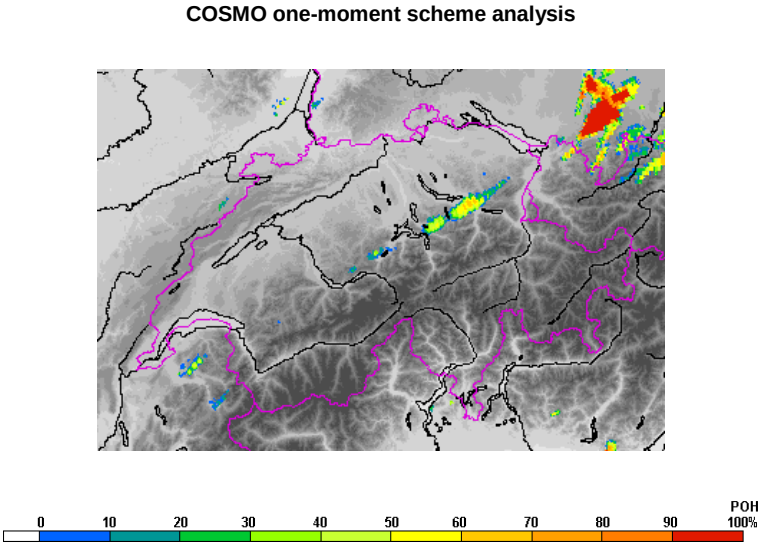

Figure 8.1.2: Synthetic daily maximum POH product [%] of July 22, 2010, of the COSMO one-moment scheme analysis cycle.

9. Appendix B

9.1. Bash Script Files

make_gif_radaroperator.sh

Connects and controls different IDL routines (see below) in order to run the computation process of synthetic radar products automatically, including the transfer of synthetic COSMO reflectivity files from the CSCS to the MeteoSwiss servers and the transfer to the CCS4 radar server.

make_anim_radarproducts.sh

Produces animations of the synthetic radar products.

make_radarproducts_manually.sh

Allows computing every radar product with the CCS4 radar server (e.g. VIL, Echotops, POH (high temporal resolution), Maxecho, etc.) from previous generated PLX files.

transform_hzero.sh

Changes the syntax of the COSMO H_0 files for using the files with either to compute high temporal resolution POH products (*make_radarproducts_manually.sh*) or daily maximum POH and MESHS products (*POH_MESHS_maxDAY_radaroperator.pro*).

make_24h_plot.sh

Computes the surface total precipitation amounts automatically using the NCL *routine tot_precip_24h.ncl, tot_precip_radar_24h.ncl.*

make_1h_plot.sh

Computes the surface total precipitation amounts automatically using the NCL *routine tot_precip_1h.ncl, tot_precip_radar_1h.ncl.*

9.2. IDL Routines

read_syn_rad_data.pro

Reads the simulated synthetic reflectivity values [dBZ] of the COSMO model. This routine was directly implemented in *create_pl_file_radaroperator.pro*.

create_pl_file_radaroperator.pro

Converts synthetic reflectivity values in binary PLX files for each of the 20 elevations considering the Swiss radar network scan strategy (elevation and range). This routine includes the three sub-routines *write_pl_file_radaroperator_albis.pro*, *write_pl_file_radaroperator_dole.pro*, and *write_pl_file_radaroperator_lema.pro*.

write_pl_file_radaroperator_albis.pro

Writes PLX files for each elevation of the Albis radar with the correct header for the CCS4 radar server.

write_pl_file_radaroperator_dole.pro

Writes PLX files for each elevation of the La Dôle radar with the correct header for the CCS4 radar server.

write_pl_file_radaroperator_lema.pro

Writes PLX files for each elevation of the Monte Lema radar with the correct header for the CCS4 radar server.

show_poi_radaroperator.pro

Visualizes all radar raw products of the CCS4 radar server (adaptation of the 4th generation show_poi.pro program).

POH_MESHS_maxDAY_radaroperator.pro

Computes synthetic daily maximum POH and MESHS values using synthetic Echotops of the CCS4 radar server, as well as H_0 files of the COSMO model.

vert_sect_radaroperator.pro

Generates vertical cross sections of (synthetic) radar reflectivities for a single radar site.

plot_vert_sect_radaroperator.pro

Visualizes the vertical cross sections of reflectivities.

9.3. NCL Routines

tot_precip.ncl

Generates the 10 min total surface precipitation plots of the COSMO model.

tot_precip_1h.ncl

Generates the 1 hour total surface precipitation plots of the COSMO model.

tot_precip_24h.ncl

Generates the 24 hours total surface precipitation plots of the COSMO model.

tot_precip_radar.ncl

Generates the 10 min total surface precipitation plots of the radar.

tot_precip_radar_1h.ncl

Generates the 1 hour total surface precipitation plots of the radar.

tot_precip_radar_24h.ncl

Generates the 24 hours total surface precipitation plots of the radar.

VIL.ncl

Calculates the vertical integrated liquid content in the vertical directly from COSMO model variables.

precip_diff.ncl

Allows computing precipitation difference plots of two different COSMO runs.

make_vertical_cuts.ncl

Make vertical cross sections of hydrometeor densities.

vert_wind_1ms.ncl

Generates the vertical cross sections of hydrometeor densities with vertical wind of the COSMO one-moment scheme.

vert_wind_2ms.ncl

Generates the vertical cross sections of hydrometeor densities with vertical wind of the COSMO two-moment scheme.

make_field_plots.ncl

Allows generating a plot of every variable which is given from the COSMO model.

Declaration

under Art. 28 Para. 2 RSL 05

Last, first name: Betschart Mario

Matriculation number: 07-702-994

Programme: Master of Science in Climate Sciences

Bachelor ☐ Master **X** Dissertation ☐

Thesis title: A Study of Convective Events in Switzerland with Radar and a High-Resolution NWP Model

Thesis supervisor: Prof. Dr. Olivia Romppainen-Martius

I hereby declare that this submission is my own work and that, to the best of my knowledge and belief, it contains no material previously published or written by another person, except where due acknowledgement has been made in the text. In accordance with academic rules and ethical conduct, I have fully cited and referenced all material and results that are not original to this work. I am well aware of the fact that, on the basis of Article 36 Paragraph 1 Letter o of the University Law of 5 September 1996, the Senate is entitled to deny the title awarded on the basis of this work if proven otherwise.

Flühli,
Place, date

.....
Mario Betschart